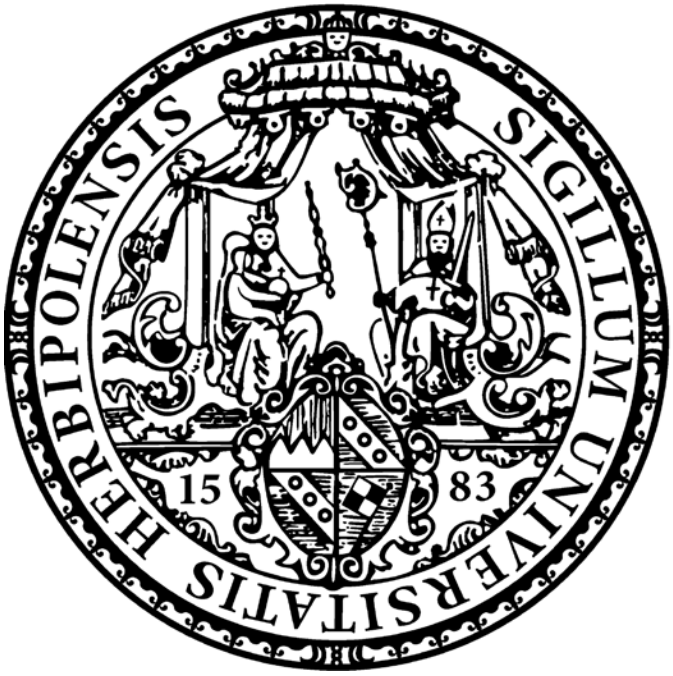


# The role of Batf3-dependent dendritic cells and the IL-23 receptor in atherosclerosis

*Die Rolle von Batf3-abhängigen dendritischen Zellen und des IL-23-Rezeptors in der Atherosklerose*

Doctoral thesis for a doctoral degree

at the Graduate School of Life Sciences,

Julius-Maximilians-Universität Würzburg,

Section **Biomedicine**

Submitted by

**Jesús Gil Pulido**

from

Córdoba, Spain

**Würzburg, 2018**

**Submitted on:**

**Members of the *Promotionskomitee*:**

| | |
|---|---|
| Chairperson: | Prof. Dr. Georg Gasteiger |
| Primary Supervisor: | Prof. Dr. Alma Zernecke-Madsen |
| Supervisor (Second): | Prof. Dr. Manfred Lutz |
| Supervisor (Third): | Dr. Ana Eulalio |

**Date of Public Defence: 14.8.2018**

**Date of Receipt of Certificates:**

A mi madre, mi padre y mi hermana, pilares de mi vida

**TABLE OF CONTENTS**

# SUMMARY

Cardiovascular diseases represent the leading cause of death worldwide, with myocardial infarction and strokes being the most common complications. In both cases, the appearance of an enlarged artery wall as a consequence of a growing plaque is responsible for the disturbance of the blood flow. The formation of plaques is driven by a chronic inflammatory condition known as atherosclerosis, characterized by an initial step of endothelial cell (EC) dysfunction followed by the recruitment of circulating immune cells into the tunica intima of the vessel. Accumulation of lipids and cells lead to the formation of atheromatous plaques that will define the cardiovascular outcome of an individual.

The role of the immune system in the progression of atherosclerosis has been widely recognized. By far, macrophages constitute the most abundant cell type in lesions and are known to be the major source of the lipid-laden foam cell pool during the course of the disease. However, other immune cells types, including T cells, dendritic cells (DCs) or mast cells, among others, have been described to be present in human and mouse plaques. How these populations can modulate the atherogenic process is dependent on their specialized function.

DCs constitute a unique population with the ability to bridge innate and adaptive immune responses, mainly by their strong capacity to present antigens bound to a major histocompatibility complex (MHC) molecule. Given their ability to polarize T cells and secrete cytokines, their role in atherosclerosis has gained attention for the development of new therapeutic approaches that could impact lesion growth. Hence, knowing the effect of a specific subset is an initial key step to evaluate its potential for clinical purposes. For example, the basic leucine zipper ATF-like 3 transcription factor (Batf3) controls the development of conventional dendritic cells type 1 (cDCs1), characterized by the expression of the surface markers CD8 and CD103. Initially, they were described to promote both T-helper 1 ($Th_1$) and regulatory T cell ($T_{reg}$) responses, known to accelerate and to protect against atherosclerosis, respectively. The first part of this thesis aimed to elucidate the potential role of Batf3-dependent DCs in

atherosclerosis and concluded that even though systemic immune responses were mildly altered they do not modify the course of the disease and may not represent an attractive candidate for clinical studies.

DCs also have the ability to impact lesion growth through the release of a broad range of cytokines, which can either directly impact atherosclerotic plaques by modulating resident cells, or by further polarizing T cell responses. Among others, interleukin (IL) 23, a member of the IL-12 family of cytokines, has received much attention during the past year due to its connection to autoimmunity.

IL-23 is known to induce pathogenicity of $Th_{17}$ cells and is responsible for the development of several autoimmune diseases including multiple sclerosis, psoriasis or rheumatoid arthritis. Interestingly, these patients often present with an accelerated course of atherosclerosis and thus, are at higher risk of developing cardiovascular events. Several epidemiological studies have pointed toward a possible connection between IL-23 and its receptor IL-23R in atherosclerosis, although their exact contribution remains to be elucidated. The second part of this thesis showed that resident antigen-presenting cells (APCs) in the aorta produced IL-23 during the steady state but this secretion was greatly enhanced after incubation with oxidized low-density lipoprotein (oxLDL). Furthermore, disruption of the IL-23R signaling led to decreased relative necrotic plaque area in lesions of *Ldlr*$^{-/-}$*Il23r*$^{-/-}$ mice fed a high-fat diet (HFD) for 6 and 12 weeks compared to *Ldlr*$^{-/-}$ controls. A proposed mechanism involves that increased IL-23 production in the context of atherosclerosis may promote the pathogenicity of IL-23-responding T cells, especially IL-23R$^{+}$ γδ T cells in the aortic root. Response to IL-23 might increase the release of granulocyte-macrophage colony-stimulating factor (GM-CSF) and IL-17 and alter the pro- and anti-inflammatory balance of cytokines in the aortic root. Altogether, these data showed that the IL-23 / IL-23R axis play a role in plaque stability.

# ZUSAMMENFASSUNG

Kardiovaskuläre Erkrankungen sind weltweit die häufigste Todesursache, wobei Myokardinfarkt und Schlaganfall die häufigsten Komplikationen darstellen. In beiden Fällen ist das Auftreten einer verbreiterten Arterienwand als Folge eines wachsenden Plaques für die Störung des Blutflusses verantwortlich. Die Bildung von Plaques wird durch einen chronischen Entzündungszustand, bekannt als Atherosklerose, ausgelöst. Zunächst kommt es dabei zur Entstehung einer endothelialen Dysfunktion, die zur Rekrutierung zirkulierender Immunzellen in die Tunica Intima des Gefäßes führt. Die Akkumulation von Lipiden und Zellen wiederum führt zur Bildung von atheromatösen Plaques, die den kardiovaskulären Gefäßstatus eines Individuums bestimmen.

Die Rolle des Immunsystems bei der Progression der Atherosklerose wurde weithin anerkannt. Makrophagen stellen bei weitem den häufigsten Zelltyp innerhalb der Läsionen dar und sind bekanntermaßen die Hauptquelle des mit Lipid beladenen Schaumzellpools im Verlauf der Erkrankung. Es wurde jedoch auch beschrieben, dass andere Arten von Immunzellen, einschließlich der T-Zellen, dendritischen Zellen (DCs) und Mastzellen, in humanen und murinen Plaques vorhanden sind. Wie diese Populationen den atherogenen Prozess modulieren können, hängt von ihrer spezialisierten Funktion ab.

DCs bilden eine einzigartige Population, der es möglich ist, angeborene und adaptive Immunartworten zu überbrücken. Dies geschieht hauptsächlich aufgrund ihrer ausgeprägten Fähigkeit, Antigene zu präsentieren, die an einen Haupthistokompatibilitätskomplex gebunden sind. Angesichts ihrer Rolle in der Polarisierung von T-Zellen und der Sezernierung von Zytokinen haben sie bisher Aufmerksamkeit bei der Entwicklung neuer therapeutischer Ansätze zur Beeinflussung des Läsionswachstums erlangt. Die Kenntnis der Wirkung einer bestimmten Subpopulation ist ein erster wichtiger Schritt, um ihr Potenzial für klinische Zwecke zu bewerten. Zum Beispiel steuert der Transkriptionsfaktor „basic leucine zipper ATF-like 3“ (Batf3) die Entwicklung von herkömmlichen dendritischen Zellen Typ 1, welche durch die Expression der Oberflächenmarker CD8 und CD103 gekennzeichnet sind.

Anfänglich wurde beschrieben, dass sie sowohl die Antworten von T-Helfer 1 als auch von regulatorischen T-Zellen fördern, welche je nach Zellfunktion die Atherosklerose beschleunigen oder vorbeugen. Im ersten Teil dieser Arbeit wurde die potentielle Rolle von Batf3-abhängigen DCs für die Entstehung der Atherosklerose aufgeklärt. Trotz diese einer leichten Veränderungen der systemischen Immunantwort den Krankheitsverlauf nicht beeinflussen und daher keine attraktiven Kandidaten für klinische Studien darstellen.

DCs haben auch die Fähigkeit das Läsionswachstum durch Freisetzung einer breiten Palette an Zytokinen zu beeinflussen, die atherosklerotische Plaques entweder direkt durch Modulation von ortsständigen residenten Zellen oder durch weiteres Polarisieren von T-Zell-Reaktionen beeinflussen können. Unter anderem hat interleukin (IL) 23, ein Mitglied der IL-12-Zytokinfamilie, aufgrund seines Zusammenhangs mit Auto-immunität im vergangenen Jahr viel Aufmerksamkeit erhalten.

Es ist bekannt, dass IL-23 die Pathogenität von $Th_{17}$-Zellen induziert und für die Entwicklung von mehreren Autoimmunkrankheiten einschließlich multipler Sklerose, Psoriasis oder rheumatoider Arthritis verantwortlich ist. Interessanterweise haben alle diese Erkrankungen gemeinsam, dass sie die Entstehung einer Atherosklerose beschleunigen. Die betroffenen Patienten haben ein höheres Risiko für ein kardiovaskuläres Ereignis. Mehrere epidemiologische Studien haben auf einen möglichen Zusammenhang zwischen IL-23 und seinem Rezeptor IL-23R bei Atherosklerose hingewiesen, auch wenn die genaue Relevanz dieser Hinweise noch zu klären ist. Im zweiten Teil dieser Arbeit konnte es gezeigt werden, dass ortsständige antigenpräsentierende Zellen in der Aorta IL-23 zwar bereits im Steady State produzieren, diese Sekretion jedoch nach Inkubation mit oxLDL stark erhöht ist. Darüber hinaus führte eine Störung der IL-23R-Signalgebung nach 6 bis 12 Wochen einer fettreichen Diät (HFD) zu einer verringerten relativen nekrotischen Plaque-Fläche in Läsionen von *Ldlr*$^{-/-}$*Il23r*$^{-/-}$ Mäusen verglichen mit *Ldlr*$^{-/-}$ Mäusen. In Bezug auf den zugrunde liegenden Mechanismus wurde diskutiert, dass eine erhöhte IL-23-Produktion im Zusammenhang mit Atherosklerose die Pathogenität von IL-23R-reaktiven T-Zellen, insbesondere von IL-23R$^{+}$ γδ T-Zellen in der Aortenwurzel, fördern

kann. Reaktionen auf IL-23 könnten die Freisetzung von Granulozyten-Monozyten-Kolonie-stimulierendem Faktor und IL-17 erhöhen und das pro- und antiinflammatorische Gleichgewicht von Zytokinen innerhalb der Aortenwurzel verändern. Insgesamt zeigen diese Daten, dass die IL-23 / IL-23R Achse eine wichtige Rolle in der Etablierung der Plaquestabilität einnimmt.

# ABBREVIATIONS

| | |
|---|---|
| AHR | Aryl hydrocarbon receptor |
| AP | Activator protein |
| APC | Antigen-presenting cell |
| APO | Apolipoprotein |
| BATF | Basic leucine zipper transcription factor ATF-like |
| BM-APC | Bone marrow-derived antigen-presenting cells |
| BMDM | Bone marrow-derived macrophages |
| BFA | Brefeldin A |
| BSA | Bovine serum albumin |
| CAD | Coronary artery disease |
| cDC | Classical dendritic cell |
| cDNA | Complementary DNA |
| CPD | Common DC precursor |
| CTL | Cytotoxic T lymphocyte |
| DC | Dendritic cell |
| DN | Double negative |
| DP | Double positive |
| DTR | Diphtheria toxin receptor |
| EBI3 | Epstein-Barr virus induced gene 3 |
| EC | Endothelial cell |
| EDTA | Ethylenediaminetetraaceit acid |
| ELISA | Enzyme-linked immunosorbent assay |
| FA | Formaldehyde |
| FACS | Fluorescence-activated cell sorting |

| | |
|---|---|
| FCS | Fetal calf/bovine serum |
| FITC | Fluorescein |
| FLT3L | FMS-like tyrosine kinase 3 ligand |
| FOXP3 | Forkhead-Box-Protein 3 |
| GM-CSF | Granulocyte-macrophage colony-stimulating factor |
| HDL | High-density lipoprotein |
| HEPES | 4-(2-hydroxyethyl)-1-piperanzineethanesufonic acid |
| HFD | High fat diet |
| HDL | High-density lipoprotein |
| ICAM | Intercellular adhesion molecule |
| IDL | Intermediate-density lipoprotein |
| IFN | Interferon |
| IL | Interleukin |
| IRF | Interferon-regulatory factor |
| JAK | Janus kinases |
| LDL | Low-density lipoprotein |
| LDLR | LDL receptor |
| LPS | Lipopolysaccharide |
| LOX | Lectin-like oxLDL receptor |
| M-CSF | Macrophage colony-stimulating factor |
| MHC | Major Histocompatibility complex |
| NEEA | Non-essential aminoacids |
| NFAT | Nuclear factor of activated T cells |
| NF-κB | Nuclear factor kappa-light-chain-enhancer of activated B cells |
| NRF | Nuclear erythroid-related factor |
| OVA | Ovalbumin |

| | |
|---|---|
| oxLDL | Oxidized Low-density lipoprotein |
| PAD | Peripheral artery disease |
| PAMP | Pathogen-associated molecular pattern |
| PBMCs | Peripheral blood mononuclear cells |
| PBS | Phosphate-buffered saline |
| PD | Programmed cell death |
| pDC | Plasmacytoid dendritic cell |
| PDL | Programmed cell death ligand |
| PFA | Paraformaldehyde |
| PMA | Phorbol-12-myristate-13-acetate |
| PMB | Polymyxin B |
| PPAR | Peroxisome proliferation-activated receptor |
| PVAT | Perivascular adipose tissue |
| ROR | RAR-related orphan receptor |
| ROS | Reactive Oxygen Species |
| SMC | Smooth muscle cell |
| SNP | Single nucleotide polymorphism |
| SR | Scavenger receptor |
| STAT | Signal transducer and activator of transcription |
| TCR | T cell receptor |
| TGF | Transforming growth factor |
| TLR | Toll-like receptor |
| TNF | Tumor necrosis factor |
| TREG | Regulatory T cell |
| TYK | Tyrosine kinase |
| SMC | Smooth muscle cell |

| | |
|---|---|
| VCAM | Vascular cell adhesion protein |
| vLDL | Very low-density lipoprotein |
| WT | Wild type |
| ZBTB46 | Zinc-finger transcription factor zDC |

# 1. INTRODUCTION

## 1. Atherosclerosis and cardiovascular diseases: a general overview

Cardiovascular diseases represent a group of disorders affecting muscular arteries supplying different organs and locations, such as the heart (coronary artery disease, CAD), the brain (cerebrovascular disease, stroke) or the arms and legs (peripheral artery disease, PAD). According to the World Health Organization, they remain the leading cause of death worldwide with around 17 million deceases reported in 2015. Predictions show that these numbers will rise in the following years. By far, myocardial infarction (a complication of CAD) and ischemic stroke represent the vast majority of reported cases, accounting for up to 80% of all deaths. Both manifestations have in common a slowly progressing chronic disorder of large and medium-sized arteries known as atherosclerosis [1].

Our current understanding of the pathogenesis of atherosclerosis has revealed that this condition is a complex entity comprising a broad range of mediators which finally results in the formation of plaques in the intima of blood vessels. Several compounds and conditions promote the dysfunction of the endothelium lining the vasculature and lead to increased permeability and retention of circulating lipoproteins. As a consequence, there is an upregulation of adhesion molecules on the surface of ECs allowing the recruitment of circulating immune cells, promoting the progression of atherosclerosis. During the lifetime of the individual bigger and more complex plaques can develop until the blood flow is disrupted. Alternatively, erosion of the endothelial barrier or rupture of the fibrous cap covering plaques can lead to the initiation of a coagulation cascade resulting in the formation of a blood clot and acute cardiovascular events.

## 1.1. Initiation and progression of atherosclerosis

### 1.1.1. Endothelial cell dysfunction

The anatomy of healthy middle to large-sized arteries is composed of three layers, as illustrated in Figure 1: the tunica externa or adventitia, which comprises a set of collagen fibers, vasa vasorum and nerves; the tunica media, mostly composed of smooth muscle cells (SMCs) and elastic tissue; and the tunica intima, the inner part of the vessel, covered by a layer of ECs, which is in direct contact with the flowing blood. During atherogenesis, the aortic endothelial lining is damaged allowing the infiltration of circulating lipids and immune cells, which constitute the starting point of the chronic inflammatory response leading to the formation of atheromatous plaques.

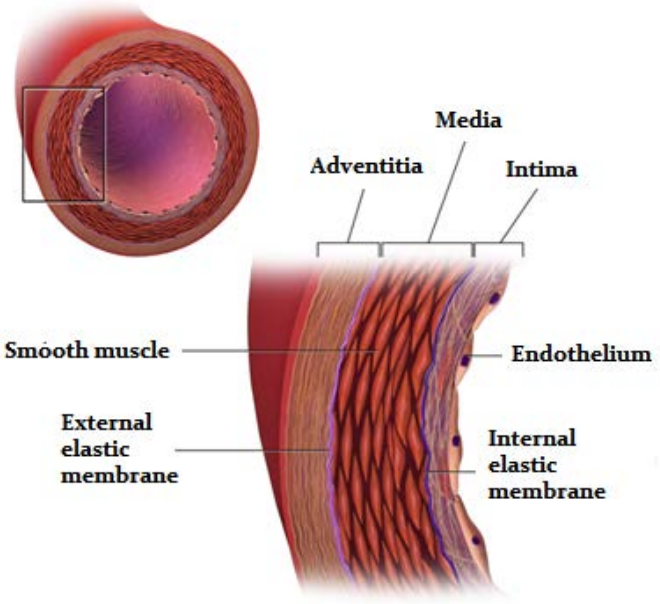


**Figure 1.** Anatomy of a healthy blood vessel (Blausen.com staff (2014). "Medical gallery of Blausen Medical 2014". Wikijournal of Medicine 1 (2). / CC BY 3.0)

The reasons why the endothelium at lesion-prone areas is damaged or get dysfunctional are not fully understood but they have been the subject of intense research since the initial consideration of Rudolph Virchow, the first evidencing a localized accumulation of lipids and other components of plasma at sites of lesion formation [2]. Decades later, Ross and Glomset proposed the Response-to-Injury-Hypothesis [3], which postulated that the initiating event in the atherogenic process was some form of overt injury to the intimal endothelial lining, induced by noxious

substances (oxidized phospholipids, compounds derived from cigarettes or hyperglycemia) or by altered hemodynamic forces, such as a blood flow disturbances generated by hypertension.

Although initially the vascular endothelium was seen as a selective permeable interface, the development of reliable methods for the in vitro culture of ECs rapidly demonstrated a broad range of metabolic functions including the enzymatic buffering of reactive oxygen species (ROS), transport and metabolism of lipoproteins and the elaboration of several growth factors, cytokines and other hormone-like substances [4, 5]. Each EC lining the vasculature can also be seen as a biomechanical transducer, with the ability to sense and transduce diverse forces imported by the pulsatile flow of blood into biological responses [6], which has a profound impact in the context of atherogenesis [7]. All these functions can be altered after challenge with certain pro-inflammatory mediators or even microbial compounds [8] that reversibly alters many of these vital functional properties and can be understood as an adaptive response to different stimuli. However, in the context of atherosclerosis, a systemic inflammation leads to a permanent dysfunctional state of the endothelium with important implications for vascular integrity. The term "endothelium dysfunction" has gained popular acceptance in the cardiovascular field and has led to an intense research focused on the discovery of the pathophysiological stimuli with the ability to trigger it. Some of these are summarized in Table 1.

**Table 1**. Pathophysiological stimuli of endothelium dysfunction in atherogenesis (adapted from [9])

- Hypercholesterolemia (e.g., oxidatively modified lipoproteins)
- Diabetes, Metabolic Syndrome (e.g., ROS, adipokines)
- Hypertension (e.g., angiotensin-II, ROS)
- Sex hormonal imbalance (e.g., estrogen deficiency, menopause)
- Aging (e.g., cell senescence)
- Oxidative stress (multi-factorial)
- Pro-inflammatory cytokines (e.g., IL-1, tumor necrosis factor (TNF))
- Infectious agents (e.g., bacterial endotoxins, viruses)
- Environmental toxins (e.g., cigarette smoke, air pollutants)
- Hemodynamic forces (e.g., disturbed blood flow)

### 1.1.2. Lipid retention and foam cell formation

Due to its nonpolar nature, cholesterol cannot be transported in the plasma without being associated with various lipoprotein particles, which include chylomicrons, very low-density lipoproteins (vLDL), intermediate-density lipoproteins (IDL), low-density lipoproteins (LDL) and high-density lipoproteins (HDL).

Lipoproteins are formed by a cholesterol and triglyceride-enriched core surrounded by a layer of phospholipids and apoproteins, the latter serving not only as a structural scaffold but also as a ligand for lipoprotein receptors and activator or inhibitor of enzymes involved in lipoprotein metabolism [10]. The basic structure of these particles is shown in Figure 2.

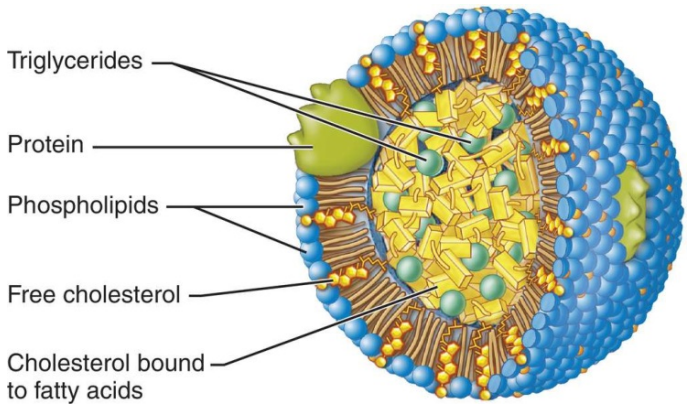


**Figure 2.** Structure of a lipoprotein (Mosby's Medical Dictionary, 9th edition, 2009. Elsevier)

The initial association between cholesterol and atherosclerosis was first described by Anitschkow, who observed that feeding cholesterol in oil to rabbits caused the formation of atheroma similar to those seen in humans [11] and demonstrated a causal role of cholesterol and increased risk for cardiovascular diseases. His study was further supported by Muller et al. after finding that families with an inherited high cholesterol history presented an increased risk of developing cardiovascular diseases [12]. Finally, compelling evidence from epidemiological studies linked increased LDL to cardiovascular diseases [13] and demonstrated an inverse relation of HDL to cardiovascular diseases [14], firmly establishing the relation of cholesterol with atherogenesis.

But how does cholesterol increase the risk of cardiovascular events? After more than two decades of work, William and Tabas postulated in 1995 the Retention Hypothesis, which can in part answer this question [15]. They demonstrated that apolipoprotein B (ApoB)-containing lipoproteins (mainly LDL) are retained within the intima layer of arteries and serve as a critical event that sparks an inflammatory response leading to the recruitment of mediators (e.g. immune cells). Thus, higher levels of circulating cholesterol promote accumulation of LDL particles and fuel the development of plaques.

Surprisingly, it was early recognized that native LDL particles are not able to induce an immune response unless the phospholipid or the apoprotein fraction have undergone chemical modification such as acetylation, carbamylation, glycation or oxidation [16]. These changes are mediated by the presence of ROS or hydroperoxidases released by ECs and other enzymes such as myeloperoxidases and lipoxygenases, described to be present in plaques [17-19].

Among all of these modifications, oxidation is the most studied process and is responsible for the generation of oxLDL, with high immunogenic properties [16]. Uptake of oxLDL by macrophages or DCs leads to a marked accumulation of cholesterol, converting them into lipid-laden cells known as foam cells [20], that initiate the development of atherosclerotic lesions. In addition to serve as a substrate for cholesterol accumulation, oxLDL also exerts a wide range of additional functions. For example it has been reported to induce the secretion of inflammatory cytokines by macrophages [21-24] and ECs [25, 26], to perpetuate the recruitment of circulating lymphocytes serving either as a chemotactic molecule [27] or inducing the surface expression of adhesion molecules in ECs, [28-32] and to induce proliferation and migration of SMCs [33-36].

### 1.1.3. oxLDL is recognized by scavenger and Toll-like receptors

Modified lipoproteins including oxLDL are not recognized by the LDL receptor (Ldlr). Instead, they can bind scavenger receptors (SRs) and Toll-like receptors (TLRs) expressed by a broad range of cell types and trigger both pro-inflammatory responses as well as anti-inflammatory responses [37]. The exact mechanisms by which oxLDL

induces a different response is not clear but it has been suggested that its pro-inflammatory properties depend on transcription factors such as nuclear factor kappa-light-chain-enhancer of activated B cells (NF-κB), activator protein 1 (AP-1), signal transducer and activator of transcription (STAT) 1 and 3, nuclear factor of activated T cells (NFAT) or specificity protein 1, among other, whereas peroxisome proliferator-activated receptor (PPAR), nuclear erythroid-related factor (NRF) 2 or heme oxygenase 1 seem to be essential to elicit an anti-inflammatory response [37].

Recognition of oxLDL by SRs has been well documented. Three main types of SRs have been described: SR-A, composed of the SR-AI and II; SR-B, including CD36 and the less studied SR-BI/II, and SR-E, with one described member, the lectin-like oxLDL receptor (LOX) 1. Their expression pattern varies among cell types, and several reports have already suggested an important role of SRs in modifying the immune response [38]. For instance, CD36 is expressed on macrophages, monocytes, and DCs and is known to be the major SR mediating oxLDL uptake contributing to the formation of foam cells [39]. Apart from this function, CD36 has been reported to function as a co-receptor for TLR-4 signaling and enhance TLR-4-driven cytokine secretion [40].

TLRs belong to the group of pattern recognition receptors, which recognize conserved pathogen-associated molecular patterns (PAMP), and play an important role in initiating innate immune responses [41]. Several TLRs have already been classified according to the PAMP they recognize [42] and their role in atherosclerosis has long been recognized [43]. Apart from PAMP recognition, some TLRs, including TLR-2 and TLR-4 have been described to recognize oxLDL and contribute both to foam cell formation [44] and to modulate cytokine secretion [45]. For example, pre-treatment of macrophages with oxLDL followed by TLR stimulation greatly increased their ability to secrete various pro-inflammatory cytokines [46, 47]

### 1.2. Latest stages of atherogenesis – the vulnerable plaque

Endothelium dysfunction is accompanied by the upregulation of adhesion molecules and recruitment of circulating immune cells (see Chapter 1.4 for further details), which initiate and perpetuate chronic inflammation in growing plaques. SMCs migrate from the media to the outer part of the plaques and contribute to the

formation of a fibrous cap enriched in collagen and proteoglycans [48]. The fibrous cap is the “physical barrier” between the lesion and the circulating blood and its thickness is associated with the appearance of cardiovascular outcomes [48].

As the plaque growths, it becomes more complex. Apart from the thickness of the fibrous cap, other features have already been recognized to contribute to the generation of the so-called “vulnerable plaques”, a term that refers to rupture-prone lesions [49]. Accumulation of immune cells, number of foam cells and disruption of efferocytotic capacities of macrophages (see Chapter 1.4.1.3) lead to the generation of a necrotic core, whose size is associated with a higher risk of cardiovascular disease [50, 51]. Moreover, ongoing inflammation also promotes plaque vulnerability [49] and it might not be surprising that chronic autoimmune disorders, characterized by systemic inflammation, are associated with increased cardiovascular risk [52].

Vulnerable plaques can break and expose their highly thrombogenic content to the blood flow. This interaction promotes the initiation of a coagulation cascade that leads to the formation of blood clots, which are responsible for cardiovascular events by disrupting or blocking the normal blood flow at different locations [53]

A general overview of atherosclerosis is summarized in Figure 3.

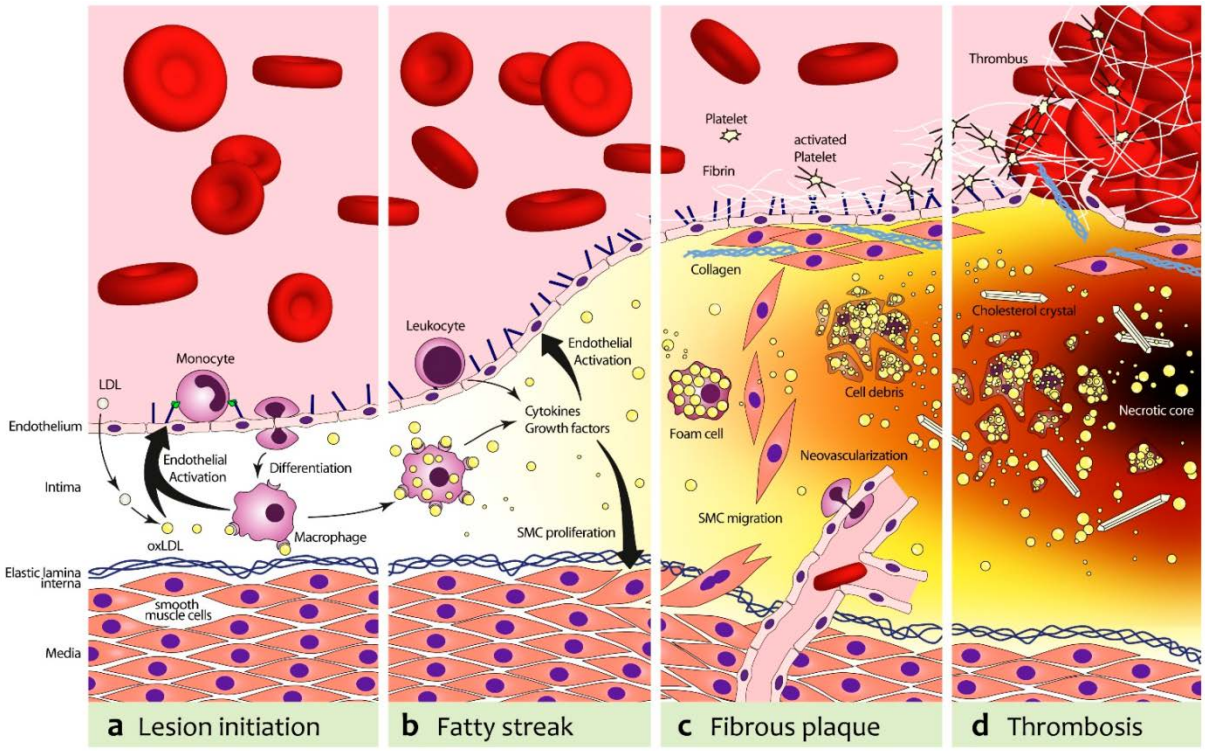


**Figure 3.** A general overview of atherosclerosis. (From [54])

### 1. 3. Animal models to study atherosclerosis: advantages and limitations

The use of experimental models to study atherosclerosis started in 1908, when Ignatowski observed for the first time that feeding rabbits with a full-fat milk, eggs, and meat diet resulted in the appearance of atherosclerotic lesions in the aortic wall [55]. Since then, several animal models have been developed, including mice, rabbits, pigs or non-primate humans [56]. Given their reduced size, easy gene manipulation and development of lesions within a reasonable timeframe, mice remain the most commonly used organism to study atherogenesis.

However, the lipid distribution of mice confers them with a natural protection against the development of lesions. Most of their cholesterol is transported associated with HDL, as opposed to humans, whose cholesterol is mainly associated with the atherogenic particles LDL and vLDL [57]. In fact, low levels of vLDL and LDL are found in unmanipulated mice and thus, genetic manipulation is mandatory to induce atherosclerosis.

Although many others have been described and are available for research, currently there are two major mice lines in use: *Lldr*$^{-/-}$ and *ApoE*$^{-/-}$. The first arises after deletion of the *Ldlr* gene [58]. This deletion is accompanied by increased plasma levels of cholesterol, mainly the LDL fraction, as is the case in humans. Deletion of the *ApoE* gene also increases plasma cholesterol but mainly in the chylomicron and vLDL remnants. Both models show higher levels of plasma cholesterol on a normal diet when compared to wild-type animals and this concentration can be further increased by feeding them with a HFD [57].

The election of *Ldlr*$^{-/-}$ versus *ApoE*$^{-/-}$ mice to study atherosclerosis should be made carefully, as both lines present marked differences (summarized in Table 2). Aged *ApoE*$^{-/-}$ mice develop lesions spontaneously when fed a chow diet, whereas *Ldlr*$^{-/-}$ mice do not. After induction of atherosclerosis with a "Western diet" or HFD, both *ApoE*$^{-/-}$ and *Ldlr*$^{-/-}$ mice develop plaques similarly to humans, although size and complexity are bigger in *ApoE*$^{-/-}$ animals. These two features have made the *ApoE*$^{-/-}$ model the preferred experimental animal in most of the studies that have been published. However, it is noteworthy that, as previously discussed, genetic deletion of *Apoe* is accompanied by an increase in the chylomicron and vLDL remnant, which does not reflect the human case. It might be possible that the atherogenic potential of these lipoproteins might differ from LDL, abundant both in *Ldlr*$^{-/-}$ mice and humans and the molecular mechanisms of atherosclerosis development in *ApoE*$^{-/-}$ mice might not fully reflect the human disease. Moreover, previous studies support a role of *ApoE* as an immunomodulatory agent. For example, it induces an anti-inflammatory phenotype in macrophages [59-61]. Contrary, disruption of the *Ldlr* gene does not alter immune responses [57].

Both *ApoE*$^{-/-}$ and *Ldlr*$^{-/-}$ mouse models have been proved invaluable to study the development of lesions during the course of atherosclerosis but they are not useful to study plaque rupture, one of the most important features affecting cardiovascular outcomes. Another disadvantage is the location where plaques develop. In mice, these locations mainly include the aortic root or the lesser curvature of the aortic arch, whereas in humans most of the clinically relevant lesions are found in coronary arteries [57].

**Table 2**. Principal features of the *ApoE*$^{-/-}$ and *Ldlr*$^{-/-}$ mouse models used to study atherosclerosis.

| | | Mouse model | |
|---|---|---|---|
| | | *ApoE*$^{-/-}$ | *Ldlr*$^{-/-}$ |
| Plasma cholesterol | Normal diet | 400-600 mg/dl | 200-300 mg/dl |
| | Western Diet | >1000 mg/dl | >1000 mg/dl |
| Spontaneous plaque development under normal diet. | | **Yes** | No |
| Human-like lipid profile (↑ LDL) | | No | **Yes** |
| Affection of immune responses | | **Yes** | No |
| Spontaneous plaque rupture | | No | No |

### 1.4. The immune system in atherosclerosis: summary

For many years it was believed that atherosclerosis was merely a passive accumulation of cholesterol in the vessel wall. Today, the picture is more complex and it has become clear that both branches of the immune system, innate and adaptive immune responses, have the ability to modulate the initiation and progression of plaques and even determine their stability [62]. Interestingly, the immune response observed in atherosclerosis sometimes resembles that characterizing autoimmune disorders such as a Crohn´s disease, psoriasis or rheumatoid arthritis. In fact, these patients are at higher risk of cardiovascular events and are known to have accelerated atherosclerosis [63]. Hence, it is not surprising that investigators have postulated an autoimmune nature for atherosclerosis [64], yet current narrative argues for a non-autoimmune condition emphasizing the active inflammatory, complex or multi-factorial and long-term nature of the disease. Understanding the nature and relationship of immune cells and mediators with the aortic environment may impact not only the early and accurate diagnosis but also the development of preventive measures and perhaps more effective therapeutic interventions.

### 1.4.1. Innate Immune responses

#### 1.4.1.1. Monocytes

Monocytes are short-lived cells produced in the bone marrow that circulate throughout the blood. Although their function under homeostatic conditions remains unresolved, they migrate from blood to lymphoid and non-lymphoid tissues in response to tissue-derived signals [65]. During the pathogenesis of atherosclerosis, endothelium dysfunction promote the upregulation of adhesion molecules such as a E-Selectin and vascular cell adhesion protein (VCAM) 1 on the surface of ECs, that act in synergy with chemokines such as CCL2, CCL5, CXCL10 and CX3CL1 to attract circulating monocytes and other immune cells [66, 67]. Once there, the inflammatory milieu determines monocyte fate and their differentiation to macrophages after exposure to EC-secreted macrophage colony stimulating factor (M-CSF) or DCs by exposure to GM-CSF [68].

In mice, two subsets of monocytes have been identified. Ly6C$^{high}$ (CCR2$^{+}$CXC3CR1$^{low}$) monocytes are regarded as "inflammatory monocytes" and give rise to inflammatory macrophages in a variety of infectious models and non-infectious models. The other subset, characterized as Ly6C$^{low}$ (CCR2$^{-}$CXC3CR1$^{high}$), is named "patrolling monocytes" due to their ability to "patrol" the luminal side of the endothelium of small blood vessels under homeostatic and inflammatory conditions [69, 70]. Whether this subset is also able to patrol the endothelium of larger vessels is currently unknown.

The majority of studies point toward a proatherogenic role of both subsets[71], although their contribution to lesion development is different. Ly6C$^{high}$ monocytes, whose numbers are increased under hypercholesterolemia [68], are the first recruited cells in developing plaques, as they strongly adhere to the activated endothelium, infiltrate early lesions and contribute to the expanding foam cell pool by differentiating to macrophages [72]. Ly6C$^{low}$ monocytes are also recruited into plaques, albeit at later stages [73]. Whether they are also able to contribute to foam cell formation is currently unknown.

#### 1.4.1.2. Neutrophils

Neutrophils are the most abundant cell type in the blood and the first cells recruited when tissue is damaged [74]. For many years, their role in atherosclerosis has been underappreciated, maybe due to initial studies showing a sparse number in human and mouse plaques [75]. However, specific neutrophil depletion in *ApoE*$^{-/-}$ mice fed a HFD resulted in significantly reduced plaque size at early stages of lesion formation [76]. In humans, the accumulation of neutrophil mediators in rupture-prone areas has been associated with plaque instability [77, 78]. In fact, leukocytosis (specifically neutrophilia) is an independent risk factor for cardiovascular diseases [79].

The role they play in the development of atherosclerosis is proatherogenic. They can impact lesion development by different mechanisms. For example, recruitment of neutrophils into developing plaques increases the recruitment of monocytes and accelerates plaque growth [76]. Production of great amounts of ROS is also a hallmark of neutrophils. This production has been reported to increase the oxidation of the LDL trapped within the intima [80] and favors the formation of foam cells [81-83]

#### 1.4.1.3. Macrophages

Macrophages constitute a complex subset with the ability to trigger many different responses depending on the environment surrounding them [84]. They represent the most abundant cell type in human and murine plaques and their important role throughout the whole process of lesion development has quickly been recognized [85].

Induction of monopoiesis by HFD is known to promote the recruitment of Ly6C$^{high}$ monocytes into developing plaques and generate inflammatory macrophages. A long stand paradigm has assumed that most of the aortic macrophages are in fact derived from circulating monocytes [85], although recent studies have provided new evidence that resident aortic macrophages have the ability to self-renew under homeostatic conditions [86]. However, as in the case of vascular resident DCs (see Chapter 1.4.1.4), their role under non-inflammatory conditions remains poorly understood.

Apart from their ability to convert into foam cells that contribute to the cell load in advanced plaques (see Chapter 1.2), macrophages are also able to phagocyte apoptotic and necrotic cells and as a response, secrete a broad range of cytokines with a

profound impact on plaque stability. Engulfment of apoptotic cells, a process known as efferocytosis, is known to induce an anti-inflammatory phenotype in macrophages by secreting IL-10 or transforming growth factor (TGF)-β, cytokines with known anti-atherogenic functions, and described to accumulate mainly at early stages of the disease [87]. The progressive accumulation of cells and lipids in the intima promotes reduced oxygen and nutrient supply. Cell death under these conditions is mainly dominated by necrosis rather than apoptosis. Engulfment of such necrotic cells by macrophages polarize them toward a pro-inflammatory phenotype [88].

#### 1.4.1.4. Dendritic cells

DCs are the most important population of cells among APCs [89]. During the steady state, immature DCs have the ability to capture and process antigens and patrol tissue to maintain homeostasis. After activation, they upregulate several chemokine receptors, lose their ability to capture antigens and migrate to lymph nodes, where they mount adaptive immune responses by presenting antigens to T cells and secrete a variety of different cytokines [90].

Ralph Steinman and Zanvil Cohn isolated DCs for the first time [91-93]. Since their discovery, many different subsets have been described to exert a unique set of activities depending on their location [89]. DCs arise in the bone marrow from a common myeloid progenitor, which give rise to a macrophage and DC precursor. It is now well accepted that the latter further differentiate either into monocytes, which can differentiate into monocyte-derived macrophages and DCs under the influence of M-CSF or GM-CSF [90], respectively or into a common DC precursor (CDP). CDP gives rise to plasmacytoid DCs (pDCs) or pre-DCs, which leave the bone marrow and generate cDCs that can be segregated into cDCs1 and cDCs2 [90]. Two types of cDCs1 have been described, one expressing CD8α, present in lymphoid tissues, and another characterized by the expression of CD103, the counterpart of CD8α in non-lymphoid tissues [94].

Opposed to monocytes and macrophages, both pDCs and cDCs rely on the presence of the FMS-like tyrosine kinase 3 ligand (Flt3L) for their development [90]. In past years, many studies have tried to characterize the expression pattern of specific

surface markers as well as unique transcription factors controlling the development of different subsets of DCs. A recent paper by Guilliams et al. [95] has provided a valuable approach to differentiate DCs among other subsets using flow cytometry. His study identified DCs as CD11c$^{+}$MHC-II$^{+}$CD26$^{+}$CD64$^{-}$F4/80$^{-}$, which allow further identification of cDCs1 by the expression of XCR1 and cDCs2 by the expression of Sirpα (CD172). pDCs are also defined as CD11c$^{+}$MHC-II$^{+}$ but can be distinguished from cDCs by their expression of B220 or Siglec-H. Next-generation sequencing and lineage-tracing studies have been performed focusing on the gene expression pattern and ontogeny to identify markers differentially expressed by distinct DCs population [96]. For example, the transcription factor zinc-finger transcription factor zDC (Zbtb46) has been identified to be expressed only in cDCs but not pDCs [97]. Moreover, recent reports revealed that BATF, interferon-regulatory factor (IRF) 8 and DNA-binding protein inhibitor 2 are essential regulators of cDCs1 development, whereas cDCs2 are dependent on the transcription factor RELB, recombining binding protein suppressor of hairless and IRF4 [90].

#### 1.4.1.4.1. Redefining dendritic cells as antigen presenting cells in atherosclerosis

Most of the studies aiming to decipher the role of DCs in health and disease rely on the use of surface markers and functional traits to differentiate them from macrophages or monocytes. For instance, CD11c is commonly referred to as a DC marker, whereas macrophages are described to mostly express CD11b, F4/80 and CD64 and be CD11c$^{-}$. Functionally, CD11c$^{+}$ cells in the aorta have been reported to have a potent antigen-presenting ability, thus resembling DCs [98], whereas CD11c$^{-}$CD11b$^{+}$cells efficiently take up lipids and resembled macrophages [94]. Noteworthy, it is now evident that CD11c is not restricted only to DCs but it can also be expressed by other cell types including monocytes and macrophages [99]. In fact, CD11c is upregulated under inflammatory conditions and is highly expressed by inflammatory macrophages [99]. Moreover, experimental models in which CD11c was depleted showed impaired responses not only restricted to “DCs” but also to other cell types, such as macrophages [99]. Studies using CD11c-depletion strategies or referring CD11c-expressing cells as “DCs” might be masking the effect of other CD11c-expressing population, including monocytes and macrophages, which also share antigen-presentation capabilities. We

here refer to CD11c-positive cells as APCs when a clear distinction from *bona fide* DCs is unclear.

#### 1.4.1.4.2. Antigen-presenting cells in atherosclerosis

APCs can be found in the aortic intima in the steady state [90]. Although it is still not clear what the major function of this subset is under homeostatic conditions, a recent report has highlighted that $CD11c^+$ APCs have the ability to capture antigens in the aorta, migrate into the lymph nodes and start an adaptive immune response [100], a process that is disrupted under hypercholesterolemia [94].

Increased numbers of APCs in the aorta have been reported in mice fed a HFD [101]. Given the presence of several DCs/APCs subsets with a unique ability to secrete cytokines and promote Th responses, which itself can impact on the development of atherosclerosis, (see Chapter 1.4.2.1.2), DCs/APCs have been rapidly recognized as a promising therapeutic target in the clinic.

Initial studies using CD11c-diphtheria toxin receptor (DTR) animals, in which $CD11c^+$ APCs can be depleted after injection of the diphtheria toxin, resulted in increased plasma cholesterol levels and it was suggested that APCs might play a role in lipid metabolism [102]. These results were partially supported by studies showing that hypocholesterolemia increased lifespan in APCs [102]. Whether DCs or macrophages were responsible for this phenotype is not clear. A recent report attempting to delete *bona fide* DCs (by disrupting the *Zbtb46* gene) have failed to report any differences in cholesterol levels in Zbtb46-DTR mice compared to control mice after feeding a HFD, although depletion of DCs was incomplete in the long term [103]. Thus, the exact cell type involved in cholesterol metabolism is still unknown.

How DCs modulate the pathogenesis of atherosclerosis depends on the subset studied. For example, pDCs are proatherogenic [90]. However, the exact contribution of cDCs during atherogenesis remains elusive.

#### 1.4.1.4.3. Current knowledge about Batf3-dependent dendritic cells in atherosclerosis

Hilder et al. were the first proving evidence that BATF3 was a critical factor in the development of CD8α$^+$ and CD103$^+$ cDCs1 [104]. In this study, specific deletion of *Batf3* was accompanied by a loss of both of these cell types in lymphoid tissues without any abnormalities among other immune cells. CD8α$^+$ and CD103$^+$ cDCs1 are well known to mediate antigen cross-presentation, a mechanism by which DCs retain the ability to present extracellular antigens bound to MHCI and to promote cytotoxic T cell responses [105]. In line with this property, *Batf3*$^{-/-}$ animals showed impaired CD8$^+$ T cell responses [104]. Apart from this ability, CD103$^+$ cDCs1 have been described to promote $T_{reg}$ responses and their depletion has been associated with a favorable outcome after infection [106]. Intriguingly, CD103$^+$ cDCs1 are also the major producers of IL-12 during infection and able to induce $Th_1$ responses, resulting in pathogen clearance. [107]. These opposing mechanisms have focused the attention on Batf3-dependent DCs as a possible mediator in atherogenesis.

The first indirect report suggesting a role in atherosclerosis came from the study of Choi et al. using *Ldlr*$^{-/-}$*Flt3*$^{-/-}$ mice [98]. They reported that in the aorta, cDCs1 expressed CD103 but not CD8α. When fed a HFD, Flt3-deficient mice presented with an increased lesion size. This phenotype was accompanied by a reduced number of aortic CD103$^+$ cells in *Ldlr*$^{-/-}$*Flt3*$^{-/-}$ mice and reduced frequencies of $T_{regs}$ in the aorta, suggesting a protective role of Batf3-dependent DCs in atherosclerosis. However, two recent reports have provided conflicting results. Legein B. et al. reported that lethally irradiated *Ldlr*$^{-/-}$ mice reconstituted with bone marrow of *Batf3*$^{-/-}$ animals showed impaired cross-presentation [108]. However, when fed a HFD, *Ldlr*$^{-/-}$→*Batf3*$^{-/-}$ mice showed similar lesion size as compared to *Ldlr*$^{-/-}$→*Ldlr*$^{-/-}$ [108] suggesting a non-relevant role of Batf3-dependent DCs. More recently, Li Y and colleagues [109] reported a strong proatherogenic role of Batf3-dependent DCs by using *ApoE*$^{-/-}$*Batf3*$^{-/-}$ mice. In their study, *ApoE*$^{-/-}$*Batf3*$^{-/-}$ fed a HFD showed greatly decreased lesion development which was accompanied by decreased $Th_1$ responses [109]. The authors hypothesized that Batf3-dependent DCs might promote the induction of $Th_1$ responses by the

described ability of $CD103^+$ DCs to secrete IL-12. Hence, the exact role of this subset remains to be elucidated.

### 1.4.2. Adaptive immune responses

#### 1.4.2.1. T cells

T cells are lymphocytes belonging to the adaptive branch of the immune system characterized by the expression of a T cell receptor (TCR) on their surface, which is linked with the adaptor molecule CD3ε, needed for intracellular signaling upon antigen encounter. All types of T cells arise in the bone marrow from a hematopoietic stem cell precursor and migrate to the thymus to undergo maturation. Newly arrived T cells (known as thymocytes) lack the expression of both CD4 and CD8 and are referred to as double negative (DN) thymocytes. At this stage, DN thymocytes rearrange genes encoding for the TCR giving rise to αβ TCR-bearing T cells (αβ T cells), constituting around 95% of rearrangements, or γδ TCR-bearing T cells (γδ T cells), which represents less than 5% of total cells [110]. After expression of a TCR, DN cells upregulate the expression of CD4 and CD8 and become double positive (DP) thymocytes, which are first positively selected to remove unproductive TCR rearrangements and later negatively selected to deplete T cells bearing a TCR with the ability to recognize self-peptides [110]. After negative selection, thymocytes become single positive cells expressing either CD4 or CD8 giving rise to $T_h$ cells or cytotoxic cells, respectively.

Together with macrophages, T cells constitute the most abundant cell type in developing plaques [111] and a myriad of studies have been trying to decipher their contribution to the pathogenesis of atherosclerosis.

##### 1.4.2.1.1. $CD8^+$ T cells

$CD8^+$ T cells become effector cytotoxic T lymphocytes (CTLs) after a naïve antigen-specific $CD8^+$ T cell encounters antigens presented by APCs bound to MHCI. The mechanisms by which CTLs kill their target include the release of the pore-forming proteins, namely perforins, together with serine proteinases known as granzymes, which induce apoptosis of the target cell, as well as the production of several cytokines, including TNF-α and interferon (IFN) γ.

How classical effector $CD8^+$ T cells modulate plaque progression is still under debate, as current literature has provided conflicting results. $CD8^+$ T cells are known to be present in human and mouse plaques [112, 113] and recruited at different stages of the disease [114] preferentially at later stages [115]. Analysis of plaque $CD8^+$ T cells has also revealed that this population is highly activated when compared to plaque $CD4^+$ T cells [116, 117]

Initial characterization using *ApoE*$^{-/-}$*CD8*$^{-/-}$ mice fed a chow diet for 18 weeks and 1 year have demonstrated that lesion size was unaltered when compared to *ApoE*$^{-/-}$ controls, suggesting a non-relevant effect of this population in the development of atherosclerosis [118]. These studies have been supported by other groups using indirect mechanisms to block MHCI-dependent responses and thus, blocking $CD8^+$ T cell responses [108, 117]. On the contrary, two independent reports using a depletion strategy using antibodies directed against CD8α or CD8β recently have pointed out a proatherogenic role of this subset [119, 120]. Both studies have shown that decreased lesion size was accompanied by decreased macrophage content and necrotic core size and it was revealed that $CD8^+$ T cells play an important role in inducing monopoiesis. Finally, evidence suggests that cytokines released by $CD8^+$ T cells, such as INF-γ, might exert proatherogenic functions [114].

Although this conflicting data might be explained by the use of different animal models, technical approaches, time point used to study plaque development and possibly compensatory mechanism involving $CD4^+$ T cells [121], another plausible explanation might be related with the discovery of a new subset of $CD8^+$ T cells with immunosuppressive properties [122], which has been clearly identified to have a protective role in atherosclerosis [123]. Depletion of total $CD8^+$ T cells might destroy not only effector cells with proatherogenic properties but also a protective population which finally could results in a non-relevant function of $CD8^+$ T cells in atherosclerosis, in line with initial studies.

#### 1.4.2.1.2. $CD4^+$ T cells

$CD4^+$ T cells, also known as $T_h$ cells, become mature after recognizing antigens presented via MHCII by APCs. Antigen-specific $CD4^+$ T cells polarize into different subpopulations, $Th_1$, $Th_2$, $Th_{17}$, $T_{regs}$, among others, depending on the cytokine milieu surrounding them (summarized in Figure 4). Each of this $T_h$ subset has a profound impact on immune responses, as they play different roles in many processes such as isotype class switching by B cells, activation and growth of CTLs and maximizing the bactericidal activity of macrophages [124].

##### 1.4.2.1.2.1. $Th_1$ and $Th_2$ cells

$Th_1$ cells are characterized by the expression of the transcription factor TBET and require the presence of IL-12 and IL-18 provided by APCs to fully differentiate [125]. Most of the T cells present in plaques are $CD4^+$ T cells that present a $Th_1$-like phenotype [126]. $Th_1$ cells are characterized by the release of IL-2 and, most notably, IFN-γ. Most, if not all, of their proatherogenic role, has been attributed to the latter [111, 127].

Initial experiments using *ApoE*$^{-/-}$*Ifng*$^{-/-}$ mice fed a HFD for 12 weeks revealed that lack of IFN-γ greatly reduced plaque size [128] whereas injection of exogenous IFN-γ aggravated atherosclerosis in ApoE-deficient mice [129]. IFN-γ aggravates lesion growth by different mechanisms. For example, it promotes activation of plaque macrophages leading to the production of pro-inflammatory cytokines, matrix metalloproteinases and ROS [130]. In vitro experiments have also reported a disruption in cholesterol efflux [131], which translated into increased macrophage foam cell formation. Moreover, it is well known that IFN-γ affects different properties of SMCs. For example, it inhibits their proliferation and reduces their collagen production while upregulating the expression of matrix metalloproteinases, mechanisms that contribute to a thinning of the fibrous cap [130]

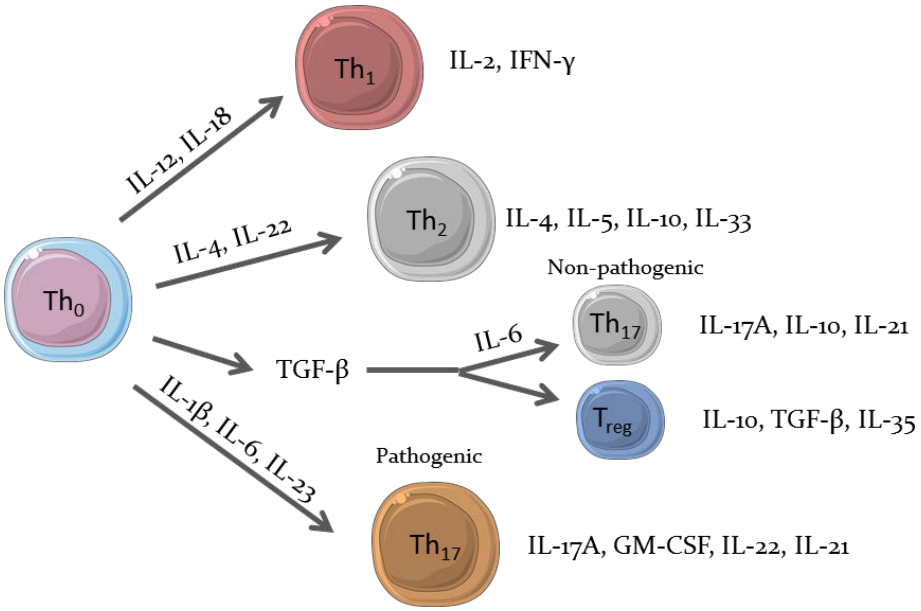


**Figure 4. Different subsets of $CD4^+$ $T_h$ cells.** Depending on the cytokine milieu provided by the environment (mainly APCs), $CD4^+$ T cells give rise to different subsets that secrete prototypical cytokines.

Polarization into the $Th_2$ lineage relies on the transcription factors GATA3 and STAT5, which are upregulated in naïve T cells in the presence of IL-4. The prototypical cytokine produced by this subset is IL-4, known to impede the production of IFN-γ [132]. This ability was initially hypothesized to infer a protective role in the development of atherosclerosis. Recent human studies have supported this idea, as increased $Th_2$ responses in peripheral blood have been linked with decreased carotid intima-media thickness and decreased risk of developing acute myocardial infarction in women [133]. However, studies in mice have shown conflicting results. Victoria L. Kind and collages studied the effect of exogenous IL-4 administration in *ApoE*$^{-/-}$ mice fed a HFD and reported no differences in plaque size when compared to *ApoE*$^{-/-}$ animals receiving a saline solution [134]. Moreover, they also analyzed the impact of *Il4* deficiency in *ApoE*$^{-/-}$ mice fed a HFD and obtained similar results as when IL-4 was administered. Contrarily, a later study using a full *Il4*$^{-/-}$ mouse model revealed that deletion of *Il4* decreased atherosclerosis lesion burden in *Ldlr*$^{-/-}$ mice fed a HFD [135]. IL-4 can promote both pro-atherogenic signals (by upregulating P-selectin or VCAM in ECs ([136],[137]) as well as anti-atherogenic signals (by inhibiting SMC proliferation and reducing macrophage adhesiveness ([138],[139], respectively). Given that $Th_2$ cells

are scarce in human plaques [126], their relevance in the human diseases requires further studies.

Animal models studying the role of the other $Th_2$-cytokines, such as IL-5 and IL-33, have revealed that deficiency in any of these cytokines greatly increased plaque size ([140],[141], respectively) due to a decreased ability of B-1 cells to produce anti-oxLDL IgM antibodies, known to be protective [142].

#### 1.4.2.1.2.2. Regulatory T cells

$T_{regs}$ are well known negative regulator of immune responses. They can be differentiated into naturally occurring $T_{regs}$ and inducible $T_{regs}$. The former arise in the thymus from developing thymocytes, whereas the latter are produced in the periphery from circulating naïve T cells and constitute one of the mechanisms of peripheral tolerance [143]. Naïve T cells acquire regulatory properties by exposure to TGF-β and upregulation of the transcription factor forkhead-box-protein 3 (FoxP3). They control immune response by cell-cell interactions, by engaging programmed cell death (PD) ligand 1 (PD-L1) expressed by $T_{regs}$ and PD-1 expressed by T cells or other effector cells, or by the secretion of immunosuppressive cytokines such as a TGF-β and IL-10 [143].

$T_{regs}$ are found in human and mouse lesions [111], albeit at lower percentages when compared to other tissues in chronic inflammatory conditions [144]. This observation led researchers to wonder if impairment of local tolerance against potential antigens in atherosclerotic lesions is a cause of inflammation and plaque formation, a mechanism described for many autoimmune disorders [145].

Many different studies have shown that their role in atherosclerosis is protective. Studies in human have shown a link between reduced numbers of peripheral $T_{regs}$ and increased frequencies of myocardial infarcts and other coronary events [146]. Neutralization of the $T_{reg}$-associated marker CD25 with anti-CD25 in *ApoE*$^{-/-}$ mice fed a HFD greatly increased lesion development [147] and adoptive transfer of $CD25^+FoxP3^+$ $T_{regs}$ decreased plaque burden in *ApoE*$^{-/-}$ animals [148]. Furthermore, *ApoE*$^{-/-}$ mice with a genetic deletion of the *Il10* gene showed increased atherosclerotic plaque when compared to wild-type (WT) mice [149]. Studies testing the role of TGF-β showed similar results [150].

But if they have anti-atherogenic properties, why do plaques progress? For example, $T_{regs}$ inhibit $Th_1$ polarization. As previously introduced (see Chapter 1.4.2.1.2.1), secretion of IFN-γ by $Th_1$ cells is strongly proatherogenic and we could expect that the immunosuppressive action of $T_{regs}$ may inhibit the negative impact of this cytokine. However, under conditions of hyperlipidemia, numbers of plaque $T_{regs}$ decrease overtime [151], favoring the generation of pathogenic $Th_1$ responses [152]. Moreover, the suppressive capacity of $T_{regs}$ derived from *ApoE*$^{-/-}$ mice has been reported to be compromised compared to cells derived from their WT littermates [148]. Finally, another report suggested that $T_{regs}$ might control lipid metabolism, as chimeric *Ldlr*$^{-/-}$ mice reconstituted with FoxP3-deficient bone marrow developed not only aggravated atherosclerosis but also hypercholesterolemia [153].

#### 1.4.2.1.2.3. Th17

Induction of $Th_{17}$ responses requires the activation of the transcription factor RAR-related orphan receptor gamma (RORγ). Although it is widely accepted that polarization into a Th17 phenotype requires the presence of TGF-β and IL-6, it is becoming evident that this pathway gives rise to a non-pathogenic subset with a protective potential and needed for maintaining tissue homeostasis (see below). On the contrary, naïve T cells have been reported to acquire a pathogenic phenotype in a TGF-β-independent mechanism when exposed to a cytokine cocktail composed of IL-1β, IL-6, and IL-23 [154], the latter being the most important mediator to induce pathogenesis in this subset (see Chapter 1.5.1). $Th_{17}$ cells are known to play an important role in the defense against extracellular pathogens but also to be a key player in the development of autoimmune diseases, including psoriasis, rheumatoid arthritis and Crohn´s disease [155].

The most studied $Th_{17}$ cytokine in the context of atherosclerosis is IL-17A. Initial studies using the *ApoE*$^{-/-}$ mouse model revealed that aged and HFD-fed mice increased IL-17A production in γδ T cells [156]. Treatment of human monocyte-derived DCs or mouse bone marrow-derived APCs (BM-APCs) with oxLDL skewed T cell polarization into a $Th_{17}$ phenotype ([157],[158], respectively), which suggests a role of IL-17A-producing cells in atherosclerosis. Given their pro-inflammatory potential, IL-17A was initially hypothesized to negatively impact atherogenesis. However, experimental

models of atherosclerosis studying IL-17A have yielded contradictory results ranging from decreased, unchanged or even increased plaque burden (reviewed in [156]). Other approaches using neutralization of IL-17A have resulted in comparable results as observed in full knock out models [156]. With regards to plaque stability, most studies have revealed that IL-17A might promote plaque instability (summarized in [159]). Thus it is difficult to finally conclude whether IL-17A might modulate lesion development or rather modify features of plaque stability.

Apart from IL-17A, both non-pathogenic and pathogenic-IL-17-producing T cells also secrete other cytokines, which have been proved to exert independent effects in atherosclerosis. Among others, IL-21 and IL-22 appear to be produced by both subsets [155] whereas other such as GM-CSF, IL-6 and IFN-γ seem to be restricted to the pathogenic subset [160].

A recent report studying CAD patients reported a positive relationship between increased serum levels of IL-21 and risk of CAD [161]. One study using *Il22*$^{-/-}$*ApoE*$^{-/-}$ mice revealed that IL-22 may play a proatherogenic role, as *Il22* deficiency showed reduced plaque size when compared to WT controls [162]. Finally, *Ldlr*$^{-/-}$*Cfs2*$^{-/-}$ (lacking GM-CSF) animals fed a HFD showed decreased atherosclerosis burden in the root [163]. The proatherogenic role of GM-CSF was also reported in humans after administration of GM-CSF to patients with stable coronary artery disease, as several of the subjects suffered acute coronary events [164]

Altogether these results suggest that $Th_{17}$ cells might exert both pro- and anti-atherogenic properties and that these differences might be attributable to the newly recognized pathogenic and non-pathogenic properties.

**1.4.2.1.3. γδ T cells**

As introduced earlier, γδ T cells also arise from the thymus but they differ from conventional αβ T cells in the chains composing their TCR, which is formed by the rearrangement of a γ and δ chain [165]. This population shares some of the classical properties of cells from the adaptive immune system (recognition of MHC-bound antigens, dependence on several activation signals) but also that of innate immune

cells (MHC-independent activation, quick responses), the reason why they are sometimes referred as innate-like cells [166].

Unlike αβ T cells, which exit the thymus and migrate to lymphoid organs, γδ T cells preferentially migrate to tissues and become resident cells [165], where they function more as innate rather than adaptive immune cells. In fact, due to their limited TCR diversity and a limited antigen repertoire, specific subsets of TCR-restricted γδ T cells populate specific niches throughout the body. For example, $V\gamma_9V\delta_2$ constitute the vast majority of peripheral blood γδ T cells in humans [165], whereas in mice, $V\gamma_3V\delta_1$ dendritic epidermal γδ T cells constitute a well-described population in the skin of rodents [167].

Although γδ T cells are an important source of cytokines, they cannot be easily classified. They can secrete IFN-γ, TNF-α, granzyme or IL-17A, among others [166] and this ability might be restricted to a specific subset, which is directly correlated with its localization in the body [166].

IL-17-producing γδ T cells ($\gamma\delta_{17}$ T cells) have long been recognized to be an important source of IL-17 in several compartments [168]. More importantly, these cells are the most prominent IL-17-producing cell type during acute infection, as conventional $Th_{17}$ cells require antigen priming, whereas γδ T cells do not [168]. This ability seems to be restricted to activated $V\gamma_2/V\gamma_4$ $CD44^{high}IL\text{-}23R^{+}CD62L^{-}$ γδ T cells[168], which raises the possibility that either IL-17-producing γδ T cells might have previously encountered the antigen or that they are committed to produce IL-17 already during their development [165].

In the context of atherosclerosis, little is known about the exact role of γδ T cells. Several studies have reported the presence of γδ T cells in human [169] and mouse atherosclerotic plaques [170]. Using experimental models it has been shown that they represent more than 50% of IL-$17^{+}$ T cells [171]. However, these studies have not characterized which population predominates in the aorta and it is unknown whether more than one subset is present at this location with different capabilities to modulate atherosclerosis.

The highest percentage of γδ T cells in the aorta has been reported to be at early stages of atherosclerosis [172] and two studies in mice have shown that their number increases under HFD regimens [170, 173]. These initial findings led researchers to propose a possible role of this subset during the early phase of atherogenesis. One study using *ApoE*$^{-/-}$*Tcrg*$^{-/-}$ mice has shown that these mice presented similar lesion size compared to the control group after fed a chow diet for 10 weeks [170], pointing out a non-relevant function in atherosclerosis. Surprisingly, a later study using the same experimental model but studying early time point of plaque formation has proposed a proatherogenic role of γδ T cells, as mice fed a HFD for 4 weeks showed decreased lesion size specifically in the arch, but not in the aortic root [173]. New studies are needed to fully elucidate the contribution of this cell type to the pathogenesis of atherosclerosis.

### 1.5. The IL-12 family of cytokines: focus on IL-23

The IL-12 family of cytokines is composed of several molecules resulting from the binding of an α-chain (p19, p28, and p35) and a β-chain (p40 and Epstein-Barr virus-induced gene 3 (Ebi3)). There are currently six members described, IL-12 (p40/p35), IL-23 (p40, 19), IL-27 (Ebi3/p28), IL-35 (Ebi3/p35) [174] and IL-39 (p19/Ebi3) as the newest addition [175].

Produced by different immune cell types, they have the ability to impact immune responses either by inducing inflammation (e.g. IL-12, IL-23 or IL-39) or by dampening immune responses (IL-27, IL-35) [174], which greatly depend on T cell polarization (as summarized in Figure 4). For instance, IL-12 is produced by DCs, macrophages and B cells and is required to generate $Th_1$ responses, whereas IL-35 is secreted by naturally-occurring $T_{regs}$ and inhibits T cell proliferation [176].

The p19 subunit was initially discovered computationally [177] and gave rise to the discovery of the already mentioned par p40/p19, known as IL-23. First attempts to characterize p19 expression revealed that the most abundant expression was found in ECs, activated macrophages or DCs and polarized $Th_1$ and $Th_2$ subsets [177]. However, only some activated APCs co-express also p40 and are currently the only known cell type to secret active IL-23 upon stimulation [177]. Why some cells produce only the p19

subunit but not p40 it still unclear. Recent evidence suggest that, although the initial study from Oppmann et al. described that only p40/p19 composites are secreted and exert biological responses, the p19 subunit may, in fact, work as an intracellular peptide. For example, Espígol-Frigolé et al. have demonstrated that overexpression of p19 in ECs led to the upregulation of several adhesion molecules such as intercellular adhesion molecule (ICAM) 1 and VCAM-1 [178]. As shown earlier, ECs do not have the ability to secrete p40 and cannot release IL-23. However, the authors showed that p19 exerts intracellular signaling by binding to gp130 and thus, unraveled a new potential therapeutic approach for giant-cell arteritis and another inflammatory-related disease such as atherosclerosis. These results also suggest that the use of the *Il23a*$^{-/-}$ mouse model could not only impact the release of IL-23 by APCs but could also affect other biological mechanisms driven by the p19 subunit.

In vitro cultures, mostly those using GM-CSF to generate inflammatory APCs, have been frequently used to study the differential regulation of each member of the IL-12 family. Of note, IL-23 has been reported to be expressed by macrophages in vivo [179] but M-CSF cultures have revealed that these cells cannot secret IL-23, presumably due to the presence of IL-10 [180]. In vitro conditions can also affect IL-23 secretion by BM-APCs. As an example, culture of bone marrow precursors in the presence of both GM-CSF and IL-4 has been described to dampen IL-23 release [181].

In vitro secretion of IL-12 and IL-23 depends on different TLR agonists. While single TLR stimulation is enough to induce secretion of IL-23, a combination of different TLR agonists are needed to promote IL-12 secretion [181]. In monocyte-derived DCs, stimulation of TLR-2, TLR-4 or TLR-7/8 has been shown to induce the expression of the p19 and p40 subunit, leading to the formation and secretion of IL-23, which can be enhanced by the addition of IFN-γ [181]. However, transcription of the p35 units requires a combination of several TLR-agonists. These observations reflect a time-dependent regulation of each cytokine by APCs which might adapt immune responses upon different challenges.

IL-23 signals through its receptor IL-23R, which comprises the subunit IL-12Rβ1 shared with the IL-12R complex and the unique subunit IL-23R, where p19 binds [182].

Both IL-12 and IL-23 activates the Janus kinase (JAK) and tyrosine kinase (TYK) 2 signaling pathways, which lead to the phosphorylation of different STAT members and promote different biological responses. IL-12 primarily acts through STAT4 whereas IL-23 mainly activates STAT3 [183]. Differences in the expression of IL-12Rβ1, IL-12Rβ2, and IL-23R determine the responsiveness of different immune cells to IL-12 and IL-23.

### 1.5.1. IL-23 induces pathogenicity in IL-23-responding T cells

As introduced in Chapter 1.4.2.1.2.3, polarization into a $Th_{17}$ phenotype can be achieved after exposure to two main different cytokine cocktails, which in turn will determine the pathogenic fate of the cells. Naive T cells differentiate into a host-protective or non-pathogenic $Th_{17}$ subset when exposed to TGF-β and IL-6 [184]. This non-pathogenic subset is characterized by the expression of IL-17 and IL-10 and plays an important role in host defense against pathogens. Exposure to IL-23 gives rise to highly inflammatory or pathogenic $Th_{17}$ subsets with the ability to secrete IL-17, IL-22, GM-CSF, and co-expression of IFN-γ [184].

Apart from $Th_{17}$ cells, other cells expressing the transcription factor RORγ can respond to IL-23. For example, γδ T cells [168], NKT cells [185], natural $Th_{17}$ [186, 187] and innate lymphoid cells [188] rapidly respond to IL-23 due to the expression of the IL-23R. More recently, a subset of myeloid cells in lymph nodes defined as $CD11c^+$ "DCs" or $CD11b^+$ macrophages, has been reported to express both IL-23R and RORγ and respond to IL-23 binding [189].

Although non-pathogenic $Th_{17}$ cells can acquire a highly inflammatory phenotype after exposure to IL-23, naïve T cells have also been reported to directly generate a pathogenic phenotype in a TGF-β-independent manner after exposure to the cytokine cocktail IL-6, IL-1β and IL-23 [154]. IL-23 triggers a STAT3-dependent signaling cascade, which leads to the stabilization of the $Th_{17}$-signaling signature (*Rorc*, *Il17a*), downregulation of other lineage-genes (aryl hydrocarbon receptor (*Ahr)*, *Il10*, *Il2*, *Il27*, *Il12)* and upregulation of pathogenic genes including *Il22*, *Cfs2* and *Ifng* [184]. Of note, the presence of double positive $IL\text{-}17A^+IFN\text{-}\gamma^+$ cells is a hallmark of many autoimmune diseases [190] and has been described in the artery wall of human plaques to play a pro-inflammatory role by activating vascular SMCs [191].

### 1.5.2. IL-23 as an apoptotic-mediator

Apart from its well-known role in inducing pathogenic responses, IL-23 has also been described to induce apoptosis in mammalian cells lines [192] as well as in several immune cells. Cocco C. and colleagues were the first suggesting a link between IL-23 and apoptosis. By studying human primary B-acute lymphoblastic leukemia cells they observed an up-regulation in IL-23R expression, which enhanced IL-23-induced apoptosis by altering miR15 and down-regulating the anti-apoptotic signal B-cell lymphoma 2 (Bcl2) [193]. In an elegant study, Li H et al. described that IL-23 could mediate depletion of self-reactive DP thymocytes during negative selection in mice. Interestingly, this subset expressed IL-23R and could respond to IL-23 in a TCR-dependent manner by upregulating *Rorc* and decreasing the proto-oncogene *c-rel*, which led to enhanced apoptosis [194]. In a similar way, another study provided evidence that IL-23 increased cell death susceptibility in 7-ketocholesterol or oxLDL-treated BM-ACPs and bone marrow-derived macrophages (BMDM). The proposed mechanisms involved an interaction between IL-23 and IL-23R, which results in decreased levels of the anti-apoptotic signal Bcl2 [179]. Finally, a recent study has highlighted that overexpression of IL-23 in a reperfusion model increased apoptosis of cardiac tissue [195]. These studies suggest two different signaling cascades in IL-23R expressing cells: 1) inducing IL-23-dependent cytokines, as previously mentioned, such as IL-17, IL-22 or GM-CSF and 2) altering *Bcl2* mRNA levels, which might increase apoptosis susceptibility in several immune cells. Understanding how IL-23 might induce different signaling pathways depending on the environment might be of particular relevance, as several antibodies against the p19 subunit of IL-23 have been – or are being- tested as a therapeutic target for the treatment of psoriasis or Crohn's Disease [183].

### 1.5.3. Current knowledge of IL-23 and IL-23R in cardiovascular diseases

The direct contribution of IL-23 and IL-23R to atherosclerosis remains to be fully elucidated, although several studies have already proposed a link between both molecules in cardiovascular diseases. Increased plasma or serum levels of IL-23 have been reported by David et al. in a study comparing patients affected with PAD [196] and also by Abbas et al. when comparing patients with carotid atherosclerosis versus

healthy controls [197]. The study from Abbas further showed that plaques contained a sustained amount of IL-23 and IL-23R that were co-localized with $CD68^+$ macrophages. Furthermore, levels of circulating IL-23 were also associated with mortality. On the other hand, a report investigating Iranian patients affected with CAD reported that un-stimulated peripheral blood mononuclear cells (PMBCs) from CAD patients, showed less *Il23a* mRNA transcripts and this was associated with a decreased risk of CAD [198]. Using an experimental model of stroke, Gelderblom et al. recently reported that cDCs2 infiltrating the ischemic tissue were the major source of IL-23, which promoted the production of IL-17A by IL-23R-bearing γδ T cells in the brain. As a consequence, the number of infiltrating neutrophils was reduced both in CD11c-deficient mice and in *Il23r*$^{-/-}$ mice [199].

The role of IL-23R in cardiovascular diseases has been less studied. Three single nucleotide polymorphisms (SNPs) for IL-23R, rs6682925T/C, rs1884444 T/G and rs1109026 A/G (R381Q) have been reported. The former has been described to increase the relative abundance of mRNA levels of *Il23r,* whereas the two last presumably affect the signaling pathway and promote alternative splicing [200, 201]. Zhang et al. reported that the rs6682925T/C SNPs was overrepresented in CAD patients from China and represented an independent risk factor to develop CAD, especially in patients with hypertension [202]. Moreover, patients bearing this SNP had increased levels of mRNA of *Il23r* and thus pointed out that overexpression of IL-23R might have a negative impact on CAD. On the contrary, no association was found with regards to the rs1884444T/G SNP [202].

The R381Q polymorphism has been extensively studied and is associated with increased risk of developing Crohn´s disease [203], rheumatoid arthritis [204] and psoriasis [205]. Mechanistically, this SNP is associated with disrupted IL-23R signaling, which may block the development of pathogenic responses associated with autoimmunity [204]. Kave et al. reported that R381Q was more frequent among patients afflicted with coronary heart disease [206] and suggested that IL-23R signaling might contribute to the development of atherosclerosis, in line with the previously mentioned report of Zhang et al. However, a report by Mangino et al. indicated no

association between R381Q and myocardial infarction [201]. In summary, whether IL-23 or IL-23R play a direct role in cardiovascular diseases remain elusive.

## 1.6. Aim of this thesis

The role that cDCs play in atherosclerosis is not clear. $CD8^+$ and $CD103^+$ cDCs1 rely on the transcription factor BATF3 for their development. Given that these DCs have been reported to secrete pro-atherogenic cytokines such as IL-12 and retain regulatory T cell responses, the first part of this thesis aimed to elucidate the role of Batf3-dependent DCs in atherosclerosis.

The second part of this thesis focused on the IL-23 / IL-23R axis. Although it has been suggested that IL-23 might play a proatherogenic role in atherogenesis, current studies do not provide detailed data on the role of this cytokine/receptor axis in this disease. Thus, this work aimed to characterize IL-23 responses by APCs and to elucidate how disruption of the IL-23R signaling could modulate plaque progression and stability.

# 2. MATERIALS

## 2.1. Chemicals

| Chemical | Purchased from |
|---|---|
| 100% Ethanol | Carl-Roth |
| 2-Propanol (Isopropanol) | Sigma-Aldrich |
| 70% Ethanol | Carl-Roth |
| Acid aldehyde | Sigma-Aldrich |
| Ammonium Chloride ($NH_4Cl$) | Sigma-Aldrich |
| Basic-Fuchsin | Sigma-Aldrich |
| Citric acid ($C_6H_8O_7$) | Carl Roth |
| Ethylenediaminetetraacetic acid, disodium ($Na_2EDTA$) | Sigma-Aldrich |
| Formaldehyde (FA) 4% (Roti Histo-Fix) | Carl Roth |
| Gelatin (from bovine skin – type B) | Sigma-Aldrich |
| Glycerol | Applichem |
| Hydrogen chloride (concentrated) (HCl) | Sigma-Aldrich |
| Nile Red | Sigma Aldrich |
| Oil-Red-O | Sigma-Aldrich |
| Paraformaldehyde (PFA) | Carl Roth |
| Phosphate-buffered saline (PBS) | Thermo Fisher Scientific |
| Potassium bicarbonate ($KHCO_3$) | Sigma-Aldrich |
| Sirius Red (Direct Red 80) | Sigma-Aldrich |
| Tween 20 | Carl Roth |
| Trisodium citrate | Carl Roth |
| Xylene | Carl-Roth |

**2.2. Cell culture reagents**

| Reagent | Purchased from |
|---|---|
| 2-Mercaptoethanol (50 mM) | Thermo Fisher Scientific |
| Brefeldin A (BFA) | Sigma-Aldrich |
| Bovine serum albumin | Sigma-Aldrich |
| D-PBS | Thermo Fisher Scientific |
| Fetal calf serum (FCS), low in endotoxin | Sigma Aldrich |
| Fluorescein (FITC)-conjugated ovalbumin (OVA) | Thermo Fisher Scientific |
| 4-(2-hydroxyethyl)-1-piperanzineethanesufonic acid (HEPES) | Thermo Fisher Scientific |
| Ionomycin | Sigma-Aldrich |
| Lipopolysaccharide (LPS) from *Escherichia Coli* O111: B4 | Sigma-Aldrich |
| Nile red | Sigma-Aldrich |
| Non-Essential Amino Acids (NEAA) (100X) | Thermo Fisher Scientific |
| oxLDL | Hycultec |
| $Pam_3CSK_3$ | Invivogen |
| Penicillin-Streptomycin (10,000 U/ml) | Thermo Fisher Scientific |
| Phorbol 12-myristate 13-acetate (PMA) | Sigma-Aldrich |
| Polymyxin B (PMB) | Invivogen |
| RPMI-1640 (with 2 mM L-Glutamine) (RPMI) | Thermo Fisher Scientific |
| Sodium Pyruvate (100 mM) | Thermo Fisher Scientific |
| StemPro™ Accutase™ Cell Dissociation Reagent | Thermo Fisher Scientific |

**2.3. Cytokines**

| Cytokine | Purchased from |
|---|---|
| α-IFN-γ (XMG1.2) | Bioceros |
| rmGM-CSF | Peprotech |
| rmIL-1β | Peprotech |
| rmIL-6 | Peprotech |
| rmM-CSF | Peprotech |
| rmIL-23 | R&D |

| | |
|---|---|
| rhTGF-β | Peprotech |

**2.4. Other reagents**

| **Reagent** | **Purchased from** |
|---|---|
| Maxima SYBR Green/ROX qPCR Master Mix (2x) | Thermo Fisher Scientific |
| Collagenase I (C1030) | Sigma Aldrich |
| Collagenase XI (C7657) | Sigma Aldrich |
| HFD (15% fat, 1.25% cholesterol) | Altromin |
| Hyaluronidase type I-S (H3506) | Sigma Aldrich |
| Tissue-Tek O.C.T Compound | Sakura |
| Vectashield with DAPI | Vector Laboratories |
| Vitro-Clud | R. Langenbrinck |

**2.5. Consumables**

| **Consumable** | **Purchased from** |
|---|---|
| 384-well plates | Biozym |
| 5 ml Polystyrene Round-Bottom Tube (FACS Tubes) | Corning |
| Falcon$^{R}$ 70µm Cell Strainer | Corning |
| Micro-test plate 96 well (round and bottom) | Sarstedt |
| Microtube 1.1 ml Z-Gel (Serum tubes) | Sarstedt |
| Microtube 1.3 ml K3E (EDTA-coated tubes) | Sarstedt |
| Syringe (BD Plastipak$^{TM}$) | BD Biosciences |

**2.6. Kits**

| **Kit** | **Purchased from** |
|---|---|
| Amplex$^{TM}$ Red Cholesterol Assay Kit | Thermo Fisher Scientific |
| Fixation/Permeabilization Solution Kit | BD Biosciences |
| Fixation Buffer | BD Biosciences |
| $CD4^{+}CD62L^{+}$ T Cell Isolation Kit II | Miltenyi Biotech |

| | |
|---|---|
| CD11c$^{+}$ MicroBeads UltraPure | Miltenyi Biotech |
| eBiosciences$^{TM}$ FoxP3/Transcription Factor Staining Buffer Set | Thermo Fisher Scientific |
| EnzyChrom$^{TM}$ Triglyceride Assay Kit | Bioassay Systems |
| First strand cDNA Synthesis Kit | Thermo Fisher Scientific |
| IL-23 Mouse Uncoated ELISA (2$^{nd}$ generation) | Thermo Fisher Scientific |
| Mouse IL-23 DuoSet ELISA (1$^{st}$ generation) | R&D |
| Mouse IL-12 p70 DuoSet ELISA | R&D |
| Mouse IL-17 DuoSet ELISA | R&D |
| Nucleospin RNA II Kit | Macherey-Nagel |

**2.7. Instruments**

| **Name** | **Company** |
|---|---|
| Aspir8mini (vacuum pump) | Cell Media |
| FACSAria$^{TM}$ III | BD Biosciences |
| FACSCanto$^{Tm}$ II | BD Biosciences |
| QuantiStudio 6 Flex Thermal Cycler | Applied Biosystems |
| Leica CM3050 S Research Cryostat | Leica Biosystems |
| Leica DM 4000B Fluorescence Microscope | Leica Biosystems |
| Nanodrop 2000C | Thermo Fisher Scientific |
| Thermocycler, peqSTAR | VWR |

**2.8. Software**

| **Name** | **Company** |
|---|---|
| Diskus image analysis (V4.81.1638) | Hilgers Technisches Büro |
| FlowJo (V10.4) | Tree Star / BD Biosciences |
| GraphPad Prism (V7) | GraphPad |
| Image J | *Open source* |

## 2.9. Antibodies

### 2.9.1. Primary and secondary antibodies not used for flow cytometry

| Name (Clone) | Nature | Purchased from |
|---|---|---|
| Anti-mouse α-Actin Cy3(1A4) | Primary | Sigma Aldrich |
| Goat anti-rat IgG – Alexa Fluor 488 | Secondary | Thermo Fisher Scientific |
| Rat anti-mouse Mac-2 (M3/38) | Primary | Cedarlane |
| LEAF™ Purified anti-mouse CD28 | Primary | Biolegend |
| Ultra-LEAF™ Purified anti-mouse CD3 | Primary | Biolegend |

### 2.9.2. Primary antibodies used for flow cytometry

| Name | Clone (Company) | Dilution |
|---|---|---|
| **B220 (CD45RO)** | RA3-6B2 (BD) | 1.300 |
| **CD103** | 2E7 (Thermo FS) | 1.100 |
| **CD11b** | M1/70 (BD, Thermo FS) | 1.300 |
| **CD11c** | N418 (Thermo FS) | 1.300 |
| **CD19** | eBio1D3 (Thermo FS) | 1.300 |
| **CD115** | AF598 (Thermo FS) | 1.300 |
| **CD16/32 (Fc Block)** | 97 (Biolegend) | 1.50 |
| **CD25** | PC61.5 (Thermo FS) | 1.300 |
| **CD3** | 500A2 (BD) | 1.300 |
| **CD4** | GK1.5 (Thermo FS) | 1.300 |
| **CD4** | RM4-5 (BD, Thermo FS) | 1.300 |
| **CD44** | IM7 (Thermo FS) | 1.300 |
| **CD45** | 30-F11 (BD) | 1.300 |
| **CD62L** | MEL-15 (Biolegend) | 1.300 |
| **CD8** | 53-6.7 (BD) | 1.300 |
| **CD86** | P03.1 (Thermo FS) | 1.300 |
| **FoxP3** | FJK-16s (Thermo FS) | 1.100 |
| **GM-CSF** | MP1-22E9 (Thermo FS) | 1.100 |
| **IFN-γ** | XMG1.2 (BD) | 1.100 |

| | | |
|---|---|---|
| **IL-17A** | eBio17B7 (Thermo FS) | 1.100 |
| **LIVE/DEAD Fixable dye** | - (Thermo FS) | 1.1000 |
| **Ly6C** | HK1.4 (Thermo FS) | 1.500 |
| **Ly6G** | 1A8 (BD) | 1.500 |
| **MHCII** | M5/114.15.2 (Thermo FS) | 1.300 |
| **Siglec H** | eBio440c (Thermo FS) | 1.300 |
| **TCR-β** | H57-597 (Thermo FS) | 1.300 |
| **TCR-γδ** | eBioGL3 (Thermo FS) | 1.300 |

*BD = BD Biosciences; Thermo FS = Thermo Fisher Scientific

**2.10. Primers**

| **Gene name** | **Forward primer (5′-> 3′)** | **Reverse primer (5′-> 3′)** |
|---|---|---|
| *Batf3* | TCCACGAGGAGCACGAGA | CCACATGTACCCCTGGACAC |
| *Foxp3* | CCCAGGAAAGACAGCAACCTT | TTCTCACAACCAGGCCACTTG |
| *Hprt* | TCCTCCTCAGACCGCTTTT | CCTGGTTCATCATCGCTAATC |
| *Ifng* | GCTGTTTCTGGCTGTTACTGC | TCACCATCCTTTTGCCAGTTCC |
| *Il10* | ATTTGAATTCCCTGGGTGAGAAG | CACAGGGGAGAAATCGATGACA |
| *Il23a* | CCAGCGGGACATATGAATCT | AGGCTCCCCTTTGAAGATGT |
| *Rorc* | TGAGGCCATTCAGTATGTGG | CTTCCATTGCTCCTGCTTTC |
| *Tbet* | GCCAGGGAACCGCTTATATG | GACGATCATCTGGGTCACATTGT |

## 2.11. Buffers, solutions, and media

### Aldehyde-Fuchsin solution

- Stock solution
  2.5 g Basic-Fuchsin in 500 ml of 70% ethanol (high grade)

- Working solution
  Mix 50 ml stock solution + 2.5 ml acid aldehyde + 1 mL concentrated HCl and leave overnight. Filter prior to use.

### Antigen retrieval solution

- Stock solution
  Solution A: 21.01 g citric acid in 1 liter distilled water
  Solution B: 29.41 g tri-sodium citrate dihydrate in 1 liter distilled water

- Working solution
  1.8 ml solution A + 8.2 ml solution B + 90 ml distilled water + 50 µg Tween-20

### Cytokine stimulation cocktail

To measure intracellular cytokines, cells were stimulated with 50 ng/ml PMA, 750 ng/ml ionomycin and 2,5 µg/ml BFA in DC Medium for 4 hours.

### DC Medium

- RPMI 1640 with 2 mM L-glutamine
- 10% heat-inactivated FCS
- 100 U/ml penicillin/streptomycin
- 50 µM 2-Mercaptoethanol

### DC Stimulation Medium

- RPMI 1640 with 2 mM L-glutamine
- 0.5% heat-inactivated FCS

- 100 U/ml penicillin/streptomycin
- 50µM 2-Mercaptoethanol

**Erythrocyte Lysis Buffer (Ery-lysis-buffer)**

- 150 mM $NH_4Cl$
- 10 mM $KHCO_3$
- 0,1 M $Na_2EDTA$

**FACS Buffer**

PBS supplemented with 2% mouse serum, 2% rabbit serum, 2% BSA.

**Heat-inactivation of FCS**

Bottles of FCS were incubated at 56°C for 30 minutes, inverting them every 10 minutes.

**Kaiser´s glycerin jelly**

- Stock solution

  4 g gelatin + 21 ml distilled water + 25 ml glycerol

- Working solution

  3 parts stock solution + 7 parts distilled water

**L929 growth medium**

- RPMI-1640
- 10% heat-inactivated FCS
- 100U/ml penicillin/streptomycin
- 25 mM HEPES

**Mac staining buffer**

Following compounds were made up in 1X PBS:

- 2% mouse serum
- 2% rabbit serum
- 2% horse serum
- 1% BSA
- 0.1% Triton X100

**Oil-Red-O Solution**

- Stock solution:

  1 g Oil-Red-O in 200 ml 99% 2-Propanol (isopropanol)
- Working solution:

  160 ml Stock solution with 120 ml milli-Q water (1 hour at room temperature). The solution was filtered prior to use.

**Picrosirius red solution**

- 0.1% Sirius Red/Direct Red 80 in saturated aqueous picric acid (pH 2.0).

**T cell polarization medium**

- DC Medium
- 1 mM Sodium Pyruvate
- 1 mM NEAA
- 10 mM HEPES

# 3. METHODS

## 3.1. Mice

### 3.1.1. Mice lines

C57BL/6J and *Ldlr*$^{-/-}$ animals were purchased from The Jackson Laboratory.

*Batf3*$^{-/-}$ mice were purchased from The Jackson Laboratory and crossed with *Ldlr*$^{-/-}$ mice (both C57BL/6J background, The Jackson Laboratory) to generate *Ldlr*$^{-/-}$ *and Ldlr*$^{-/-}$*Batf3*$^{-/-}$ mice.

IL-23R knock-in mice were provided by Prof. Dr. Thomas Korn (University of Munich) [189]. In these mice, an internal ribosomal entry site green fluorescent protein (IRES GFP) cassette was introduced in the endogenous *Il23r* gene locus. In heterozygous mice (*Il23*$^{gfp/+}$), IL-23R-expressing cells can be visualized by their GFP expression. When bred as homozygotes (*Il23r*$^{-/-}$), the deletion of the IL-23R abrogates their responsiveness to IL-23. To study the effect of IL-23R in atherosclerosis, *Il23r*$^{-/-}$ mice were crossed with *Ldlr*$^{-/-}$ mice (both C57BL/6J background) to generate *Ldlr*$^{-/-}$ and *Ldlr*$^{-/-}$*Il23r*$^{-/-}$ animals.

### 3.1.2. Animal maintenance

Mice were bred and housed under specific pathogen-free conditions at the Zentrum für Experimentelle Molekulare Medizin, Würzburg. Mice were maintained on a standard light-dark cycle and have *ad libitum* access to food and water. Animal studies and number of animals used conform to the Directive 2010/63/EU of the European Parliament and have been approved by the appropriated local authorities (Regierung von Unterfranken, Würzburg, Germany. Akt.-Z 2-82, 105-14 and 2-82)

### 3.1.3. Induction of atherosclerosis

Males or females mice at the age of 6 to 8 weeks were used to study the effect of gene deletion on atherosclerosis development. They were grouped in cages (max. 3 per cage) and placed on a HFD regimen (15% milk fat, 1.25% cholesterol) for specified time points. Animals were inspected once weekly.

### 3.1.4. Euthanization of mice and organ preparation

Mice were anesthetized using isoflurane and euthanized by cervical dislocation. In non-diet experiments, mice were flushed either with PBS or RPMI 1640 before extracting the organs. When the aorta was extracted, extraneous fat was carefully removed before use. In diet experiments, mice were initially flushed with PBS followed by 4% PFA in PBS. After perfusion, organs were collected, weighted if necessary and processed as described in section 3.1.5 to 3.1.8.

To study lesion development, the heart and whole aorta were removed and carefully cleaned of extraneous fat before being post-fixed with 4% PFA in PBS. After overnight incubation, PFA was replaced with fresh PBS. *En face* preparation of the aorta and sectioning of hearts is described in 3.2.1 and 3.2.3.

### 3.1.5. Preparation of single-cell suspension from the peripheral blood

Whole blood was collected in EDTA-coated tubes, mixed gently to avoid blood clotting and placed on ice. 150 µl were transferred to 1.5 ml Eppendorf and mixed with 850 µl of Ery-Lysis-Buffer at room temperature for 10 minutes. After centrifugation at 400 Gs, 10 minutes at room temperature, a white-clear pellet was observable. The supernatant was carefully removed by aspiration and cells were resuspended in cold PBS 1%FCS according to the number of mixes needed for each experiment. For example, for 4 different staining, the cell pellet was resuspended in 800 µl of PBS 1%FCS and 200 µl were transferred to 96-well plates for FACS analysis.

### 3.1.6. Preparation of single cell suspension from spleen or lymph nodes

Spleen or lymph nodes were disrupted and passed through a 70 µm filter. Cells were centrifuge at 400 Gs, 5 minutes at 4°C. In the case of the spleen, red blood cells were lysed by adding 3 ml of Ery-Lysis-Buffer and incubated on ice for 7 minutes, when 7 ml of cold PBS 1%FCS were added to stop the reaction. After a new centrifugation step, cells were resuspended in 10 ml of PBS 1%FCS and filtered again using a 70 µm filter to remove cell clumps. In both cases, 1 x $10^6$ cells were used for flow cytometry analysis.

### 3.1.7. Preparation of single cell suspension from spleen or lymph nodes for FACS-sorting

Single cell suspension from spleen was obtained as described in 3.1.6. The whole supernatant was resuspended in 250 µl of PBS supplemented with 1% FCS and 250 µl of FACS Buffer and stained with antibodies for 30 minutes in the dark when 1.5 ml of PBS supplemented with 1%FCS was added to wash cells. After centrifugation, the cell pellet was resuspended in 1 ml of PBS supplemented with 1%FCS and filtered using a 70 µm strainer to remove any clog

**3.1.** Antibody mixture used to sort splenic naïve $CD4^+$ T cells

| Name/Colour | Clone | Dilution |
|---|---|---|
| CD4 – V500 | | 1.300 |
| CD44 – PE | | 1.300 |
| CD25 – APC | | 1.300 |
| TCR-β – PerCP/Cy5.5 | | 1.300 |
| CD45 – APC/Cy7 | | 1.300 |
| CD62L – PE/Cy7 | | 1.300 |

### 3.1.8. Preparation of single cell suspension from the aorta and aortic sinus

Fat was carefully removed throughout the aorta and separated from the aortic sinus. Both tissues were separately placed in 1.5 ml tubes containing 200 µl of RPMI-1640 where they were minced and incubated 1 hour at 37°C with 450 U/ml collagenase I, 125U/ml collagenase XI and 60U/ml hyaluronidase in a final volume of 400 µl. After incubation with the enzyme cocktail, tissues were filtered using a 70 µm cell strainer and cells were centrifuged at 400 Gs, 5 minutes at 4°C. The cell pellet was resuspended in 200 µl of PBS 1%FCS and transferred to a round 96-well plate for FACS analysis.

### 3.1.9. Serum preparation

Approximately 100-150 µl of fresh blood obtained retro-orbitally were placed in Serum Tubes and placed on ice until all samples were collected. Afterward, tubes were left at room temperature for 30 minutes and then centrifuged 10.000 rpm for 5 minutes to separate serum from clogged blood. Serum was transferred to 1.5 ml tubes and kept at -80°C until use.

### 3.1.10. Serum cholesterol and triglyceride measurement

Serum was analyzed for total cholesterol and triglycerides using the Amplex™ Red Cholesterol Assay Kit and EnzyChrom™ Triglyceride Assay Kit, respectively, according to the manufacturer´s instruction.

### 3.1.11. Serum lipoprotein profile

Serum cholesterol lipoprotein profiles were determined by size exclusion chromatography. In brief, 5 µl of serum was fractioned using a Superose 6 3.2/300 gel filtration column from GE Healthcare and PBS, pH 7.4 as elution buffer, delivered by a first pump at a flow rate of 50 µl/min. The separated lipoproteins were mixed in a T-tube with 50 µl/min cholesterol reagent delivered by a second pump. Thereafter, the mixture went through a 500 µl reaction coil PEEP tubing at 37°C in a post-column reaction over. Finally, absorption was measured with an UV-VIS detector at 500 nm. Total run time for each sample was 60 min. Chromatograms were integrated by Waters Empower 3 software. vLDL, LDL and HDL concentrations were calculated as products of the area percent of total cholesterol.

## 3.2. Histology

### 3.2.1. Oil-Red O staining of aortas

The aorta was cut longitudinally and opened. Staining of lipids was achieved by Oil-Red O as follows:

| Step | Duration |
|---|---|
| First wash with 1X PBS | 5 minutes |
| Dip aortas in 60% 2-propanol 10 times | |
| Staining with Oil-Red O working solution | 15 minutes |
| Dip aortas in 60% 2-propanol 10 times | |
| Last wash with 1X PBS | 5 minutes |
| Mount aortas with Kaiser´s glycerin jelly | |

### 3.2.2. Quantification of lesion area in the aorta

Lesion size was analyzed in three sections of the aorta (abdominal, thoracic and arch) by marking red areas using the Diskus image analysis software and is expressed as the percentage of the total size of each aortic section.

### 3.2.3. Aldehyde-Fuchsin staining of aortic roots

PFA-fixed hearts were cut in the middle and embedded in a solution containing 50% 1X PBS and Tissue-Tek. After overnight incubation, hearts were initially cut using a cryostat until reaching the beginning of the valves. Once reached, three sections covering the region of the valves were collected on a slide and left at 4°C until use.

Aortic root sections were assessed for atherosclerotic plaque size after staining with Gabe´s Aldehyde-Fuchsin as follows:

| Step | Duration |
|---|---|
| Staining with Aldehyde-Fuchsin working solution | 15 minutes |
| Dip slides 5 times in 70% ethanol | |
| Stop differentiation with distilled water | 5 minutes |
| Staining with Picrosirius Red solution | 90 minutes |
| Place slides in 0.01N HCl | 1 minute |
| Dehydration (see below) | |

Dehydration protocol:

| Reagent | Duration |
|---|---|
| Distilled water | Short dip |
| 70% ethanol | 1 minute |
| 96% ethanol (first) | 1 minute (3x) |
| 100% ethanol (first) | 1 minute (3x) |
| Xylene | 5 minutes (3x) |

After dehydration, slides were covered with Vitro-Clud and air-dried at room temperature before visualization

### 3.2.4. Quantification of lesion area in the aortic root

Lesion size in the aortic root was quantified from three sections per mice. Images were recorded using a Leica microscope and quantification performed using the Diskus image analysis software. Plaque size is defined as the sum of all plaques among valves. Values represent the average of plaque among the three sections analyzed.

### 3.2.5. Quantification of collagen content in the aortic root

The content of collagen in plaques from the aortic root was analyzed using the open sourced program Image J and is expressed as the percentage of total plaque.

### 3.2.6. Antigen retrieval

Heat treatment for antigen retrieval was applied to aortic root sections before immunostaining. Slides were placed in a slide holder containing 150 ml of working solution and heated for 10 minutes in a microwave (medium settings). To prevent boiling over of the solution, the process was stopped every 3 minutes for 10 seconds. After 10 minutes, half of the solution was replaced with 150 ml of fresh working solution and samples were heated again for 10 minutes (medium settings) following the same strategy as described above to avoid boiling, but stopping the reaction every other minute. Next, the container was placed at room temperature followed by a final two-step wash with PBS for 5 minutes. Sections were later processed as described in the next section.

### 3.2.7. Macrophage and smooth muscle cell staining of aortic root sections

Selected aortic root sections that underwent antigen retrieval were first dried and then blocked with Mac Staining Buffer for 30 minutes in a wet incubation chamber followed by incubation with the primary antibody mixture at 4°C. After overnight incubation, slides were washed once with 1X PBS for 15 minutes and then once more for 5 minutes. Secondary antibody for the identification of macrophages was added to slides for 1 hour at room temperature. Slides were washed once with 1X PBS for 15 minutes, then once more for 5 minutes and left dried before adding one drop of DAPI-containing Vectashield per tissue and covering slides with coverslips. Borders were sealed with nail polish and slides were stored in dark at 4°C.

| | **Antibody** | **Dilution** |
|---|---|---|
| **Primary antibody mixture** | Mac-2 (rat anti-mouse) | 1.600 |
| | α-SM Actin Cy3 (mouse anti-mouse/human/rat) | 1.200 |
| **Secondary antibody** | Anti-rat 488 | 1.500 |

### 3.2.8. Quantification of macrophage, smooth muscle cell, necrotic core and collagen content in plaques

Stained slides containing three sections per mouse were recorded with a fluorescence microscope and a JVC KZ-F75U camera. Quantification of the macrophage content (Green-positive area), smooth muscle cell content (strong red-positive area) and necrotic area (DAPI-blue-negative area) was calculated as a percentage of the total lesion per section using the Diskus image analysis software.

## 3.3. In vitro experiments

### 3.3.1. Generation of BM-APCs

Femurs and tibiae were removed from donor mice and bone marrow was flushed with DC Medium. Cells were counted and 5 x $10^6$ cells were cultured in 10 cm-Petri dishes in DC Medium containing 20 ng/ml GM-CSF. After 3 days, another 10 ml of medium supplemented with 20 ng/ml GM-CSF were added to plates. At day 6, half of the medium was aspirated, centrifuged, resuspended in 10ml containing 20 ng/ml GM-

CSF and put back to the plate. At day 7, around 80-90% of cells were $CD11c^+$ and were used for experiments.

For phagocytosis assay, all experiments were carried out in 24-well plates and down-scaled 1/10 (e.g. 5 x $10^5$ starting cells in a final volume of 1 ml). 20 ng/ml of GM-CSF were used.

### 3.3.2. BM-APCs priming and stimulation

To study the effect of oxLDL in cultured cells, 5 x $10^5$ BM-APCs were transferred to 24-well plates and cultured in DC Stimulation Medium in a final volume of 500 µl. Cells were further stimulated with LPS (100 ng/ml), oxLDL (10 or 50 µg/ml) or a combination of both. For priming analysis, immature BM-APCs were stimulated with 100 ng/ml of LPS for 3 hours at 37°C 5%$CO_2$. Non-adherent cells were then centrifuged 10 minutes, 400 GS at room temperature and the supernatant was carefully removed to eliminate any residual LPS. BM-APCs were resuspended in fresh DC Stimulation Medium containing a specified amount of the secondary stimuli.

### 3.3.3. Generation of BMDMs

Bone marrow was flushed as described in 3.3.1. and 2 x $10^6$ cells were cultured in 24-well plates in DC Medium supplemented with 15% L-929 cell-conditioned medium. At days 3 and 5 medium was renewed. Cells at day 7 were used as mature BMDMs.

### 3.3.4. Generation of L929-conditioned media

As a source of M-CSF for the generation of BMDM, conditioned medium collected after culturing the M-CSF-expressing L929 mouse cell line was used.

Frozen aliquots of L929 were thawed and washed to remove DMSO. The cell pellet was resuspended in 5 ml of L929 growth medium and seeded in T25 flasks until reaching 100% confluence, when the cells were split at ratio 1:30 into T175 flasks. Medium renewal was every other day.

To obtain conditioned medium, five confluent T175 flasks were split into 26 T175 flasks, each supplemented with 55 ml of L9292 growth medium. After 10 days of incubation at 37°C, 5% $CO_2$, media was collected, centrifuged at 350 Gs for 5 minutes

and sterile filtered using bottle-top vacuum filters. 50ml aliquots were stored at -80°C until use.

### 3.3.5. Foam cell formation

To induce foam cell formation, BMDMs were first starved with RPMI-1640 containing 2% BSA for 4 hours and then washed once with warmed PBS. Using the same medium as mentioned, cells were stimulated with 50 µg/ml oxLDL and cultured overnight at 37°C. Cells were detached using StemPro™ Accutase™ Cell Dissociation Reagent for 5 minutes at room temperature and transferred to a round 96-well plate for fixing them with 100 µl of 10% Fixation Buffer for 5 minutes at room temperature. Cells were centrifuged and incubated with Nile red (1.2000) in 200 µl of PBS for 10 minutes in the dark at room temperature. After two washes with PBS cells were measured by flow cytometry.

### 3.3.6. Non- and pathogenic $Th_{17}$ polarization of splenic naïve T cells

Naïve $CD4^+CD62L^+CD25^-$ T cells were FACS-sorted from spleens of specified mice. The purity of naïve T cells was close to 99% in all cases, as measured by flow cytometry. 2 x $10^5$ naïve T cells were cultured in pre-coated anti-CD3ε (5 µg/ml) flat-bottom 96-well plates and stimulated with a non-pathogenic $Th_{17}$ cocktail containing anti-CD28 (1 µg/ml), IL-6 (20 ng/ml), TGF-β (4 ng/ml) and α-IFN-γ (10 µg/ml) or a pathogenic $Th_{17}$ cocktail composed of CD28 (1 µg/ml), IL-6 (20 ng/ml), IL-1β (20 ng/ml), IL-23 (50 ng/ml) and α-IFN-γ (10 µg/ml) for at 37°C and 5% $CO_2$. After 96 hours cells were stimulated as described in 3.4.2. to induce IL-17A production and cells were measured by flow cytometry.

### 3.3.7. Phagocytosis assay

BM-APCs were either left untreated or stimulated with oxLDL (20 or 50 µg/ml) or LPS (100 ng/ml) in DC Stimulation Medium. Cells were then collected, washed and 2 x $10^5$ cells incubated with 0.5 mg/ml of FITC-conjugated OVA in RPMI supplemented with 0.5%FCS for 30 minutes at 37°C. Phagocytosis controls were performed by incubating cells at 4°C. After incubation cells were washed twice with PBS and stained with the LIVE/DEAD Fixable dye, CD11c, and MHC-II and measured by flow cytometry

### 3.3.9. $T_{reg}$ polarization

5 x $10^5$ splenocytes or 2 x $10^5$ FACS- or magnetic-sorted $CD4^+CD6L^+$ naïve T cells were cultured in round-bottom 96-well plates and stimulated with soluble (total splenocytes) or pre-coated (naïve T cells) anti-CD3ε (5 µg/ml), soluble anti-CD28 (1 µg/ml) and TGF-β (4 ng/ml) at 37°C and 5°$CO_2$. After 72 hours the percentage of $CD25^+FoxP3^+$ $T_{regs}$ was measured by flow cytometry.

## 3.4. Flow cytometry

### 3.4.1. Flow cytometry analysis of surface antigens

Cells were transferred to round 96-well plates and centrifuged at 400 Gs, 5 minutes at 4°C and the supernatant was removed by inverting the plate. For experiments requiring the analysis of DCs populations or macrophages, cells were first resuspended in 50 µl of FACS Buffer containing an Fc Block and incubated for 20 min at 4°C. After washing with 150 µl of PBS 1%FCS cells were again resuspended in 50 µl of FACS Buffer containing the antibody mixture and incubated for 30 min at 4°C. Cells were washed once more and resuspended in 200 µl of PBS 1%FCS for flow cytometry analysis.

### 3.4.2. Flow cytometry analysis of intracellular cytokines or transcription factors

For the study of transcription factors such as a FoxP3, the FoxP3/Transcription Factor Staining Buffer kit was used, whereas to study intracellular cytokines such as IFN-γ and IL-17A, the Fixation/Permeabilization Solution Kit was selected. When intracellular cytokines were measured, 1 x $10^6$ cells (except in the case of blood) were transferred to round 96-well plates and resuspended in 200 µl of RPMI containing the Cytokine Stimulation Cocktail (see Material) to induce production and accumulation of cytokines. Cells were incubated for 4 hours at 37°C and 5% $CO_2$ and then washed once with PBS 1%FCS. After staining of surface antigens, cells were fixed and permeabilized using 100 µl of the corresponding buffer for 20 min at 4°C. Cells were washed twice using the washing buffer provided for each manufacturer, resuspended in 50 µl of washing buffer containing the antibodies against intracellular antigens and incubated for 30 min at 4°C. After a final wash, cells were finally resuspended in 200 µl of PBS 1%FCS and left at 4°C for measurement.

### 3.4.3. Flow cytometry analysis for the co-detection of intracellular GFP and intracellular cytokines

To co-detect intracellular cytokines in IL-23R$^{+}$ (GFP$^{+}$) animals, cells were fixed using formaldehyde (FA) as previously described [207]. Briefly, after surface staining, cells were fixed using 2% FA for 1 hour at 4°C and then washed once using the wash buff provided in the kit from ThermoFisher Scientific used for FoxP3 detection. Intracellular antibodies against specified cytokines were used in a final volume of 50 µl and incubated for 30 minutes at room temperature. After one wash, cells were resuspended in 200 µl of PBS 1%FCS and measured by flow cytometry.

## 3.5. Enzyme-linked immunosorbent assay (ELISA)

### 3.5.1. IL-23 and IL-17 measurement by ELISA

Serum IL-23 and supernatant IL-23 was measured using a second generation mouse ELISA and a mouse IL-23 DuoSet ELISA respectively, following manufacturer instructions. For serum IL-23, samples were left overnight at 4°C to obtain the highest sensitivity. For IL-17 measurement 2 x $10^5$ splenocytes were cultured in round-bottom 96-well plates and stimulated with soluble anti-CD3 (5 µg/ml), anti-CD28 (1 µg/ml) and IL-23 (10 or 25ng/ µl) or conditioned-supernatant from treated BM-APCs supplemented with 10%FCS, 1mM NEAA, 1mM sodium pyruvate and 1mM HEPES to avoid cell death. After 24 and 72 hours, supernatant was collected and analyzed using a mouse IL-17 ELISA.

### 3.5.2. Ex vivo aortic culture

Cytokine analysis from ex vivo aortic culture was done following a previous protocol [208]. Briefly, fat-free aortas were cut in 15 rings of 2 mm and transferred to a 1.5 ml tube containing cold PBS. Rings were washed twice with PBS and incubated overnight in a 24-well plate in DC Stimulation Media containing specified stimuli in a final volume of 200 µl. Supernatant was collected and IL-23 measured using the mouse IL-23 DuoSet ELISA. Results were normalized to the content of total DNA extracted from cultured rings.

### 3.6. Quantitative real-time PCR (qPCR)

#### 3.6.1. Tissue processing

Isolated specified tissues from mice were immediately transferred to a 1.5ml tube and stored in liquid nitrogen until all samples were collected. After total collection, probes were conserved at -80°C until use.

#### 3.6.2. qPCR conditions

Total RNA from specified sources was isolated using the NucleoSpin RNA kit according to the manufacturer´s recommendation. 100 ng of complementary DNA (cDNA) was reverse transcribed from total RNA using the first strand cDNA synthesis kit. Quantitative real-time PCR analysis was performed from 10ng cDNA using SYBR green mix following conditions:

| Stage | Temperature | Time |
|---|---|---|
| **1** | 95°C | 15 minutes |
| **2 (Repeats: 40)** | 95°C | 15 seconds |
| | 60°C | 30 seconds |
| | 72°C | 50 seconds |
| **3** | 95°C | 15 seconds |
| | 60°C | 15 second |
| | 95°C | 15 seconds |

# 4. RESULTS I

## 4.1. The role of Batf3-dependent dendritic cells in atherosclerosis.

### 4.1.1 *Batf3* deficiency depletes CD103$^+$ DCs in the aortic root under homeostatic conditions

The transcription factor BATF3 has been shown to be highly expressed in CD8α$^+$ and CD103$^+$ cDCs1 and is lowly expressed or absent in other immune cell populations, including pDCs [104]. Although initial studies have shown that *Batf3*$^{-/-}$ mice specifically lacked both subsets in several lymphoid compartments [104, 209], further studies reported that mice on a C57BL/6 background still showed some splenic CD8α$^+$ DCs [210]. The impact of *Batf3* deficiency on CD8α$^+$ and CD103$^+$ DCs under homeostatic conditions was analyzed. As described previously, spleens from *Ldlr*$^{-/-}$*Batf3*$^{-/-}$ mice presented some CD8α$^+$ and CD103$^+$ DCs, although knock out animals showed an 80% reduction in each population compared to wild-type animals (Figure 1b). No differences in pDCs were noted (0.37% ± 0.08% *versus* 0.32% ± 0.03% of CD11c$^{low/-}$ SiglecH$^+$ pDCs among CD45$^+$ cells in *Ldlr*$^{-/-}$ compared to *Ldlr*$^{-/-}$*Batf3*$^{-/-}$ mice, respectively; p=0.26).

At the steady state, APCs with a dendritic-like phenotype are primarily localized in the aortic root and only express CD103 but not CD8α [98]. Analysis of the aortic root of *Ldlr*$^{-/-}$*Batf3*$^{-/-}$ mice revealed a complete loss of the CD103$^+$ cell population (Figure 2b, left) and this was accompanied by increased frequencies of CD11b$^+$ cells (Figure 2b, right). Similar results were obtained in the aorta (11.27% ± 3.16% *versus* 0% of CD103$^+$ DCs among CD11c$^+$MHCII$^+$ APCs in *Ldlr*$^{-/-}$ compared to *Ldlr*$^{-/-}$*Batf3*$^{-/-}$ mice, respectively; ***p<0.001; and 66.55%± 5.73% *versus* 81.75% ± 8.41% of CD11b$^+$ DCs among CD11c$^+$MHCII$^+$ APCs in *Ldlr*$^{-/-}$ compared to *Ldlr*$^{-/-}$*Batf3*$^{-/-}$ mice, respectively; ***p<0.001)

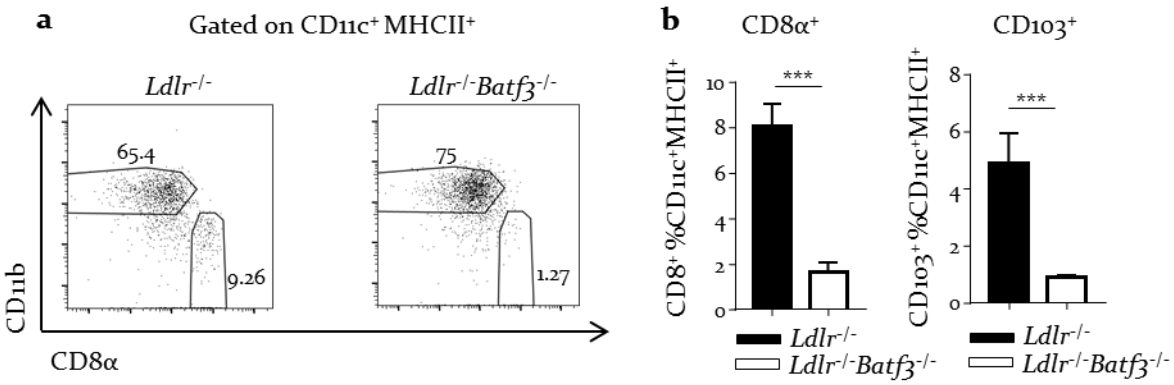


**Figure 1. *Batf3* deficiency reduced the frequency of CD8α⁺ and CD103⁺ DCs in the spleen.** Splenocytes from *Ldlr*$^{-/-}$ (n=4) and *Ldlr*$^{-/-}$*Batf3*$^{-/-}$ mice (n=4) were analyzed by flow cytometry. First, CD45⁺ leukocytes were gated and APCs were defined as CD11c⁺ MHCII⁺ (a) Representative dot plots of CD8α⁺ and CD11b⁺ DCs among the CD11c⁺ MHCII⁺ population. (b) Percentages of CD8α⁺ and CD103⁺ DCs in the spleen. Data are presented as mean ± SEM; ***p<0.001.

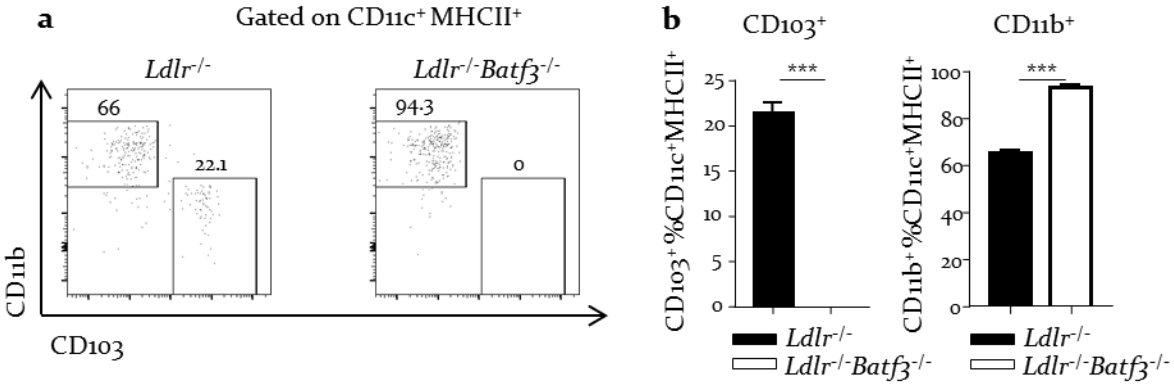


**Figure 2. Aortic sinus of *Ldlr*$^{-/-}$*Batf3*$^{-/-}$ mice lacked CD103⁺ DCs.** Single cell suspensions from the aortic sinus were obtained from *Ldlr*$^{-/-}$ (n=2) and *Ldlr*$^{-/-}$*Batf3*$^{-/-}$ mice (n=2) and measured by flow cytometry. Cells were first incubated with Fc block to avoid non-specific binding. First, total live CD45⁺ leukocytes were gated and CD19⁺ and TCR-β⁺ cells excluded to remove B and T cell populations. (a) Representative dot plots of CD103⁺ and CD11b⁺ DCs among CD11c⁺ MHCII⁺ cells. (b) Percentages of CD103⁺ (left) and CD11b⁺ (right) cells in the aortic sinus. Data are presented as mean ± SEM; ***p<0.001.

### 4.1.2. Lack of *Batf3* in macrophages does not alter foam cell formation in vitro

A recent study has found that BATF3 is highly expressed in pre-macrophages and its expression decreases as macrophages become mature [211]. Although several studies have shown that *Batf3* deficiency does not alter any macrophage population [212, 213], it is not clear whether it might impact other features such as foam cell formation, a key hallmark of atherosclerosis. First, mRNA levels of *Batf3 in* cultured BMDM were

analyzed. Compared to the isolated CD11c$^+$ splenic fraction, which contains a Batf3-enriched population of APCs, BMDM only expressed residual mRNA levels of *Batf3* (Figure 3a). In line with these findings, foam cell formation was not changed among BMDM derived from *Ldlr*$^{-/-}$ and *Ldlr*$^{-/-}$*Batf3*$^{-/-}$ mice (Figure 3b), which further confirm that *Batf3* deletion does not play a major role in macrophages.

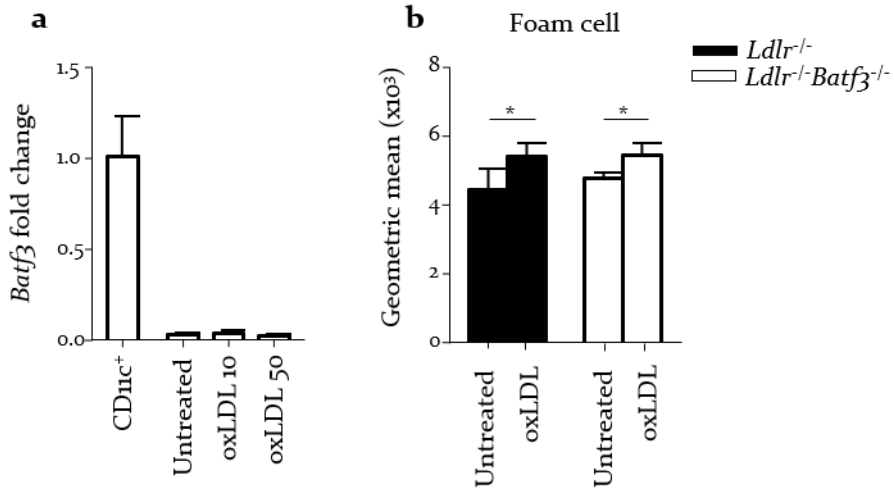


**Figure 3. Loss of *Batf3* in BMDM did not affect foam cell formation.** BMDMs were generated from *Ldlr*$^{-/-}$ (n=3) and *Ldlr*$^{-/-}$*Batf3*$^{-/-}$ mice (n=3). Splenic CD11c$^+$ cells were enriched from *Ldlr*$^{-/-}$ animals. (a) BMDMs were left untreated or treated with different concentrations of oxLDL (10 or 50 µg/ml) for 24 hours. Results were normalized to *Hprt* mRNA and are presented relative to splenic CD11c$^+$ cells. (b) BMDMs were left untreated or were stimulated with oxLDL (50 µg/ml) for 24 hours. Cells were stained with the intracellular dye Nile red and the mean fluorescence intensity was measured by flow cytometry. One of two representative experiments is shown. Data are presented as mean ± SEM; *p<0.05.

### 4.1.3. Under homeostatic conditions *Ldlr*$^{-/-}$*Batf3*$^{-/-}$ animals showed mildly altered innate and adaptive immune responses

It has previously been described that Batf3-deficient mice do not show any differences in total splenic B or T cells [104], although no data regarding other immune cells with the ability to impact the development of atherosclerosis is available. Apart from CD8α$^+$ and CD103$^+$ DCs, monocytes also express *Batf3*, albeit at lower levels [104]. Immune responses of *Ldlr*$^{-/-}$*Batf3*$^{-/-}$ mice under homeostatic conditions compared to *Ldlr*$^{-/-}$ controls were analyzed.

No differences in the number of circulating monocytes (Figure 4a) or in Ly6C$^{high}$ or Ly6C$^{low}$ populations (Figure 4b) were observed in the blood between groups. *Ldlr*$^{-/-}$

*Batf3*$^{-/-}$ mice showed unaltered percentages of CD115$^{+}$ in spleen (Figure 5a), although decreased percentages of inflammatory Ly6C$^{high}$ and increased Ly6C$^{low}$ monocytes were noted at this location (Figure 5b).

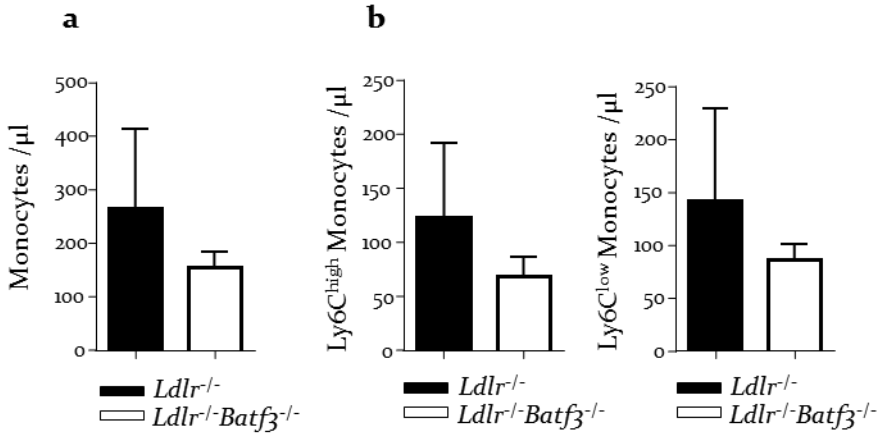


**Figure 4. *Ldlr*$^{-/-}$ and *Ldlr*$^{-/-}$*Batf3*$^{-/-}$ animals showed similar numbers of circulating monocytes under homeostatic conditions.** PBMCs were obtained from *Ldlr*$^{-/-}$ (n=6) and *Ldlr*$^{-/-}$*Batf3*$^{-/-}$ mice (n=5) fed with a chow diet and measured by flow cytometry. (a) Numbers of monocytes (CD115$^{+}$) per µl of blood and (b) numbers of inflammatory Ly6C$^{high}$ (left) and non-conventional Ly6$^{low}$ monocytes (right) per µl of blood. Data are presented as mean ± SEM.

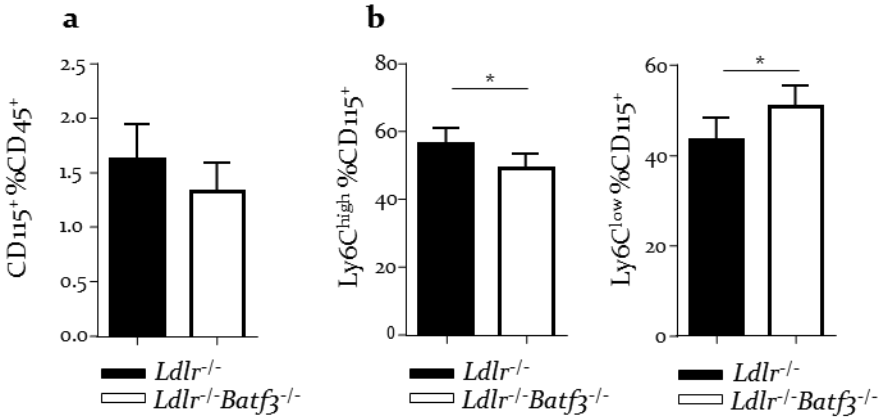


**Figure 5. Batf3-deficient *Ldlr*$^{-/-}$ mice showed decreased percentages of Ly6C$^{high}$ inflammatory monocytes in the spleen.** Splenocytes were obtained from *Ldlr*$^{-/-}$ (n=6) and *Ldlr*$^{-/-}$*Batf3*$^{-/-}$ mice (n=5) and analyzed by flow cytometry. (a) Percentages of CD115$^{+}$ monocytes from total CD45$^{+}$ cells and (b) percentages of inflammatory Ly6C$^{high}$ and non-conventional Ly6$^{low}$ monocytes among CD115$^{+}$ cells. Data are presented as mean ± SEM; *p<0.5

In line with previous reports [104], the number of circulating T cells in the blood and the frequency of total $CD3^+$ T cells in the spleen were similar in both groups (Figure 6a). However, *Ldlr*$^{-/-}$*Batf3*$^{-/-}$ mice showed decreased splenic $CD8^+$ T cell frequencies, whereas the $CD4^+$ T cell fraction was increased (Figure 6b). No differences in the $T_{reg}$ compartment in blood (3.88% ± 0.66% *versus* 4.32% ± 1.27% of $CD25^+FoxP3^+$ among $CD4^+$ T cells in *Ldlr*$^{-/-}$ compared to *Ldlr*$^{-/-}$*Batf3*$^{-/-}$ mice, respectively; p=0.48) or in spleen (12.75% ± 0.50% *versus* 12.82% ± 1.23% of $CD25^+FoxP3^+$ among $CD4^+$ T cells in *Ldlr*$^{-/-}$ compared to *Ldlr*$^{-/-}$*Batf3*$^{-/-}$ mice, respectively; p=0.90) were observed under homeostatic conditions.

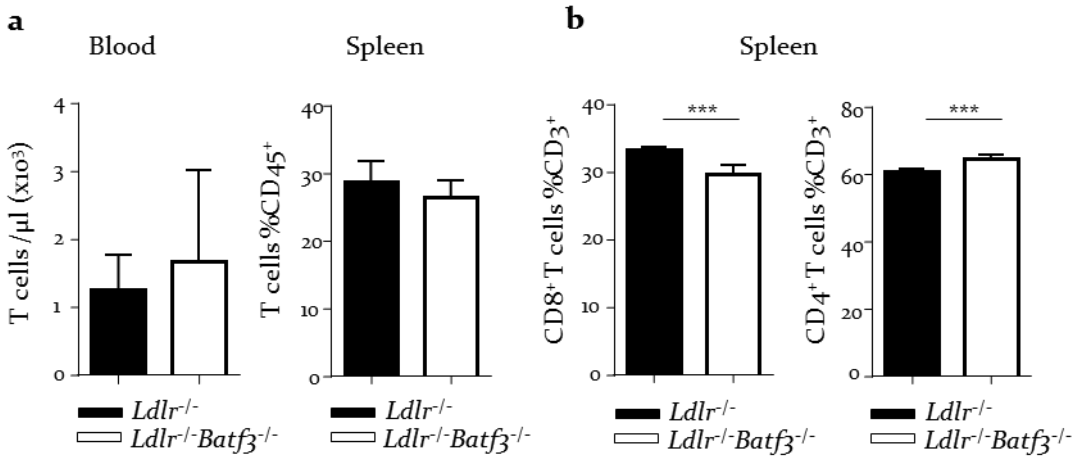


**Figure 6. Frequencies of splenic $CD8^+$ T cells were reduced in *Ldlr*$^{-/-}$*Batf3*$^{-/-}$ mice.** PBMCs and splenocytes were obtained from *Ldlr*$^{-/-}$ (n=6) and *Ldlr*$^{-/-}$*Batf3*$^{-/-}$ mice (n=5) and measured by flow cytometry. (a) Numbers of circulating $CD3^+$ T cells per µl of blood (left) and the percentage of splenic $CD3^+$ T cells among total $CD45^+$ leukocytes (right). (b) Percentages of splenic $CD8^+$ T cells (left) and $CD4^+$ T cells (right) among $CD3^+$ T cells. Data are presented as mean ± SEM; ***p<0.001.

### 4.1.4. Long-term depletion of Batf3-dependent DCs after feeding mice a HFD

Next, to assess how Batf3-dependent DCs might impact the course of atherosclerosis, age and sex sex-matched *Ldlr*$^{-/-}$ and *Ldlr*$^{-/-}$*Batf3*$^{-/-}$ mice were fed a HFD for 8 or 12 weeks. After 8 weeks of HFD, both groups showed similar body weight and white blood cell counts (Table 1).

**Table 1. Body weight and white blood cell (WBC) count of *Ldlr*$^{-/-}$ and *Ldlr*$^{-/-}$*Batf3*$^{-/-}$ fed a HFD for 8 weeks.**

| | *Ldlr*$^{-/-}$ | *Ldlr*$^{-/-}$*Batf3*$^{-/-}$ | *p-value* |
|---|---|---|---|
| **Body weight (g)** | 27.4 ± 1.61 | 28.19 ± 1.27 | 0.24 |
| **WBC count (10³/ µl)** | 7.47 ± 1.64 | 6.83 ± 1.54 | 0.34 |

Several studies have reported that infected *Batf3*$^{-/-}$ animals still retain the ability to cross-present antigens in vivo due to an expansion of the CD8α$^{+}$ DC fraction in a Batf3-independent manner [214]. Further studies have demonstrated that the other two members of the BATF family, BATF, and BATF2, can compensate for the lack of BATF3 during infection [215]. As HFD regimens induce systemic inflammation [49], the percentage of CD103$^{+}$ cDCs1 in the aortic root in mice fed a HFD was analyzed. After 8 weeks of diet, aortic roots from *Ldlr*$^{-/-}$*Batf3*$^{-/-}$ animals still showed a complete loss of CD103$^{+}$ cells accompanied by increased frequencies of CD11b$^{+}$ cells (Figure 7). Similar results were observed in the aorta (8.8% ± 5.74% *versus* 0% of CD103$^{+}$ DCs among CD11c$^{+}$MHCII$^{+}$ APCs in *Ldlr*$^{-/-}$ compared to *Ldlr*$^{-/-}$*Batf3*$^{-/-}$ mice, respectively; ***p<0.001; and 80% ± 6.14% *versus* 95.72% ± 2.13% of CD11b$^{+}$ DCs among CD11c$^{+}$MHCII$^{+}$ APCs in *Ldlr*$^{-/-}$ compared to *Ldlr*$^{-/-}$*Batf3*$^{-/-}$ mice, respectively; ***p<0.001)

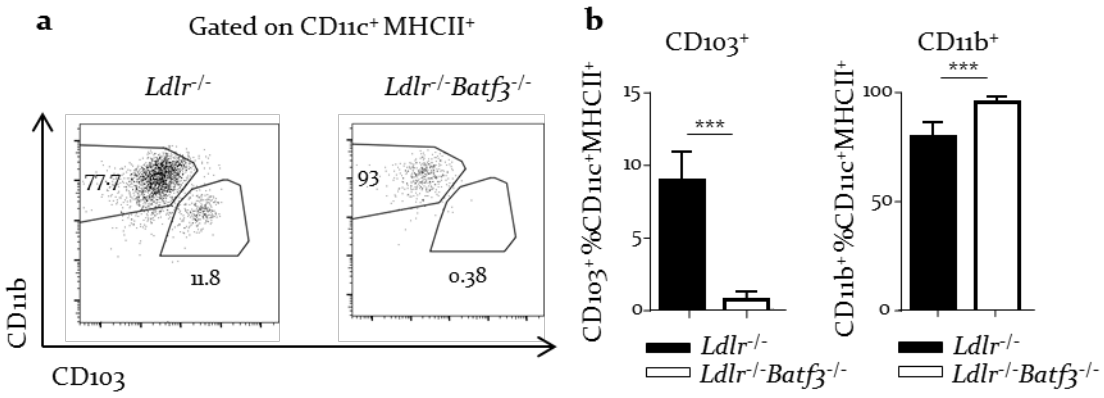


**Figure 7. Long-term depletion of Batf3-dependent DCs in *Ldlr*$^{-/-}$ mice fed 8 weeks a HFD.** Single cell suspensions from the aortic sinus were obtained from *Ldlr*$^{-/-}$ (n=7) and *Ldlr*$^{-/-}$*Batf3*$^{-/-}$ mice (n=6) fed a HFD for 8 weeks and measured by flow cytometry. Cells were first incubated with Fc block to avoid non-specific binding. Total CD45$^{+}$ leukocytes were gated and CD19$^{+}$ and TCR-β$^{+}$ were excluded to remove B and T cell populations. (a) Representative dot plot of CD103$^{+}$ and CD11b$^{+}$ cDCs1 among CD11c$^{+}$ MHCII$^{+}$ cells. (b) Percentages of CD103$^{+}$ (left) and CD11b$^{+}$ (right) in the aortic sinus. Data are presented as mean ± SEM; ***p<0.001.

Levels of CD8α$^{+}$ DCs were still reduced in spleen (6.02% ± 2.26% versus 2.37% ± 0.70% of CD8α$^{+}$ cells among CD11c$^{+}$ MHCII$^{+}$ APCs in *Ldlr*$^{-/-}$ versus *Ldlr*$^{-/-}$*Batf3*$^{-/-}$ mice, respectively; ***p<0.001) and no differences in the pDC compartment were noted between groups (0.26% ± 0.05% *versus* 0.29% ± 0.07% of CD11c$^{low/-}$ SiglecH$^{+}$ pDCs among CD45$^{+}$ cells in *Ldlr*$^{-/-}$ *versus Ldlr*$^{-/-}$*Batf3*$^{-/-}$ mice, respectively; p=0.18).

Of note, frequencies of CD11c$^{low}$ F4/80$^{+}$ cells, which are described to have a macrophage-like phenotype in the aortic tissue [98], were unaltered in the aorta of both wild-type and Batf3-deficient *Ldlr*$^{-/-}$ mice after 8 weeks of HFD (Figure 8b). Similar frequencies of CD64$^{+}$F4/80$^{+}$ macrophages were also observed in spleens from both groups (Figure 8a); further demonstrating that deletion of the transcription factor BATF3 does not alter macrophage development, as previously suggested.

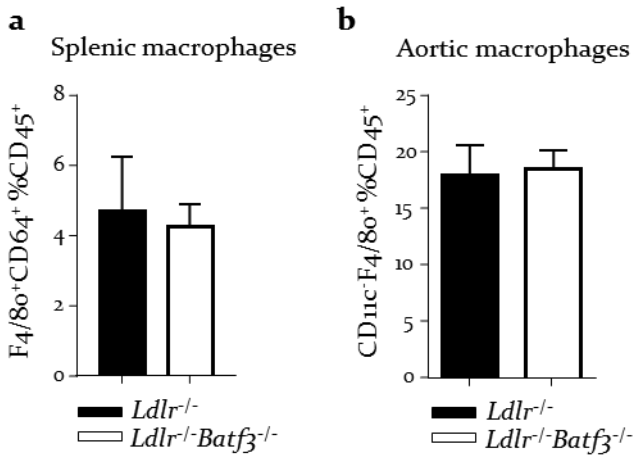


**Figure 8. *Ldlr*$^{-/-}$*Batf3*$^{-/-}$ animals fed a HFD for 8 weeks showed unaltered percentages of splenic and aortic macrophages.** Splenocytes or single cell suspensions from the aorta were obtained from *Ldlr*$^{-/-}$ (n=7) and *Ldlr*$^{-/-}$*Batf3*$^{-/-}$ mice (n=6) fed 8 weeks a HFD and analyzed by flow cytometry. (a) CD64$^{+}$ F4/80$^{+}$ macrophages among total CD45$^{+}$ cell in spleen. (b) CD11c$^{-}$ F4/80$^{+}$ macrophage-like cells in the aorta expressed as percentages of total CD45$^{+}$ cells. Data are presented as mean ± SEM

### 4.1.5. Innate and adaptive immune responses stayed mildly affected after 8 or 12 weeks of HFD

HFD induces an alteration of immune responses, for example by increasing monopoiesis (see Chapter 1.4.1.1) and hence, different immune responses might be observed between homeostatic and atherosclerotic-inducing conditions.

No differences in circulating neutrophils (719 ± 272.60 *versus* 668.50 ± 427.90 of Ly6G$^{+}$ cells per µl of blood in *Ldlr*$^{-/-}$ compared to *Ldlr*$^{-/-}$*Batf3*$^{-/-}$ mice, respectively; p=0.74) and percentages of neutrophils in spleen (1.91% ± 0.49% *versus* 2.85% ± 1.65% of Ly6G$^{+}$ cells among CD45$^{+}$ in *Ldlr*$^{-/-}$ compared to *Ldlr*$^{-/-}$*Batf3*$^{-/-}$ mice, respectively; p=0.08) were noted among groups after 8 weeks of diet. The number of circulating monocytes in the blood and the frequency of splenic CD115$^{+}$ monocytes were also similar (Figure 9a-d). Unaltered percentages of Ly6$^{high}$ inflammatory and Ly6C$^{low}$ non-conventional monocytes were noted after HFD-feeding, as opposed to homeostatic conditions. Similar results were obtained after 12 weeks of diet (data not shown).

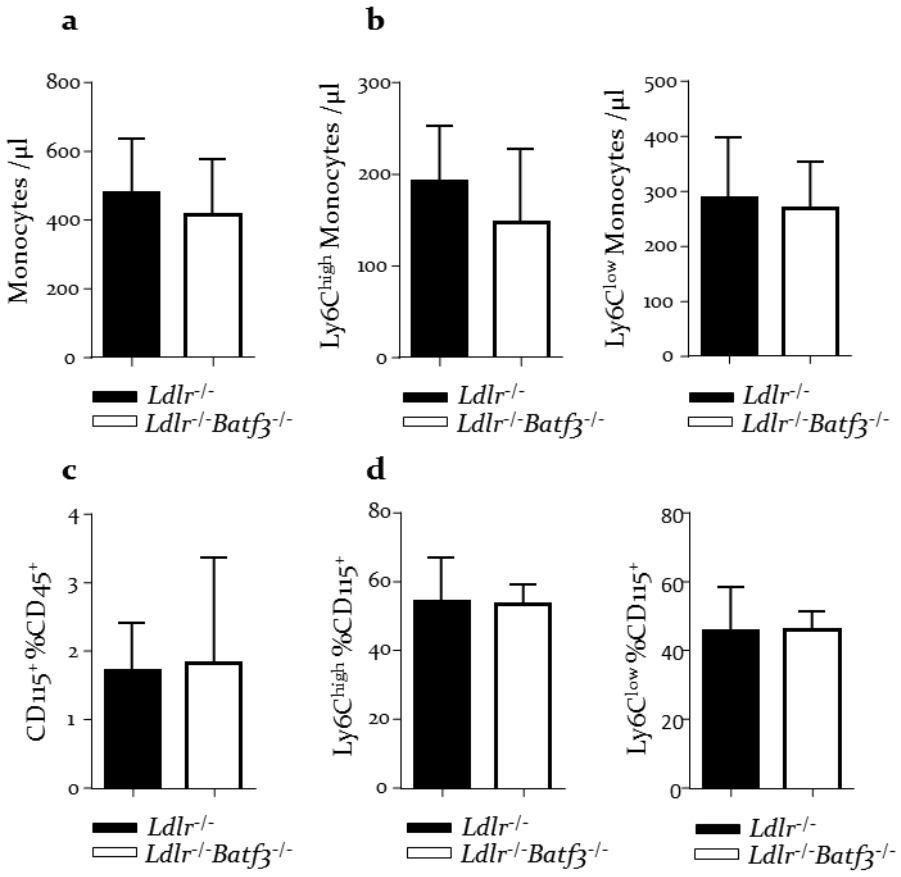


**Figure 9. Unaltered frequencies and percentages of monocytes in *Ldlr*$^{-/-}$ and *Ldlr*$^{-/-}$*Batf3*$^{-/-}$ mice fed a HFD for 8 weeks.** PBMCs and splenocytes from *Ldlr*$^{-/-}$ (n=11) and *Ldlr*$^{-/-}$*Batf3*$^{-/-}$ mice (n=10) fed a HFD for 8 weeks were analyzed by flow cytometry. (a) Numbers of CD115$^{+}$ monocytes per µl of blood and (c) percentages of splenic monocytes among CD45$^{+}$ cells, and (b) numbers of inflammatory Ly6C$^{high}$ and non-conventional Ly6$^{low}$ monocytes per µl of blood and (d) percentages among CD115$^{+}$ cells in the spleen. Data are presented as mean ± SEM.

Animals fed a HFD showed similar levels of circulating T cells and no differences in circulating CD4$^{+}$ or CD8$^{+}$ T cell subsets were noted between groups (Figure 10a, b). The percentage of splenic T cells was unaltered, but similar to homeostatic conditions, *Ldlr*$^{-/-}$*Batf3*$^{-/-}$ animals showed decreased percentages of CD8$^{+}$ T cells and increased CD4$^{+}$ T cells compared to *Ldlr*$^{-/-}$ controls (Figure 11a, b).

Analysis of T cell activation revealed that the percentage of activated $CD44^+$ $CD4^+$ T cells in spleens of Batf3-deficient *Ldlr*$^{-/-}$ mice was unaltered (14.46% ± 1.40% *versus* 17.28% ± 4.69% of $CD44^+$ cells among $CD4^+$ T cells in *Ldlr*$^{-/-}$ compared to *Ldlr*$^{-/-}$*Batf3*$^{-/-}$ mice, respectively; p=0.06), whereas the percentage of $CD44^+CD8^+$ T cells was markedly reduced in *Ldlr*$^{-/-}$*Batf3*$^{-/-}$ mice fed a HFD for 8 weeks (Figure 12b). No differences in the percentage of CD44+ $CD62L^+$ central memory $CD8^+$ T cells were noted (Figure 12b).

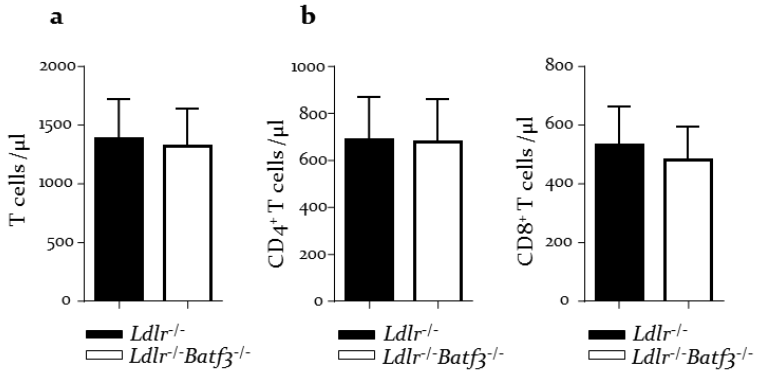


**Figure 10. Batf3-deficient *Ldlr*$^{-/-}$ mice fed a HFD for 8 weeks showed similar numbers of circulating T cells.** PBMCs were obtained from *Ldlr*$^{-/-}$ (n=11) and *Ldlr*$^{-/-}$*Batf3*$^{-/-}$ mice (n=10) fed a HFD for 8 weeks and analyzed by flow cytometry. (a) Numbers of $CD3^+$ T cells per µl of blood and (b) numbers of $CD4^+$ and $CD8^+$ T cells per µl of blood. Data are presented as mean ± SEM.

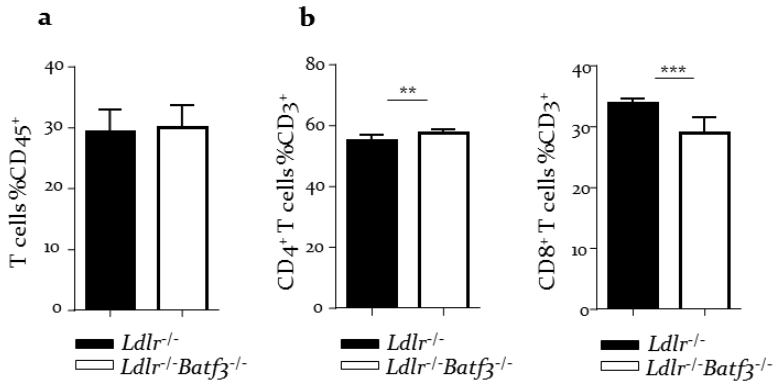


**Figure 11. Decreased percentages of $CD8^+$ T cells in Batf3-deficient *Ldlr*$^{-/-}$ mice after 8 weeks of HFD-feeding.** Splenocytes were obtained from *Ldlr*$^{-/-}$ (n=11) and *Ldlr*$^{-/-}$*Batf3*$^{-/-}$ mice (n=10) and analyzed by flow cytometry. (a) Percentages of $CD3^+$ T cells among $CD45^+$ cells, and (b) percentages of $CD4^+$ and $CD8^+$ T cells among $CD3^+$ T cells. Data are presented as mean ± SEM; **p<0.01, ***p<0.001.

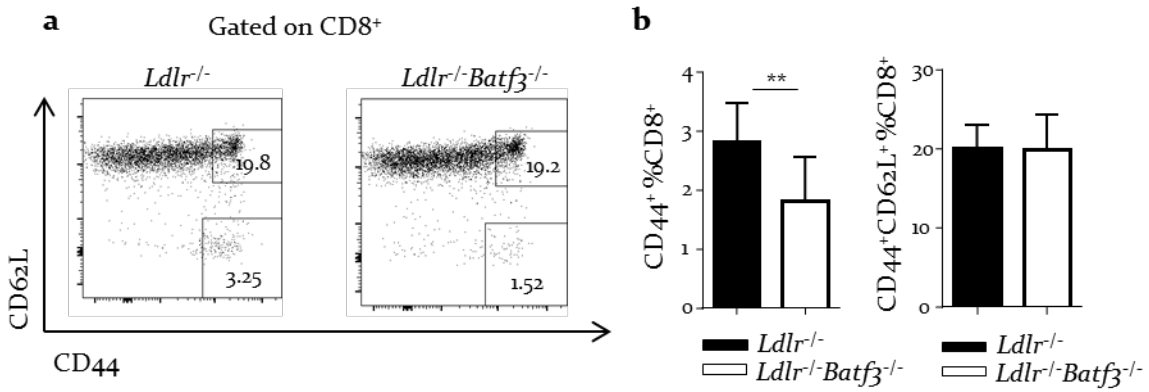


**Figure 12. Decreased percentages of splenic CD44$^+$ CD8$^+$ T cells in Batf3-deficient *Ldlr*$^{-/-}$ mice fed a HFD for 8 weeks.** Splenocytes were obtained from *Ldlr*$^{-/-}$ (n=11) and *Ldlr*$^{-/-}$*Batf3*$^{-/-}$ mice (n=10) and measured by flow cytometry. (a) Representative dot plots of activated CD8$^+$ T cells, defined as CD44$^+$CD62L$^-$, and central memory CD8$^+$ T cells, defined as CD44$^+$CD62L$^+$. (b, left) Percentages of activated CD8$^+$ T cells and (right) central memory CD8$^+$ T cells. Data are presented as mean ± SEM; **p<0.01.

Both CD8α$^+$ and CD103$^+$ cDCs1 have been described to be the major producers of IL-12 and promote Th$_1$ responses after bacterial challenge [107]. To decipher whether *Batf3* deficiency might impair Th$_1$ or Th$_{17}$ responses after feeding mice a HFD for 8 weeks, percentages of INF-γ-producing CD4$^+$ and CD8$^+$ and IL-17A-producing CD4$^+$ T cells were analyzed. As expected, percentages of IFN-γ-producing CD4$^+$ T cells were decreased in *Ldlr*$^{-/-}$*Batf3*$^{-/-}$ animals compared to *Ldlr*$^{-/-}$ controls (Figure 13a), whereas no differences in IL-17A$^+$ CD4$^+$ T cells were noted (Figure 13b). IFN-γ secretion by CD8$^+$ T cells remained unaltered (Figure 13c).

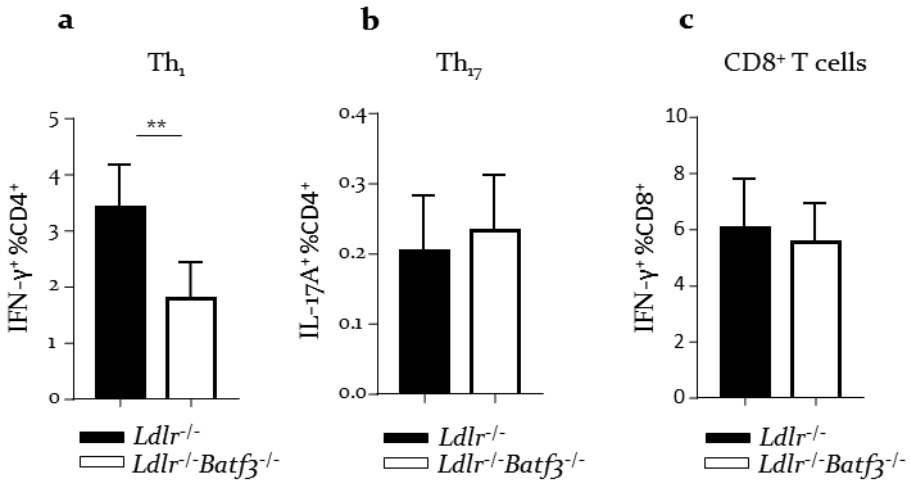


**Figure 13. Decreased percentages of IFN-γ$^+$CD4$^+$ T cells in the spleen of Batf3-deficient *Ldlr*$^{-/-}$ mice fed a HFD for 8 weeks.** Splenocytes were obtained from *Ldlr*$^{-/-}$ (n=6) and *Ldlr*$^{-/-}$*Batf3*$^{-/-}$ mice (n=6) and were stimulated with PMA (50 ng/ml), ionomycin (750 ng/ml) and BFA (2.5 μg/ml) for 4 hours to induce cytokine secretion. Cytokine production was detected by intracellular staining and flow cytometry. (a) Percentages of IFN-γ$^+$ cells among CD4$^+$ T cells. (b) Percentages of IL-17A$^+$ cells among CD4$^+$ T cells. (c) Percentages of IFN-γ$^+$ cells among CD8$^+$ T cells. Data are presented as mean ± SEM; **p<0.01.

The percentage of CD25$^+$FoxP3$^+$ $T_{regs}$ at different locations were similar between groups (data not shown). Altogether this data supports the hypothesis that *Batf3* deficiency only mildly affects immune responses under homeostatic conditions or under atherosclerosis-inducing regimens.

### 4.1.6. Loss of Batf3-dependent DCs does not impact cholesterol levels

It has been proposed that CD11c$^+$ APCs might control lipid metabolism, as CD11c-DTR *ApoE*$^{-/-}$ mice, depleted of CD11c$^+$ cells by DT administration, showed an elevation in plasma cholesterol levels, whereas an expanded lifespan of APCs resulted in hypocholesterolemia and in decreased levels of vLDL and LDL [90]. Analysis of cholesterol levels after 8 weeks of HFD showed that Batf3-deficient *Ldlr*$^{-/-}$ mice showed similar values of serum cholesterol and triglycerides levels when compared to *Ldlr*$^{-/-}$ controls (Table 2). Moreover, vLDL, LDL and HDL fractions were unaltered between groups (Figure 14), suggesting that Batf3-dependent DCs do not play a role in controlling cholesterol homeostasis.

**Table 2. Lipid levels of *Ldlr*$^{-/-}$ and *Ldlr*$^{-/-}$*Batf3*$^{-/-}$ mice fed a HFD for 8 weeks.**

| | *Ldlr*$^{-/-}$ | *Ldlr*$^{-/-}$*Batf3*$^{-/-}$ | *p-value* |
|---|---|---|---|
| **Serum cholesterol (µg/ml)** | 23378 ± 4656 | 21533 ± 6962 | 0.46 |
| **Serum triglycerides (mmol/L)** | 4.70 ± 1.20 | 3.70 ± 1.00 | 0.06 |

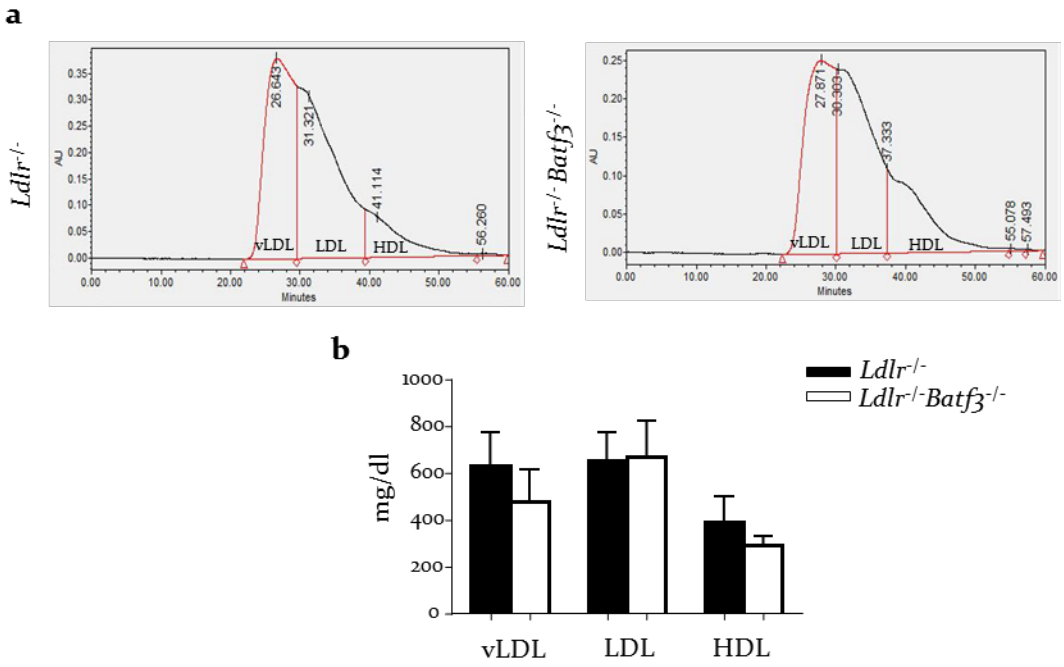


**Figure 14. Lipid profiles were similar between *Ldlr*$^{-/-}$ controls and Batf3-deficient *Ldlr*$^{-/-}$ mice after 8 weeks of HFD diet.** Serum samples were fractioned to reveal vLDL, LDL and HDL content. (a) Representative lipoprotein profile and (b) serum lipid profile in *Ldlr*$^{-/-}$ (n=7) and *Ldlr*$^{-/-}$*Batf3*$^{-/-}$ mice (n=6) fed a HFD for 8 weeks. Data are presented as mean ± SEM.

### 4.1.7. *Batf3* deficiency in *Ldlr*$^{-/-}$ mice had no effect on atherosclerosis progression and plaque composition after 8 and 12 weeks of HFD

Analysis of atherosclerotic lesion burden in *Ldlr*$^{-/-}$*Batf3*$^{-/-}$ mice compared to *Ldlr*$^{-/-}$ controls after 8 or 12 weeks of HFD revealed no differences in lesion size when considering the total aorta (Figure 15a). Similar results were obtained from mice fed a HFD for 12 weeks (Figure 15b).

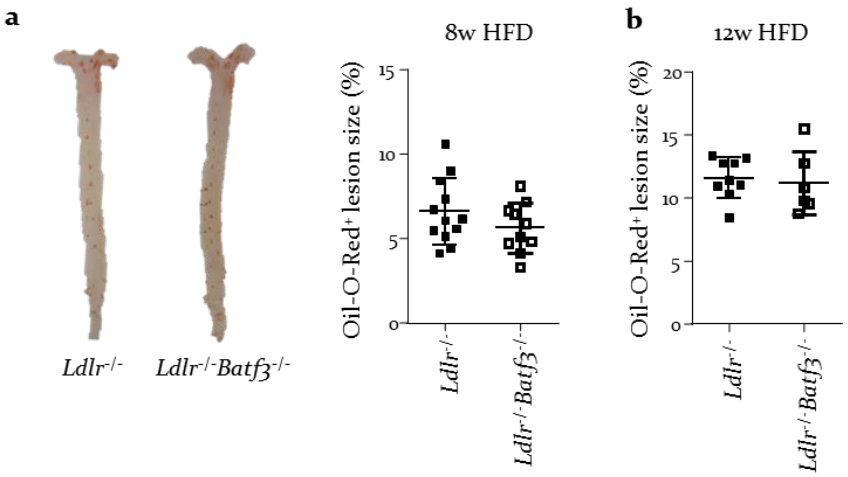


**Figure 15. Deficiency of *Batf3* in *Ldlr*$^{-/-}$ mice did not alter atherosclerotic lesion development**. Quantification of plaque area in Oil-Red-O stained aortas in mice fed a HFD for (a) 8 weeks (*Ldlr*$^{-/-}$ n=13 and *Ldlr*$^{-/-}$*Batf3*$^{-/-}$ n=10) and (b) 12 weeks (*Ldlr*$^{-/-}$ n=9 and *Ldlr*$^{-/-}$*Batf3*$^{-/-}$ n=6). Representative images of the aorta of mice fed 8 weeks a HFD are shown. Data are presented as mean ± SEM.

The analysis of plaque size in the aortic root in both *Ldlr*$^{-/-}$ and *Ldlr*$^{-/-}$*Batf3*$^{-/-}$ mice after 8 or 12 weeks or HFD reported no differences between groups at either time point studied (Figure 16a). Plaque composition analysis further revealed that macrophage content was similar (Figure 17a, b).

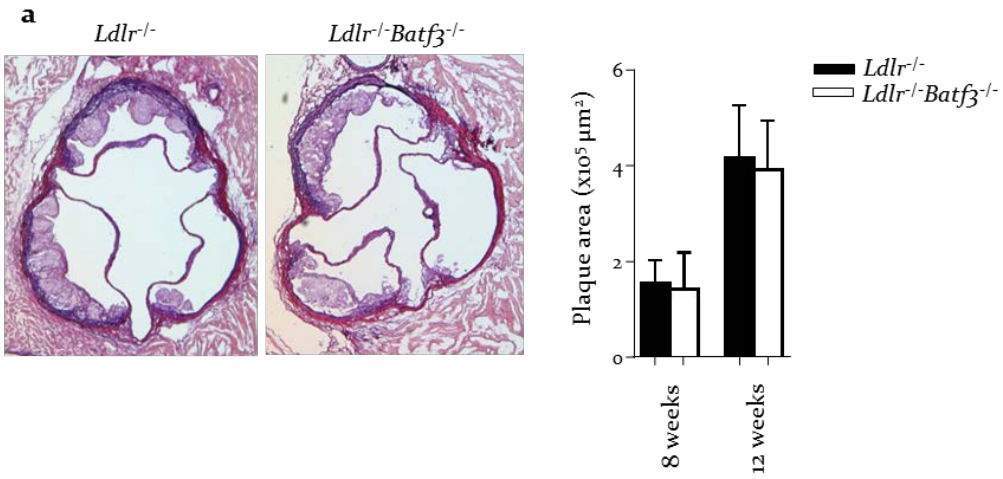


**Figure 16. Deficiency of *Batf3* in *Ldlr*$^{-/-}$ mice did not alter atherosclerotic lesion development in the aortic root in mice fed a HFD for 8 or 12 weeks.** (a) Quantification of plaque area in Aldehyde-Fuchsin-stained aortic roots sections in atherosclerotic *Ldlr*$^{-/-}$ (8 weeks HFD, n=13; 12 weeks HFD, n=6) and *Ldlr*$^{-/-}$*Batf3*$^{-/-}$ mice (8 weeks HFD, n=10, 12 weeks HFD, n=6). Representative images of aortic root sections from mice after 8 weeks of HFD are shown. Data are presented as mean ±SEM.

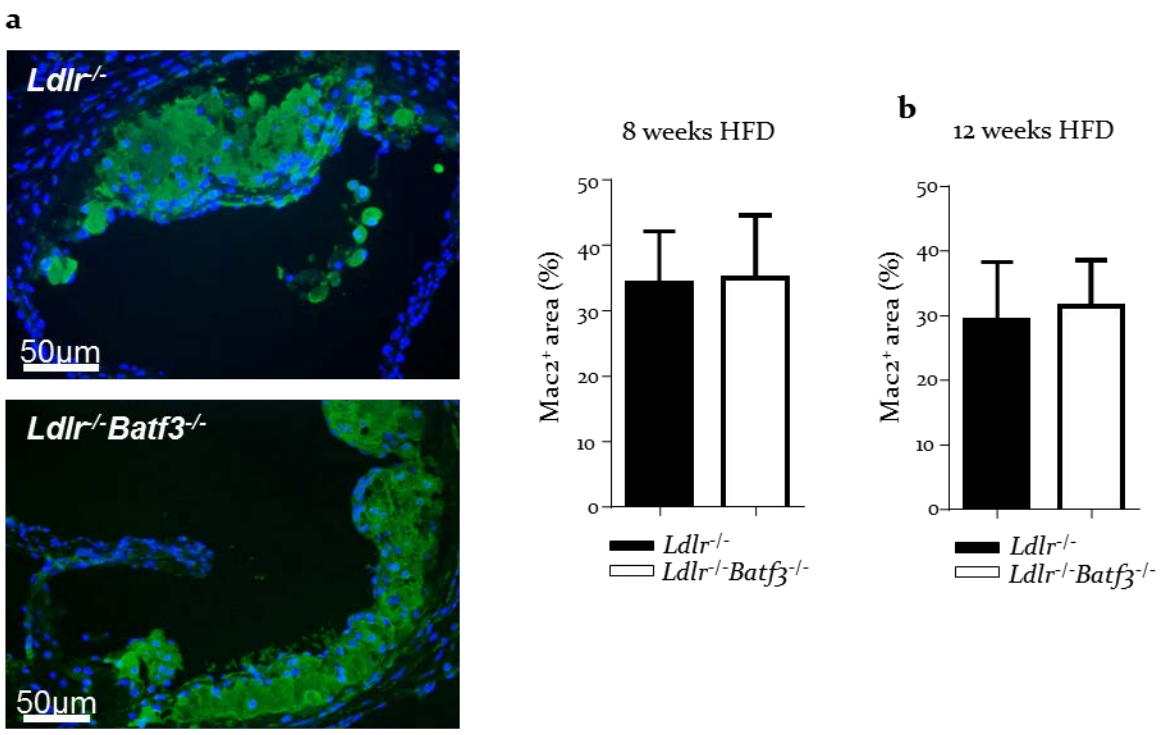


**Figure 17. Macrophage content in plaques was not altered in *Ldlr*$^{-/-}$*Batf3*$^{-/-}$ mice after 8 or 12 weeks of HFD-feeding. (a)** Quantification of the area positive for Mac-2; representative images of immunofluorescence staining from plaques of mice (*Ldlr*$^{-/-}$ mice n=13; *Ldlr*$^{-/-}$*Batf3*$^{-/-}$ mice n=10) fed a HFD for 8 weeks are shown; scale bars: 50µm; cell nuclei were counterstained with DAPI (blue). (b) Macrophage content in plaques of mice fed a HFD for 12 weeks (*Ldlr*$^{-/-}$ mice n=6; *Ldlr*$^{-/-}$*Batf3*$^{-/-}$ mice n=6). Data are presented as mean ± SEM.

Stability of plaques can predict cardiovascular outcomes (introduced in Chapter 1.2). Features of plaque instability comprise decreased collagen and SMC accumulation and an enlarged necrotic core. In line with previous results demonstrating no differences in atherosclerotic lesion burden, these features were also similar between *Ldlr*$^{-/-}$ and *Ldlr*$^{-/-}$*Batf3*$^{-/-}$ mice fed a HFD for 8 (Figure 18a-c) or 12 weeks (data not shown), demonstrating that *Batf3* deficiency does not impact on atherosclerosis development or affect plaque composition.

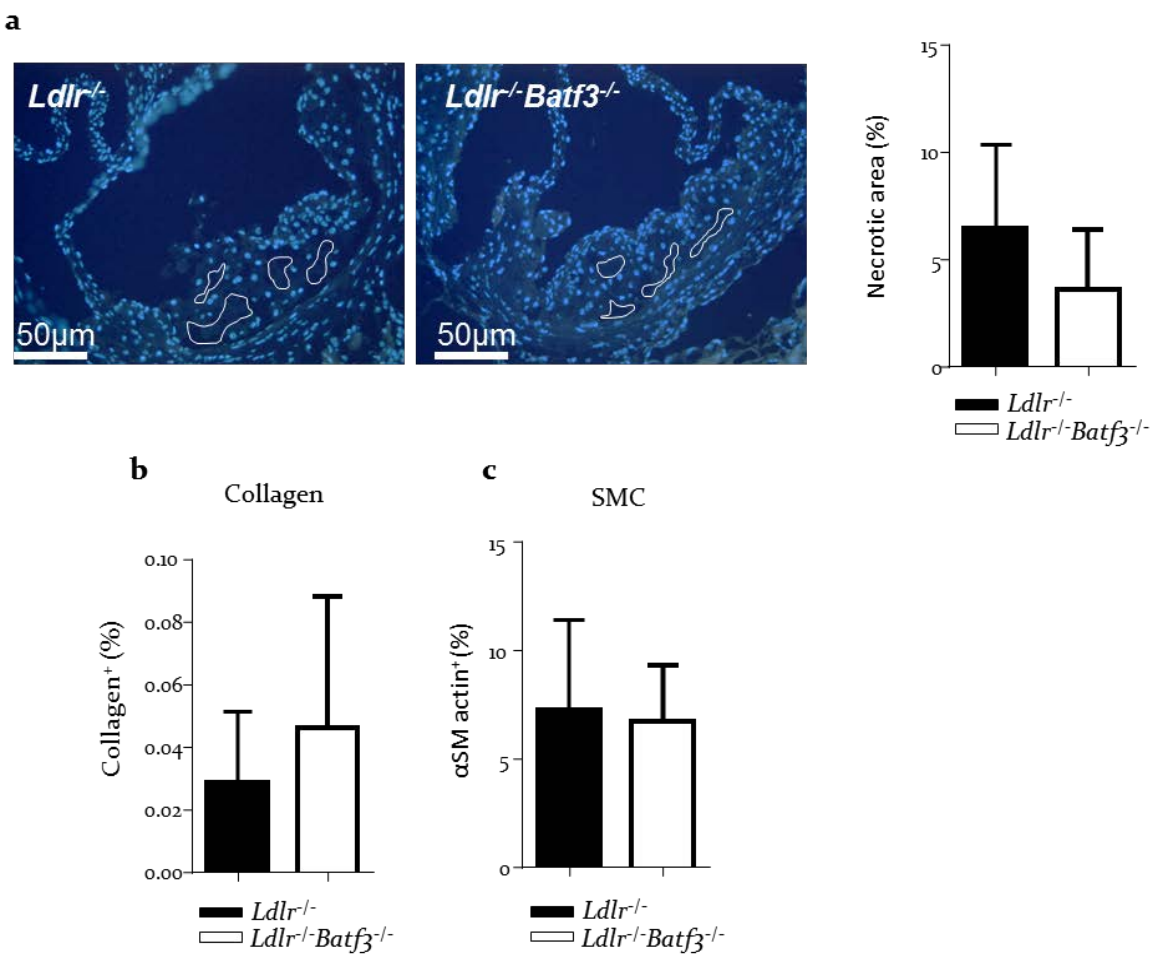


**Figure 18. Plaque composition is not altered by *Batf3* deficiency**. (a) Quantification of the necrotic core area in the aortic root of *Ldlr*$^{-/-}$ (n=13) and *Ldlr*$^{-/-}$*Batf3*$^{-/-}$ mice (n=10) fed a HFD for 8 weeks. Representative images of immunofluorescence staining are shown, scale bars: 50µm. For collagen and smooth muscle cell content, slides were stained with (b) α-smooth muscle cell actin or (c) Sirius red. Data are presented as mean ± SEM.

# 4. RESULTS II

## 4.2. The role of the IL-23 receptor in atherosclerosis

### 4.2.1. oxLDL does not induce a fully activated phenotype in BM-APCs

Only activated APCs can secrete IL-23 in vitro (introduced in Chapter 1.5). To elucidate whether oxLDL can modulate IL-23 secretion, the effect of oxLDL in APC activation in vitro and in vivo was studied. After 24 hours of stimulation, levels of CD80 were increased in BM-APCs treated with oxLDL (Figure 19a), whereas levels of CD86 and CD40 remained unaltered (Figure 19b, c). As expected, treatment with LPS induced a strong upregulation of all markers (Figure 19 a-c).

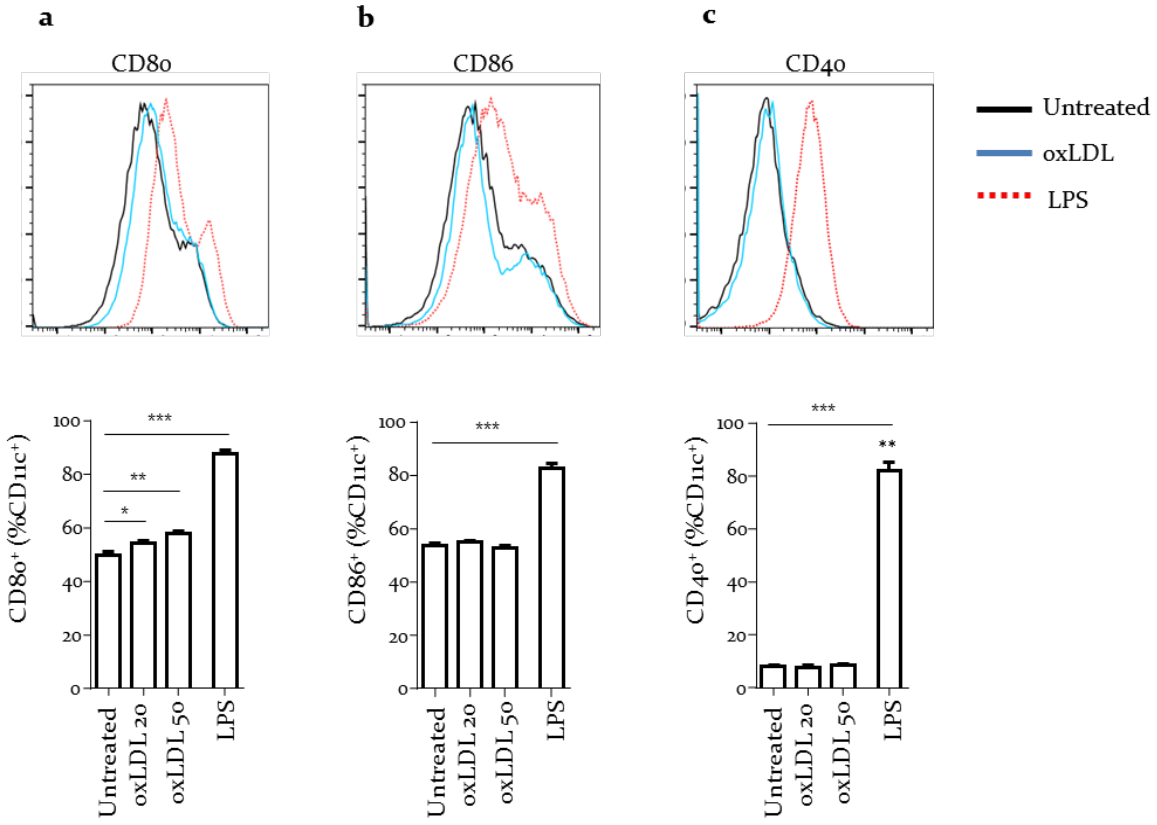


**Figure 19. oxLDL increased CD80 expression in BM-APCs but not CD86 or CD40.** BM-APCs were left untreated or were treated with oxLDL (20 or 50 μg/ml) or LPS (100 ng/ml) for 24 hours. After incubation, nonadherent cells were collected, stained and analyzed by flow cytometry. Percentages of cells expressing CD80 (a), CD86 (b) and CD40 (c) among live CD11c⁺ are shown. One of two (n=4) representative experiments are shown. Only treatment with 50 μg/ml of oxLDL is shown in histograms. Data are presented as mean ± SEM; *p<0.05, **p<0.01; ***p<0.001.

Next, the expression of the activation markers CD80, CD86 and CD40 on CD11c$^{+}$MHCII$^{+}$ APCs from the aorta of *Ldlr*$^{-/-}$ mice fed a HFD for 8 weeks was analyzed. In line with in vitro findings, CD80 was markedly upregulated after HFD (Figure 20a), whereas CD86 remained unaltered (Figure 20b). Interestingly, the expression of CD40 in CD11c$^{+}$MHCII$^{+}$ APCs was increased in *Ldlr*$^{-/-}$ mice fed a HFD compared to those fed a chow diet (Figure 20c).

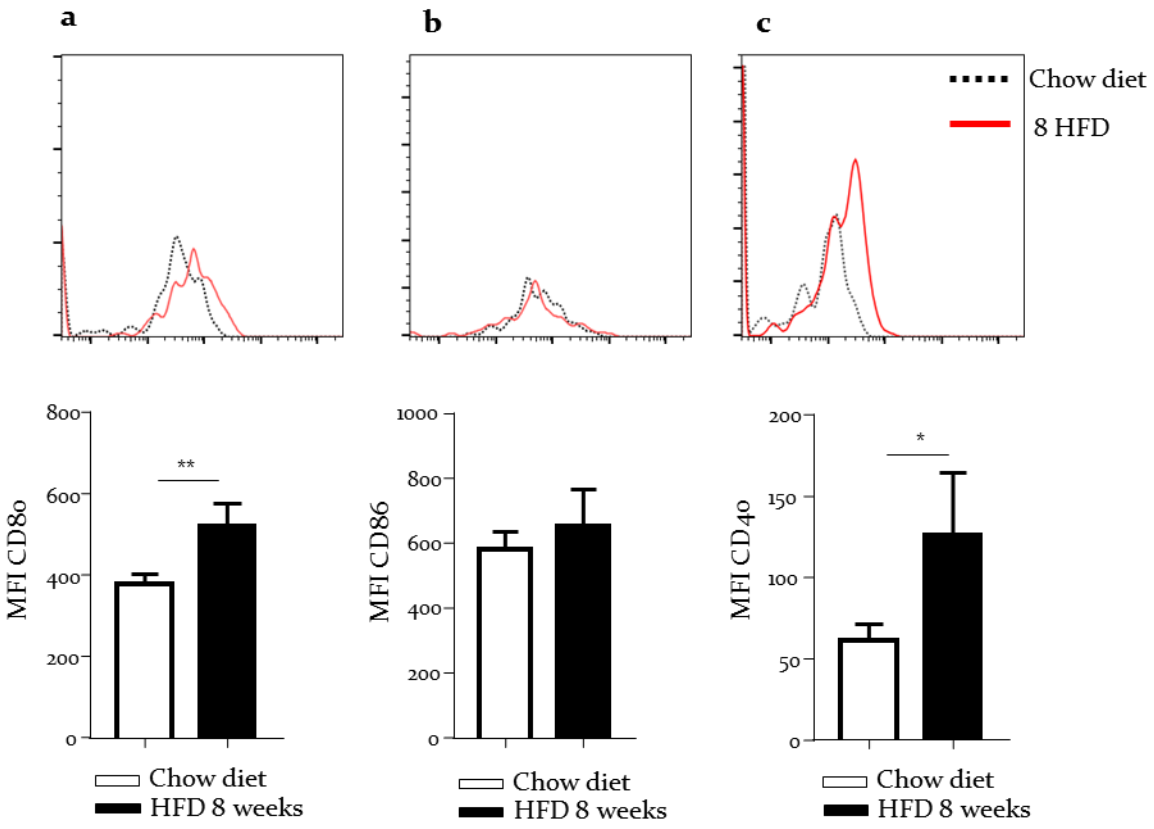


**Figure 20. HFD promoted the upregulation of activating markers on the surface of aortic CD11c$^{+}$ MHCII$^{+}$ APCs.** *Ldlr*$^{-/-}$ mice were fed a chow diet (n=4) or a HFD for 8 weeks (n=4). Aortas were collected and digested enzymatically to obtain a single cell suspension. FC receptors were blocked to avoid unspecific binding. Aortic cells were stained and measured by flow cytometry. Expression of CD86 (a), CD80 (b) and CD40 (c) was measured on CD11c$^{+}$ MHCII$^{+}$ cells. Representative histograms are presented. Data are presented as mean ± SEM; *p<0.05, ***p<0.001.

Immature and mature APCs can be distinguished by their ability to take up particles [216]. While the former are able to efficiently engulf antigens, the latter lose this function and mainly promote antigen presentation to T cells. Given that stimulation with oxLDL had a mild effect on the upregulation of several activation

markers, an OVA-uptake assay to test whether oxLDL might modulate the ability of cultured BM-APCs to engulf particles was used. BM-APCs were treated with different concentrations of oxLDL for 24 hours, and thereafter cells were incubated with FITC-stained OVA at 37°C to promote particle uptake. Even though treatment with LPS led to reduced percentages of FITC$^+$ cells (as it induces a mature phenotype), incubation of BM-APCs with different concentrations of oxLDL did not alter FITC-uptake when compared to untreated cells (Figure 21). Together, these data support the hypothesis that oxLDL alone induces a mild activation status in cultured APCs.

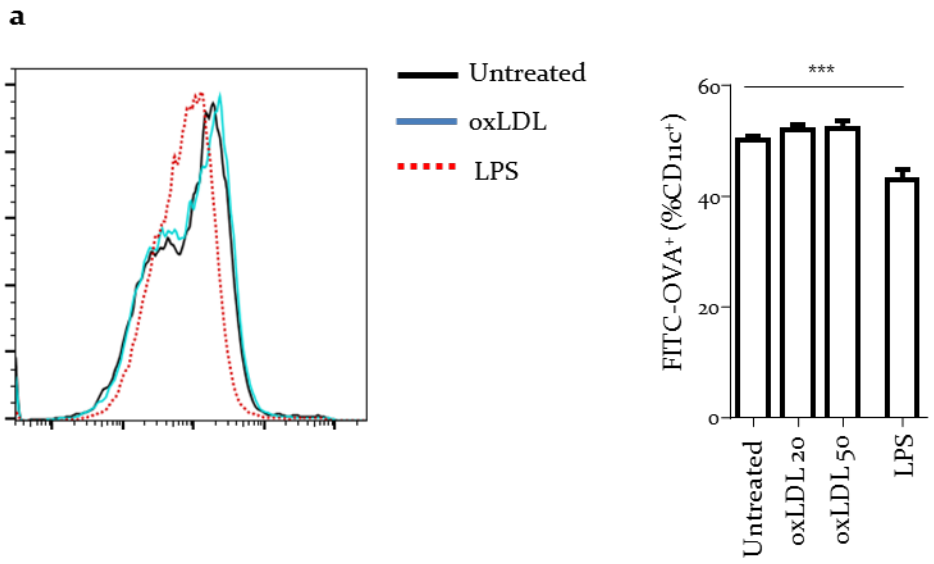


**Figure 21. oxLDL did not affect particle uptake by BM-APCs.** BM-APCs were left untreated or were treated with oxLDL (20 or 50 µg/ml) or LPS (100 ng/ml) for 24 hours in RPMI supplemented with 0.5% FCS. Cells were then washed and incubated with 0.5 mg/ml of FITC-OVA for 30 minutes at 37°C. Cells incubated at 4°C were used as a control to confirm efficient phagocytosis and LPS-treated cells were used as a positive control for the analysis. Cells were then washed twice and measured by flow cytometry. After dead cell exclusion, CD11c$^+$ cells were gated and percentages of cells positive for OVA were analysed. One of two (n=4) representative experiments are shown. Data are presented as mean ± SEM; ***p<0.001.

### 4.2.2. oxLDL sustains IL-23 secretion by TLR-stimulated cells

Previous experiments suggest that oxLDL might not induce IL-23 secretion by BM-APCs. In fact, BM-APCs treated with oxLDL did not show any increase in mRNA levels of *Il23a* compared to the untreated group, as opposed with a robust increase after treatment with LPS (Figure 22a). Analysis of supernatants from oxLDL- and LPS-

treated BM-APCs collected after 3 or 24 hours of stimulation confirmed that oxLDL did not induce secretion of IL-23 (Figure 22b), whereas LPS induced the release of high amounts of the cytokine after 3 hours and declined over time (Figure 22b), as described previously [180, 217].

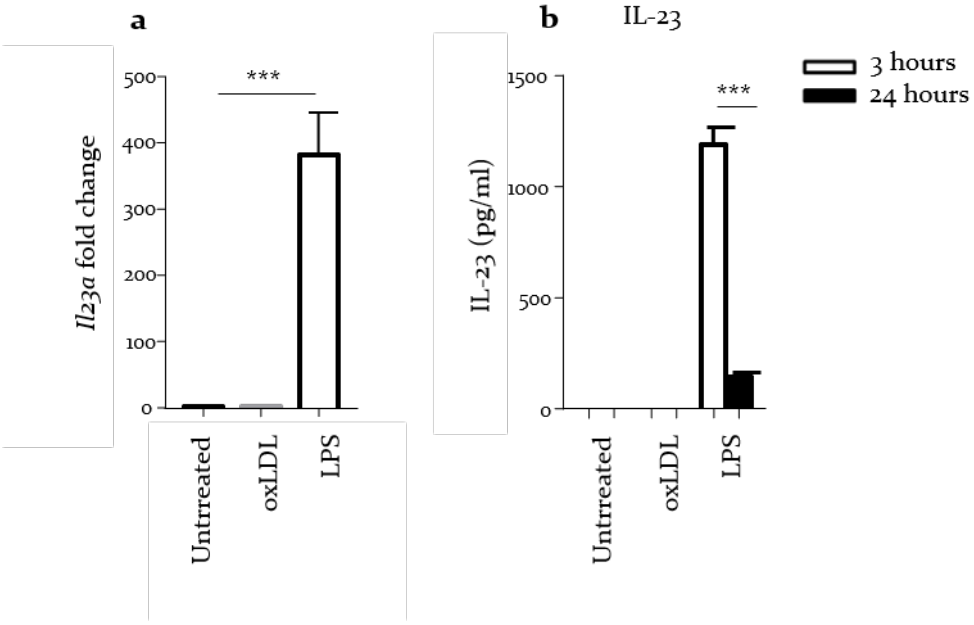


**Figure 22. oxLDL alone could not promote IL-23 secretion by BM-APCs.** BM-APCs were left untreated or were treated with oxLDL (50 μg/ml) or LPS (100 ng/ml). After 3 and 24 hours, non-adherent cells were collected and (a) the amount of *Il23a* mRNA was measured by quantitative real-time PCR. Results were normalized to *Hprt* mRNA and are presented relative to untreated cells. (b) Cell-free supernatant was collected after the indicated time points and IL-23 concentration was measured by ELISA. One of three (n=3) independent experiments is shown. Data are presented as mean ± SEM; **p<0.01; ***p<0.001.

It has been reported that BM-APCs secrete IL-23 upon activation with different TLR agonists, such as LPS (TLR4-agonist) or Pam3CSK4 (TLR-1/2) [217]. Moreover, oxLDL has been reported to potentiate TLR-driven responses [218, 219]. During the progression of atherosclerosis, TLR-activated APCs might encounter oxLDL and alter their ability to secrete IL-23. Two different approaches were performed to ascertain this: 1) incubation of BM-APCs in the presence of different TLR agonists (LPS and Pam3CSK4) together with oxLDL and 2) induction of BM-APCs maturation for 3 hours before adding oxLDL (which will be referred to as "priming"). Surprisingly, oxLDL dramatically increased the amount of IL-23 secreted by BM-APCs when cells were co-

stimulated with LPS or Pam3 together (Figure 23a). The effect was also pronounced when cells were first primed with a TLR agonist, washed and then stimulated with oxLDL alone (Figure 23b). This effect was specific for oxLDL as incubation with native LDL (nLDL) did not change IL-23 secretion either in combination with LPS or after priming (Figures 23a, b). As stimulation with LPS induced a greater response compared to Pam3 stimulation, it was selected for priming in all subsequent experiments.

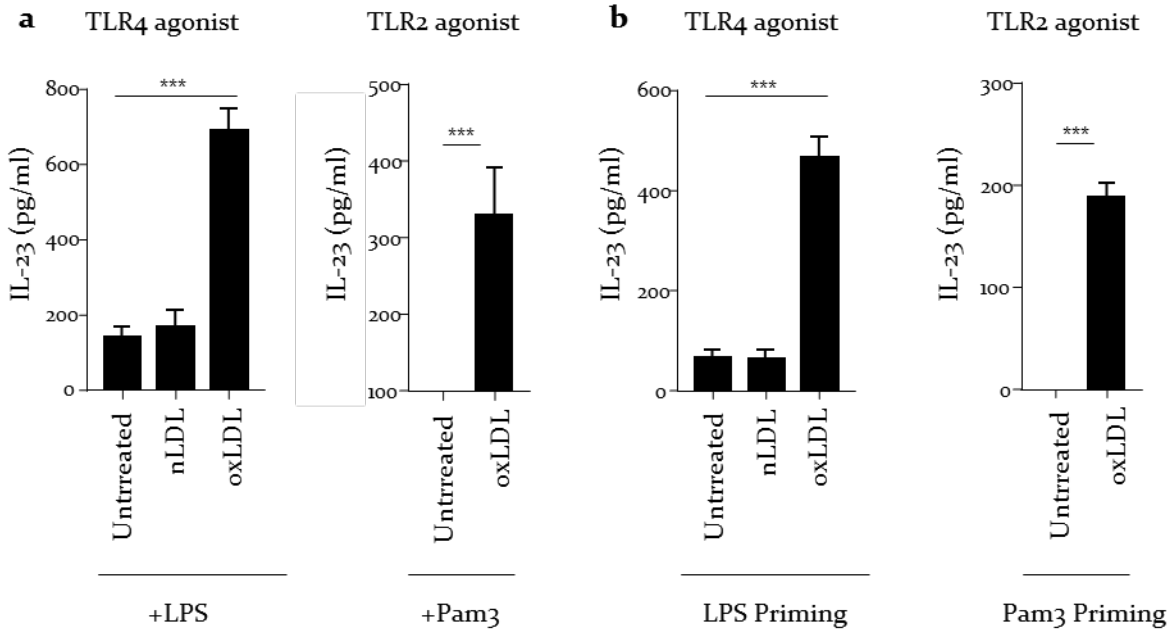


**Figure 23. IL-23 secretion was sustained by oxLDL in TLR-activated BM-APCs**. (a) BM-APCs were stimulated with LPS (100 ng/ml) or $Pam_3CSK_4$ (100 ng/ml) alone or in combination with nLDL (50 µg/ µl) or oxLDL (50 µg/ml) for 24 hours. Cell-free supernatants were collected and IL-23 concentration was measured by ELISA. (b) BM-APCs were primed with LPS (100 ng/ml) or $Pam_3CSK_4$ (100 ng/ml) for 3 hours. Cells were then washed and stimulated with fresh medium containing nLDL (50 µg/ml) or oxLDL (50 µg/ml) overnight. Cell-free supernatant was collected and IL-23 concentration was measured by ELISA. One of three (n=3) independent experiments is shown. Data are presented as mean ± SEM; ***p<0.001.

Sustained IL-23 secretion was concentration-dependent. Low doses (10 µg/ml) of oxLDL significantly increased the amount of the cytokine in the supernatant, which rises with higher (50 µg/ml) concentrations (Figure 24a). This increase was not due to any LPS trace contamination in oxLDL, as priming of BM-APCs and stimulation with oxLDL in the presence of the LPS inhibitor PMB, did not block the ability of oxLDL to upregulate IL-23 secretion (Figure 24b).

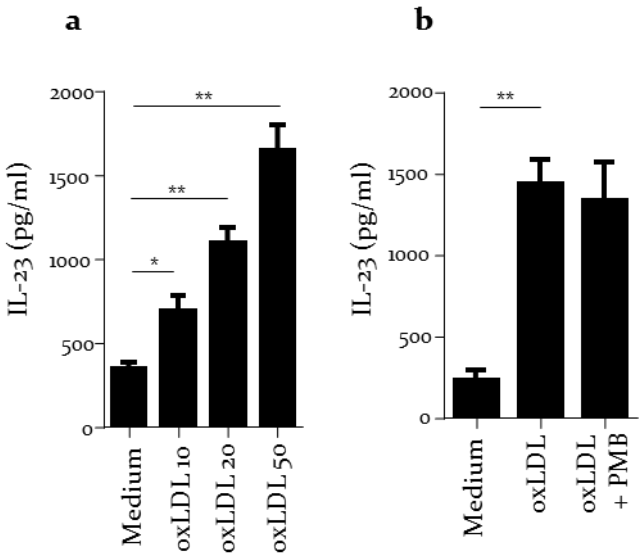


**Figure 24. Sustained IL-23 secretion by oxLDL was concentration dependent.** (a) BM-APCs were primed with LPS (100 ng/ml) for 3 hours and then washed and stimulated in fresh medium containing different concentrations of oxLDL (10, 20 and 50 µg/ml). (b) BM-APCs were treated as described in (a) and in the absence or presence of the gram-negative bacteria inhibitor PMB (10 µg/ml). 24 hours later, cell-free supernatants were collected and measured by ELISA. One of three (n=3) independent experiment is shown. Data are presented as mean ± SEM; *p<0.05; **p<0.01; ***p<0.001.

As both IL-12 and IL-23 share the p40 subunit, it might be possible that the ability of oxLDL to sustain IL-23 secretion in TLR-stimulated BM-APCs was also observable when studying IL-12 secretion. oxLDL stimulation alone did not induce IL-12 secretion either after 3 or 24 hours (Figure 25a). In response to LPS, IL-12 was not detected in the supernatant after the first hours of stimulation, whereas a marked secretion was observed after 24 hours (Figure 25a). Surprisingly, treatment of BM-APCs with both LPS and oxLDL completely abrogated IL-12 secretion after 24 hours (Figure 25b). Again, this effect was mediated by oxidized particles only, as the addition of nLDL did not abrogate secretion (Figure 25b). Using the priming strategy, LPS-primed cells did not secrete IL-12 either when left untreated or treated with oxLDL overnight. These results reveal that oxLDL specifically increased IL-23 but not IL-12 secretion in TLR-activated BM-APCs.

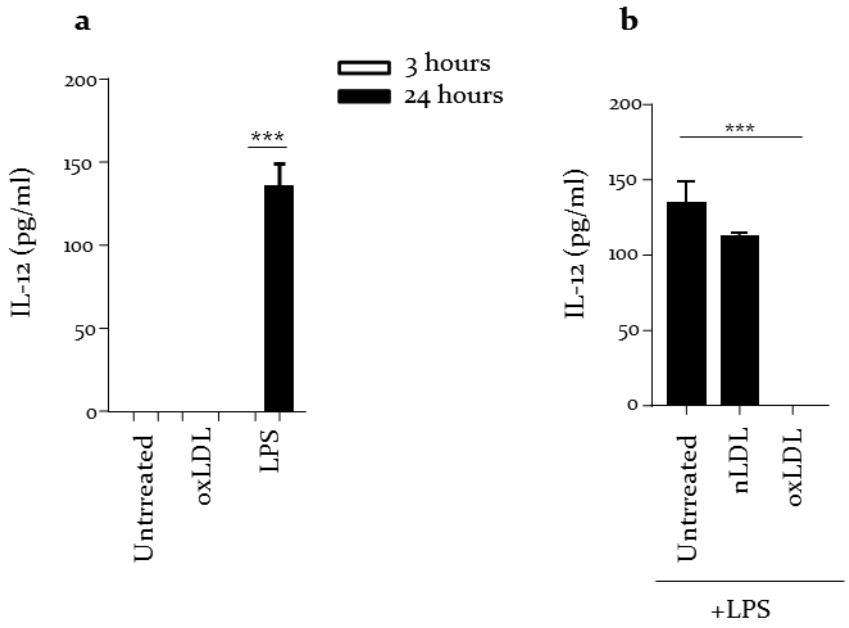


**Figure 25. oxLDL blocked IL-12 secretion in LPS-stimulated BM-APCs.** (a) BM-APCs were left unstimulated or were stimulated with oxLDL (50 μg/ml) or LPS (100 ng/ml) for 3 or 24 hours. (b) BM-APCs were treated with LPS alone (100 ng/ml) or in combination with nLDL (50 μg/ml) or oxLDL (50 μg/ml) for 24 hours. After incubation cell-free supernatant was collected and measured by ELISA. One of two independent experiments is shown. Data are presented as mean ± SEM; ***p<0.001.

Finally, to test whether the observed effect on IL-23 was also reproducible ex vivo, sectioned mice aorta were sectioned (as described in the Methods) and cultured overnight in the presence of LPS, oxLDL or a combination of both. After 24 hours, the supernatant was analyzed and the amount of IL-23 relative to the total DNA content measured. As expected, treatment with LPS increased the secretion of IL-23 when compared to the untreated group (Figure 26a). Stimulation with both LPS and oxLDL further increased the amount of IL-23 detected in the supernatant (Figure 26a). Unexpectedly, treatment with oxLDL alone also induced the secretion of IL-23 (Figure 26a). These results suggest that oxLDL can modify IL-23 secretion in cultured BM-APCs and cultured aortic cells.

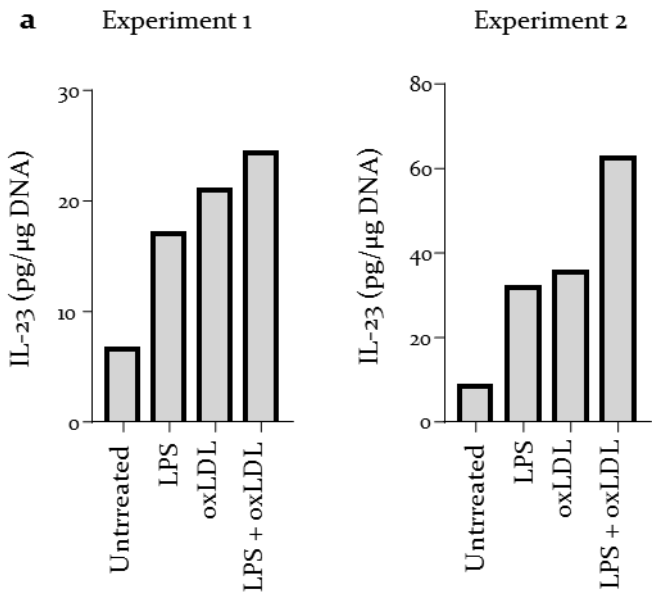


**Figure 26. Aortic cells produced IL-23 in response to LPS and oxLDL.** Aortas from C57B6/J animals (n=1 for each condition) were first cleaned of any associated perivascular adipose tissue (PVAT) and then sectioned in 15 rings of 2mm starting from the aortic arch. Rings were maintained in RPMI and washed twice with PBS before culturing overnight either unstimulated or stimulated with LPS (100 ng/ml), oxLDL (50 µg/ml) or both. 24 hours later, rings and supernatants were collected. DNA concentration isolated from rings was measured with Nanodrop and used to relativize the amount of IL-23 detected by ELISA. Two representatives experiments are shown.

### 4.2.3. *Il23a* mRNA levels were increased in the aortic sinus in mice fed a HFD

It has been shown that in humans, serum IL-23 is increased in patients affected by PAD [196] and that IL-23 levels are high in symptomatic patients affected by CAD [220]. Increased IL-23 production by TLR-activated APCs after treatment with oxLDL might have raised serum levels of IL-23 during the progression of atherosclerosis. To ascertain this, *Ldlr*$^{-/-}$ mice were fed a HFD for 4, 6 and 8 weeks and serum IL-23 was analyzed by ELISA. Unexpectedly, IL-23 was not detected at any time point studied.

Next, modulation of IL-23 in the spleen, aortic sinus, and aorta in *Ldlr*$^{-/-}$ mice fed a HFD for 6 weeks was studied. Although *Il23a* mRNA levels were unaltered in spleen and aorta when comparing *Ldlr*$^{-/-}$ mice fed a chow diet with *Ldlr*$^{-/-}$ mice fed a HFD for 6 weeks, an increase in expression levels specifically in the aortic sinus was observed (Figure 27). These data suggest a localized effect of IL-23 in the aortic sinus.

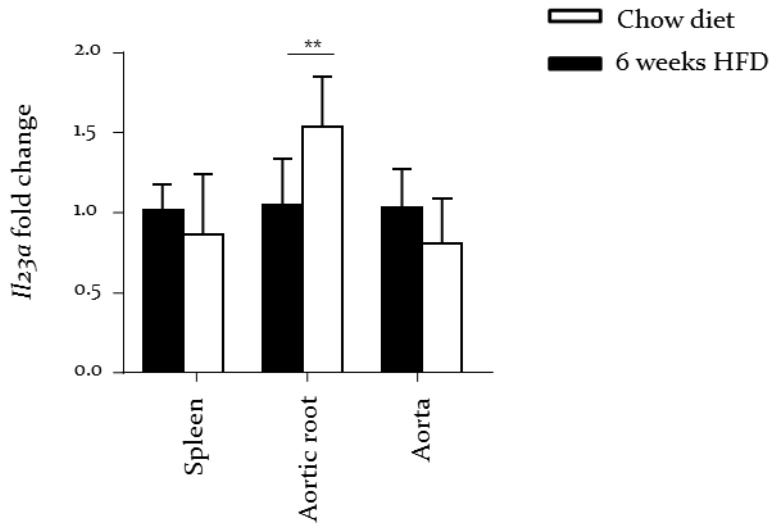


**Figure 27. 6 weeks of HFD increased mRNA levels of *Il23a* specifically in the aortic root of *Ldlr*$^{-/-}$ mice.** *Ldlr*$^{-/-}$ mice were fed a chow diet (n=4) or a HFD for 6 weeks (n=5). RNA from spleen, aortic sinus and aorta was extracted, and mRNA levels of *Il23a* were analyzed by qPCR. Results were normalized to *Hprt* mRNA and are presented relative to the group fed a chow diet. Data are presented as mean ± SEM; **p<0.01.

### 4.2.4. Decreased circulating monocytes in IL-23R-deficient *Ldlr*$^{-/-}$ mice

In vitro and in vivo data revealed that IL-23 expression can be modulated by oxLDL and HFD. However, it is still not clear whether altered levels of IL-23 cause or inhibit atherosclerosis or are a response encountered during the progression of the disease. Previously, a study using an *Il23p19*$^{-/-}$ mouse model showed that the p19 subunit of IL-23 can function as an intracellular peptide altering the expression of adhesion markers on ECs [178]. Thus, the use of this model to study the effect of IL-23 in atherosclerosis may be taken with caution, as not only the release of IL-23 by APCs is affected, but also other mechanisms reported to have a profound effect in atherosclerosis, such as the modulation of adhesion molecules by ECs [221]. To overcome this effect, an IL-23R-knock-in mouse model crossed with *Ldlr*$^{-/-}$ mice was used, in which signaling through the IL-23R is abrogated in homozygous animals.

First, immune responses under homeostatic conditions were characterized. In line with previous results [189], similar percentages of total T cells, $CD4^+$ or $CD8^+$ T cells, γδ T cells, B cells, $CD11c^+$ and $CD11b^+$ cells in the blood, spleen or lymph nodes were observed (data not shown). Furthermore, levels of Tregs in the blood (7.26% ± 1.55%

*versus* 6.36% ± 1.19% of $CD25^+FoxP3^+$ cells among $CD4^+$ T cells in *Ldlr*$^{-/-}$ mice compared to *Ldlr*$^{-/-}$*Il23r*$^{-/-}$ mice; p=0.32), lymph nodes (5.28% ± 0.85% *versus* 5.56% ± 0.33% of $CD25^+FoxP3^+$ cells among $CD4^+$ T cells in *Ldlr*$^{-/-}$ mice compared to *Ldlr*$^{-/-}$*Il23r*$^{-/-}$ mice; p=0.56) or spleen (10.85 % ± 0.62% *versus* 11.2% ± 1.00% of $CD25^+FoxP3^+$ cells among $CD4^+$ T cells in *Ldlr*$^{-/-}$ mice compared to *Ldlr*$^{-/-}$*Il23r*$^{-/-}$ mice; p=0.55) were similar among groups. However, decreased percentages and absolute numbers of circulating monocytes in *Ldlr*$^{-/-}$*Il23r*$^{-/-}$ mice compared to *Ldlr*$^{-/-}$ controls were detected (Figure 28a), whereas the percentage of monocytes was unaltered in spleen (Figure 28c, left). The percentage of neutrophils was similar between groups at both locations (Figure 28b, c). No differences were noted in body weight between groups (23.1g ± 2.36g in *Ldlr*$^{-/-}$ mice *versus* 24.18g ± 1.32g *Ldlr*$^{-/-}$*Il23r*$^{-/-}$ mice).

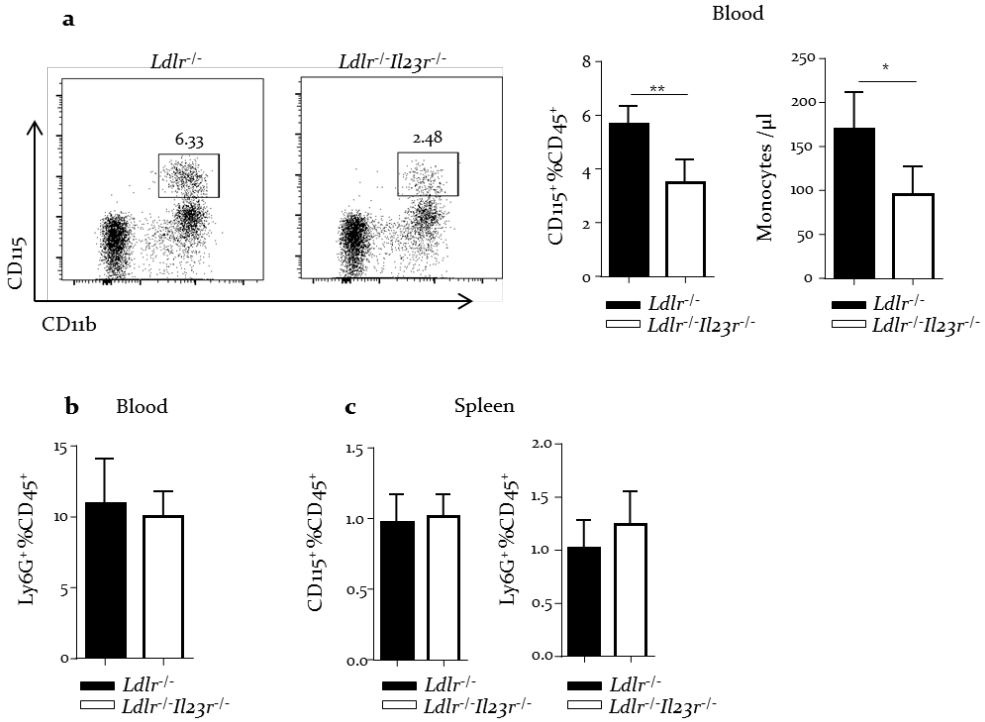


**Figure 28. *Il23r* deficiency led to decreased numbers of circulating monocytes**. Single cell suspension from the blood and spleen from *Ldlr*$^{-/-}$ (n=4) and *Ldlr*$^{-/-}$*Il23r*$^{-/-}$ mice (n=4) were analyzed by flow cytometry. Monocytes were defined as $CD11b^+CD115^+$ cells and neutrophils were defined as $CD11b^+Ly6G^+$ cells. (a) Representative dot plots and quantification of percentages of monocytes (left) and cells per µl of blood (right). (b) Percentages of circulating neutrophils. (c) Percentages of monocytes (left) and neutrophils (right) in the spleen. Data are presented as mean ± SEM; *p<0.05 **p<0.01.

As IL-23 promotes IL-17 secretion in IL-23R-expressing cells (see Chapter 1.5.1), IL-17 responses in IL-23R-deficient *Ldlr*$^{-/-}$ mice were compared to *Ldlr*$^{-/-}$ controls. Of note, levels of IL-17 were unaltered in *Ldlr*$^{-/-}$*Il23r*$^{-/-}$ compared to *Ldlr*$^{-/-}$ mice, both in the $Th_{17}$ $CD4^+$ fraction and in IL-17-producing γδ T cells in the blood and spleen (Figure 29b, d, f, and h). Similarly, unaltered levels of IFN-γ –secreting cells were noted (Figure 29a, c, and e), although a slight increase in IFN-γ-producing γδ T cells in the spleen was observed in IL-23R-deficient *Ldlr*$^{-/-}$ mice (Figure 29g). Importantly, IL-17 production was severely impaired in the aortic root of *Ldlr*$^{-/-}$*Il23r*$^{-/-}$ animals (Figure 30).

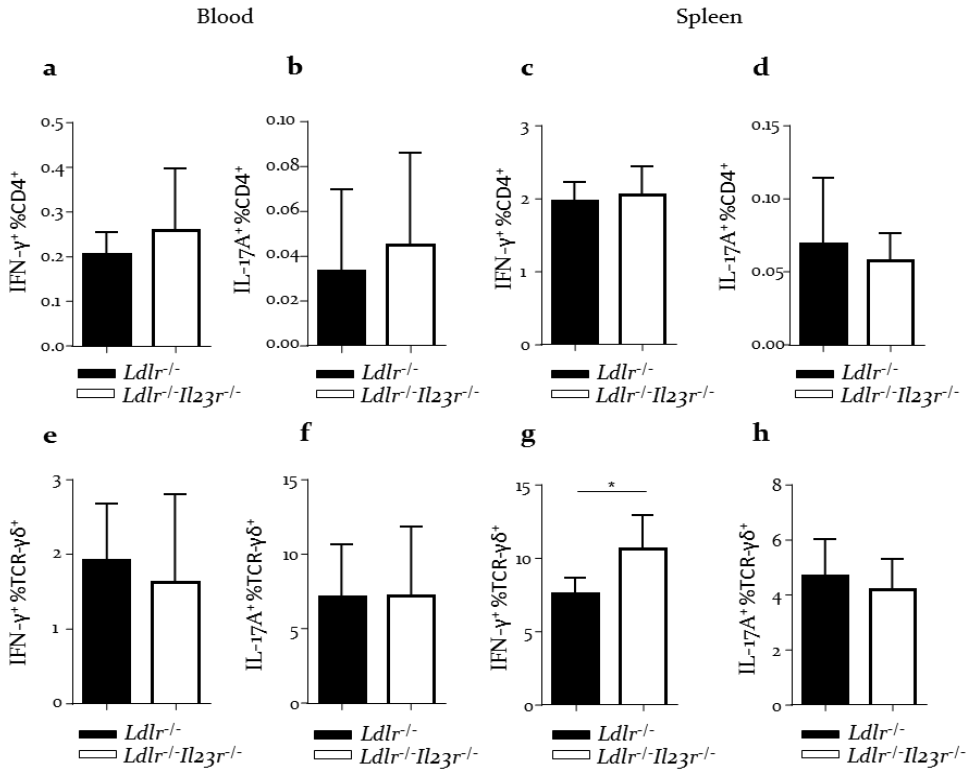


**Figure 29. IL-17 responses in blood and spleen were unaltered in *Ldlr*$^{-/-}$*Il23r*$^{-/-}$ compared to *Ldlr*$^{-/-}$ mice.** Blood and splenocytes from *Ldlr*$^{-/-}$ (n=5) and *Ldlr*$^{-/-}$*Il23r*$^{-/-}$ mice (n=6) were stimulated with PMA (50 ng/ml), ionomycin (750 ng/ml) and BFA (2.5 μg/ml) for 4 hours and then analyzed by flow cytometry. (a-d) $Th_1$ and $Th_{17}$ responses were analyzed in the blood and spleen, defined as IFN-$\gamma^+$ and IL-$17A^+$ $CD4^+$ T cells, respectively. (e-f) Production of IFN-$\gamma^+$ and IL-$17A^+$ among TCR-$\gamma\delta^+$ cells. Data are presented as mean ± SEM; *p<0.05.

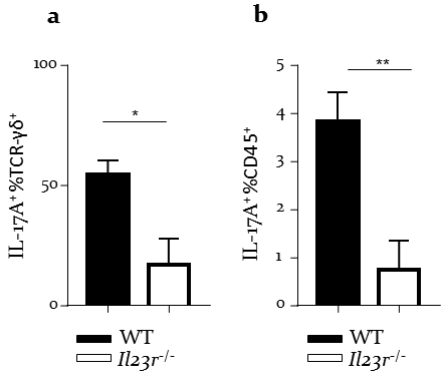


**Figure 30. IL-17 secretion was markedly impaired in the aortic root of IL-23R-deficient mice**. Single cell suspensions from the aortic sinus were obtained from WT (n=3) and *Il23r*$^{-/-}$ mice (n=3) and measured by flow cytometry. Cells were treated with PMA (50 ng/ml), ionomycin (750 ng/ml) and BFA (2,5 μg/ml) to stimulate cytokine production as described in the Methods. (a) First, total live CD45$^{+}$ leukocytes and TCR-γδ$^{+}$ cells were gated to study IL-17 production. (b) Total IL-17-producing cells were analyzed by evaluating IL-17A$^{+}$ cells among total live CD45$^{+}$ cells. Date are presented as mean ± SEM, *p<0.05; **p<0.01.

T cells can be polarized into non-pathogenic $Th_{17}$ responses, which require TGF-β and IL-6 or pathogenic $Th_{17}$ responses, that are TGF-β independent and requires the presence of IL-1β, IL-23, and IL-6. To study $Th_{17}$ cell polarization in IL-23R-deficient cells, naïve T cells were cultured in the presence of a pathogenic and non-pathogenic $Th_{17}$ cocktail. When cells were polarized in the presence of the non-pathogenic cocktail, naïve T cells from WT and *Ldlr*$^{-/-}$*Il23r*$^{-/-}$ mice produced similar amounts of IL-17 (Figure 31, left bars). However, when the pathogenic-cocktail was used, the amount of IL-17 was greatly reduced in IL-23R-deficient T cells (Figure 31, right bars). This suggests that *Il23r* deficiency impairs pathogenic but not non-pathogenic $Th_{17}$ responses.

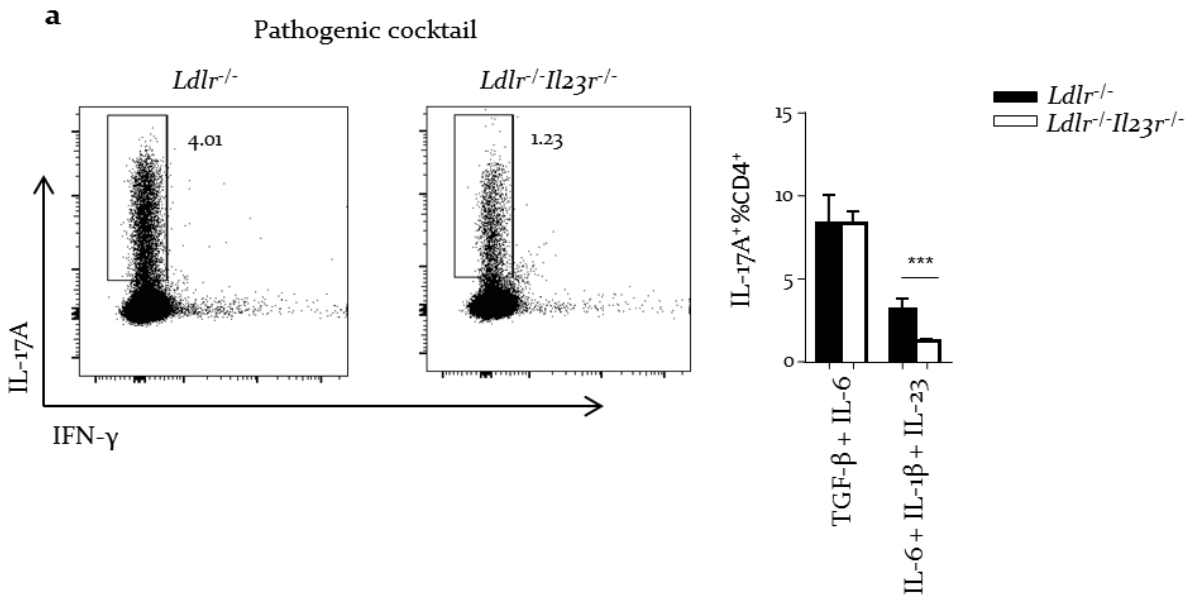


**Figure 31. *Il23r* deficiency impairs pathogenic but not non-pathogenic $Th_{17}$ responses.** Splenic naïve T cells ($CD62L^+$ $CD44^-$ $CD25^-$) were sorted from *Ldlr*$^{-/-}$ (n=4) or *Ldlr*$^{-/-}$ *Il23r*$^{-/-}$ mice (n=4) and polarized under non-pathogenic $Th_{17}$ conditions (TGF-β + IL-6, see Methods) or pathogenic $Th_{17}$ conditions (IL-6 + IL-1β + IL-23, see Methods) for 96 hours. Cells were then collected and stimulated with PMA (50 ng/ml), ionomycin (750 ng/ml) and BFA (2,5 μg/ml) to induce cytokine production, and analyzed by flow cytometry. Data are presented as mean ± SEM; ***p<0.001.

### 4.2.5. IL-23R is highly expressed in γδ T cells in the aortic root

Previous results studying IL-17 secretion showed a marked reduction of IL-17 in the aortic root of IL-23R-deficient animals. To study which immune cell type expressed the receptor in the aortic tissue, the *Il23r*$^{gfp/+}$ reporter mouse was used. Expression of IL-23R ($GPF^+$) was measured in the aortic sinus and aorta separately. As shown in Figure 32, less than 50% of γδ T cells in the aorta expressed IL-23R (average 42% ± 12.5% of IL-$23R^+$ among TCR-$γδ^+$ T cells), whereas more than 70% γδ T cells were positive in the aortic root (average 73% ± 15% IL-$23R^+$ among TCR-$γδ^+$ T cells), revealing a tissue-specific distribution. αβ T cells also expressed IL-23R but at much lower levels (Figure 32). Of note, no GFP expression in $CD11b^+$ and $CD11c^+$ cells in the aortic root and aorta was noted (Figure 33 and data not shown), suggesting that in the resting aorta, APCs might not be able to respond to IL-23.

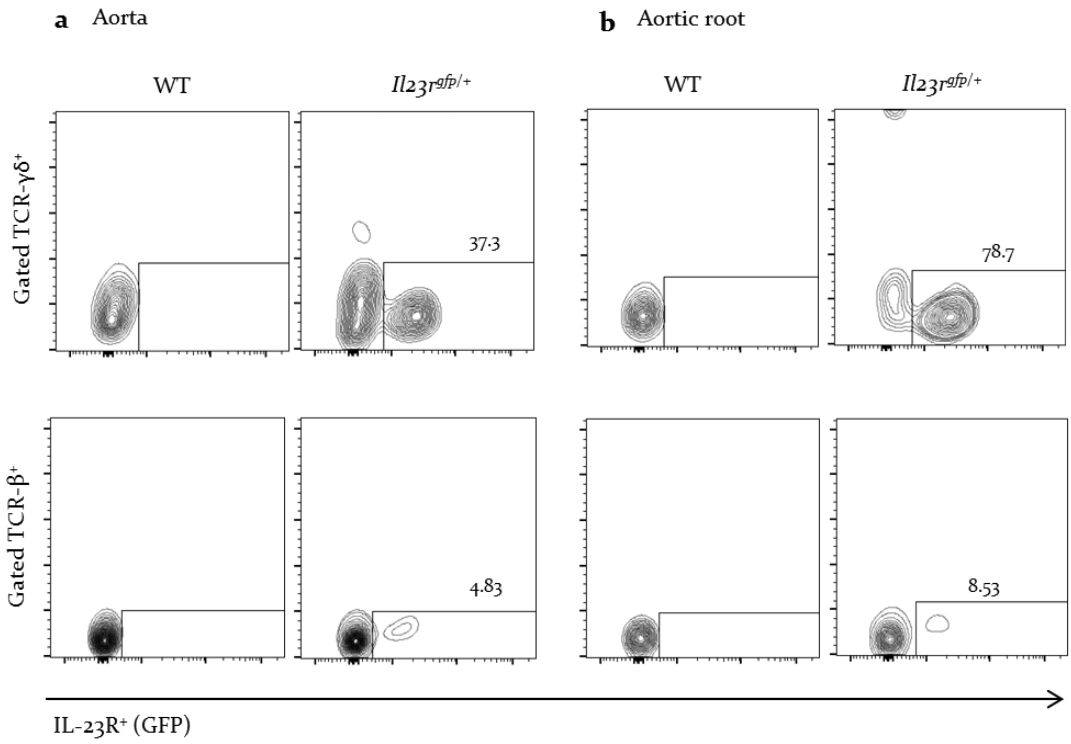


**Figure 32. IL-23R expression in the aortic sinus and aorta is primarily localized in the γδ T cell compartment.** Single cell suspensions from the aorta (a) and the aortic root (b) were obtained from *Ldlr*$^{-/-}$ and *Ldlr*$^{-/-}$ *Il23r*$^{gfp/+}$ mice and analyzed by flow cytometry. Dead cells were excluded from the analysis. IL-23R expression (GFP) in TCR-γδ$^{+}$ (upper panels) and TCR-β$^{+}$ (lower panels). Representative dot plots are shown. Numbers indicated gated events. One of three representative experiments is shown.

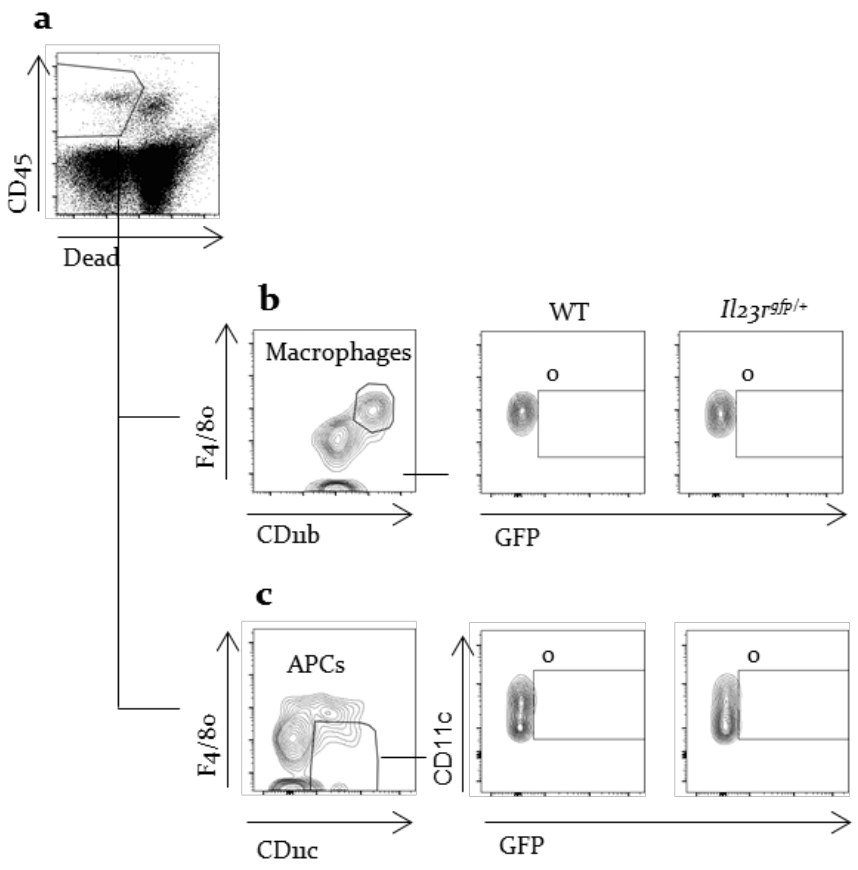


**Figure 33. Aortic CD11b$^+$F4/80$^+$ macrophages and CD11c$^+$ APCs do not express IL-23R.** Aortic sinus from *Ldlr*$^{-/-}$ (n=5) and *Ldlr*$^{-/-}$*Il23r*$^{gfp/+}$ mice (n=4) was digested and analyzed by flow cytometry. (a) Gating strategy for the detection of live lymphocytes in the aortic sinus. (b) GFP expression among CD11b$^+$F4/80$^+$ macrophages or (c) CD11c$^+$F4/80$^-$ APCs in the aortic root. Representative dot plots are shown. Numbers indicated gated events. One out of two representative experiments is shown.

As γδ T cells expressed the highest levels of GFP, the number of these cells in *Ldlr*$^{-/-}$ *Il23r*$^{-/-}$ mice was analyzed. Indeed, percentages of γδ T cells both in the aorta and in the aortic root were dramatically reduced in IL-23R-deficient *Ldlr*$^{-/-}$ mice (Figure 34).

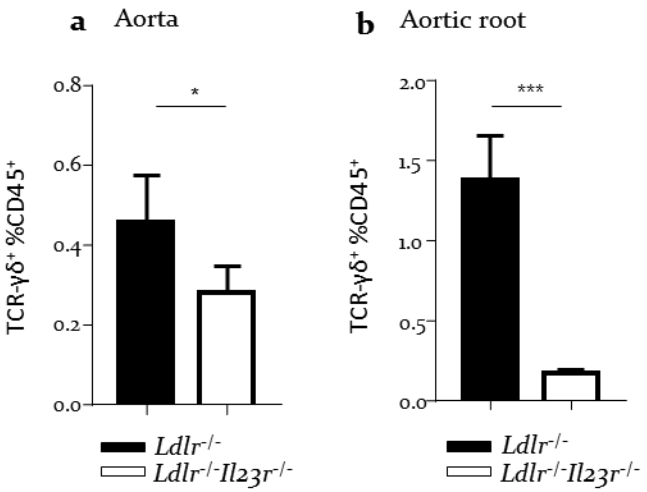


**Figure 34. Reduced frequencies of γδ T cells in the aorta and aortic sinus in IL-23R-deficient *Ldlr*$^{-/-}$ mice.** Single cell suspensions from the aorta and the aortic root were obtained from *Ldlr*$^{-/-}$ (n=5) and *Ldlr*$^{-/-}$*Il23r*$^{-/-}$ mice (n=5) fed a chow diet and were analyzed by flow cytometry. Percentages of γδ T cells in the (a) aorta and (b) aortic root among total live CD45$^{+}$ cells. Data are presented as mean ± SEM; *p<0.05; ***p<0.001.

γδ T cells were the only cell type with the ability to produce IL-17 in the root, and IFN-γ secretion was confined to the TCR-β$^{+}$ subset (Figure 35). IL-23R expression was associated with IL-17 secretion, as all IL-17$^{+}$TCR-γδ$^{+}$ T cells were IL-23R$^{+}$, compared to IFN-γ$^{+}$TCR-β$^{+}$ cells, which were IL-23R$^{-}$ (Figure 35). Interestingly, IL-23R$^{+}$ γδ T cells also expressed GM-CSF at much higher levels compared to IL-23R$^{-}$ cells (Figure 36a). Moreover, the expression of GM-CSF was reduced in γδ T cells from *Ldlr*$^{-/-}$*Il23r*$^{-/-}$ animals (Figure 36b). Noteworthy, *Ldlr*$^{-/-}$ mice fed a HFD for 6 or 12 weeks showed increased percentages of IL-17A$^{+}$GM-CSF$^{+}$ double positive γδ T cells in the aortic root (Figure 37), suggesting an expanded pathogenic capability of IL-23R$^{+}$ γδ T cells.

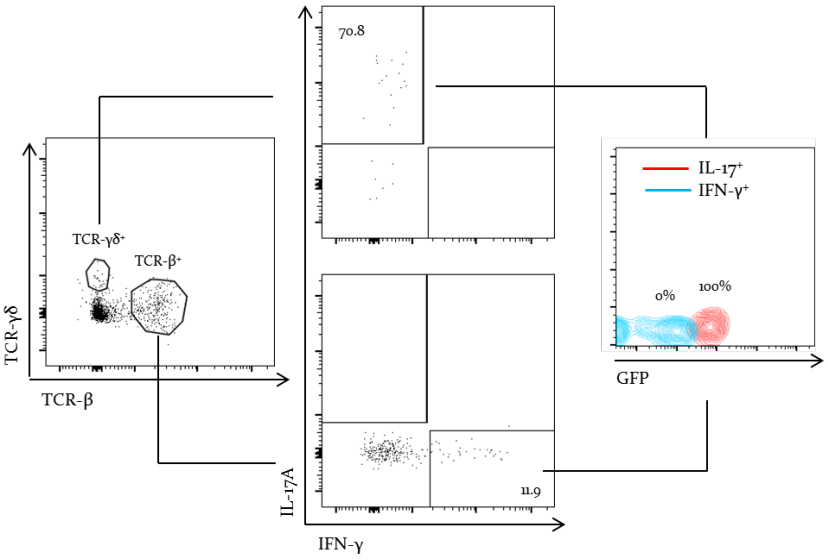


**Figure 35. Resident γδ T cells are the only producers of IL-17 in the aortic root.** Single cell suspension from the aortic root from *Ldl*$^{-/-}$*Il23r*$^{gfp/+}$ mice were stimulated to induce intracellular cytokine production as described in the Methods. One of two representative experiments is shown. Representative dot plots are shown. Numbers indicated gated events.

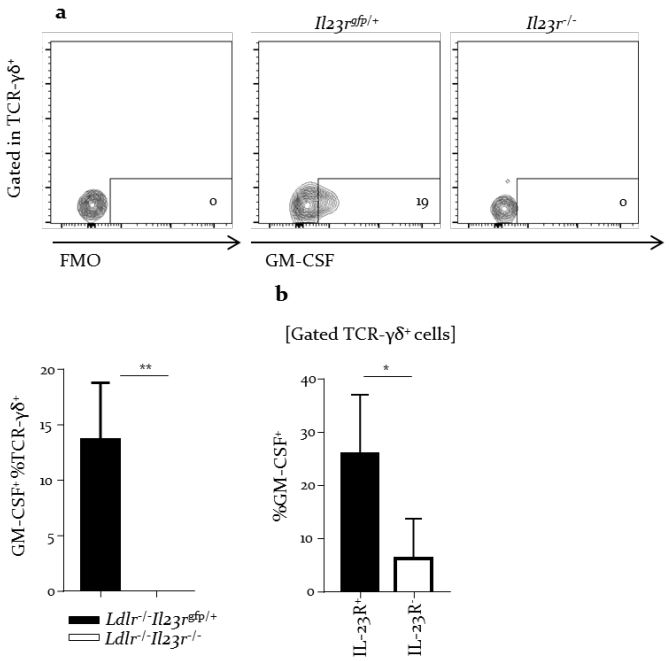


**Figure 36. Aortic resident γδ T cells elicit a pathogenic phenotype.** Single cell suspensions from the aortic root from *Ldlr*$^{-/-}$*Il23r*$^{gfp/+}$ (n=3) and *Ldlr*$^{-/-}$*Il23r*$^{-/-}$ mice (n=3) were stimulated to induce intracellular cytokine production as described in the Methods. (a) GM-CSF$^{+}$ among TCR-γδ$^{+}$ cells. Representative dot plots are shown. Numbers indicated gated events. (b) Expression of GM-CSF in IL-23R$^{+}$ and IL-23R$^{-}$ γδ T cells. Data are presented as mean ± SEM; *p<0.05; **p<0.01.

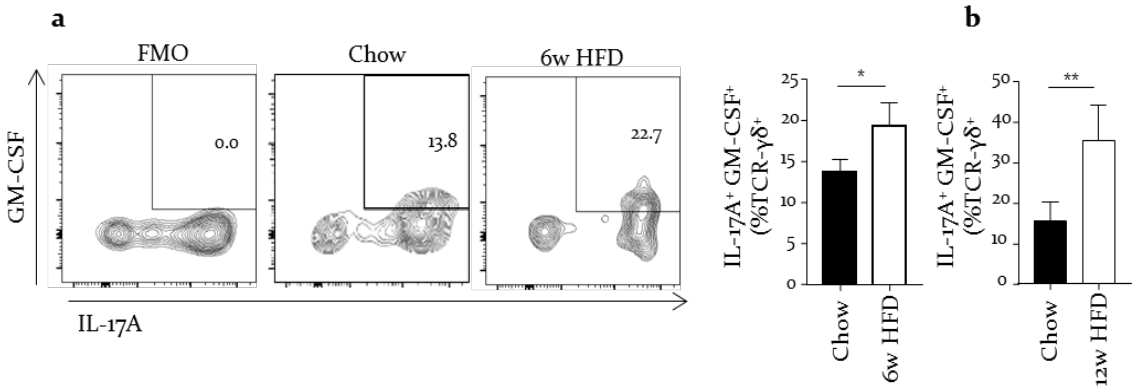


**Figure 37. Pathogenic signature in γδ T cells from the aortic root of *Ldlr*$^{-/-}$ mice fed a HFD**. *Ldlr*$^{-/-}$ mice were fed a chow diet (n=9), a HFD for 6 weeks (n=4) or a HFD for 12 weeks (n=9), aortic sinus was digested and cells were stimulated as specified in the Methods. After stimulation, cells were stained and measured by flow cytometry. Dead cells were excluded for the analysis. (a) Percentages of double positive IL-17$^{+}$GM-CSF$^{+}$ among gated TCR-γδ$^{+}$ cells in the aortic sinus after 6 weeks of HFD or (b) 12 weeks of HFD. Representative dot plots are shown. Numbers indicated gated events. Data is presented as mean ± SD. *p<0.05, **p<0.01. FMO: fluorescent minus one.

### 4.2.6. *Il23r* deficiency inhibits the development of early atherosclerosis and reduced plaque necrosis

*Ldlr*$^{-/-}$ and *Ldlr*$^{-/-}$*Il23r*$^{-/-}$ mice were fed a HFD for 6 or 12 weeks to study early and late stages of atherosclerosis. After 6 weeks of diet, body weight, white blood cell count, and serum cholesterol were similar in *Ldlr*$^{-/-}$ and *Ldlr*$^{-/-}$*Il23r*$^{-/-}$ animals (Table 3).

**Table 3. Body weight, white blood cell (WBC) counts and serum cholesterol levels in *Ldlr*$^{-/-}$ (n=13) and *Ldlr*$^{-/-}$*Il23r*$^{-/-}$ mice (n=16) mice fed a HFD for 6 weeks.**

| | *Ldlr*$^{-/-}$ | *Ldlr*$^{-/-}$*Il23r*$^{-/-}$ | *p-value* |
|---|---|---|---|
| **Body weight (g)** | 22.72 ± 3.44 | 22.6 ± 2.732 | 0.913 |
| **WBC count (10³/ µl)** | 4.62 ± 1.14 | 4.26 ± 1.566 | 0.51 |
| **Cholesterol (µg/ml)** | 22337 ± 3526 | 25164 ± 4285 | 0.06 |

Although plaque size was similar throughout the aorta between groups (Figure 38a), a decreased lesion size specifically in the aortic root was observed in IL-23R-deficient *Ldlr*$^{-/-}$ animals after 6 weeks of HFD (Figure 38b). Characterization of plaque composition revealed that plaques from *Ldlr*$^{-/-}$*Il23r*$^{-/-}$ mice showed a smaller necrotic core area compared to *Ldlr*$^{-/-}$ controls (Figure 39a), whereas macrophage, SMC and collagen content showed similar values (Figure 39b-d).

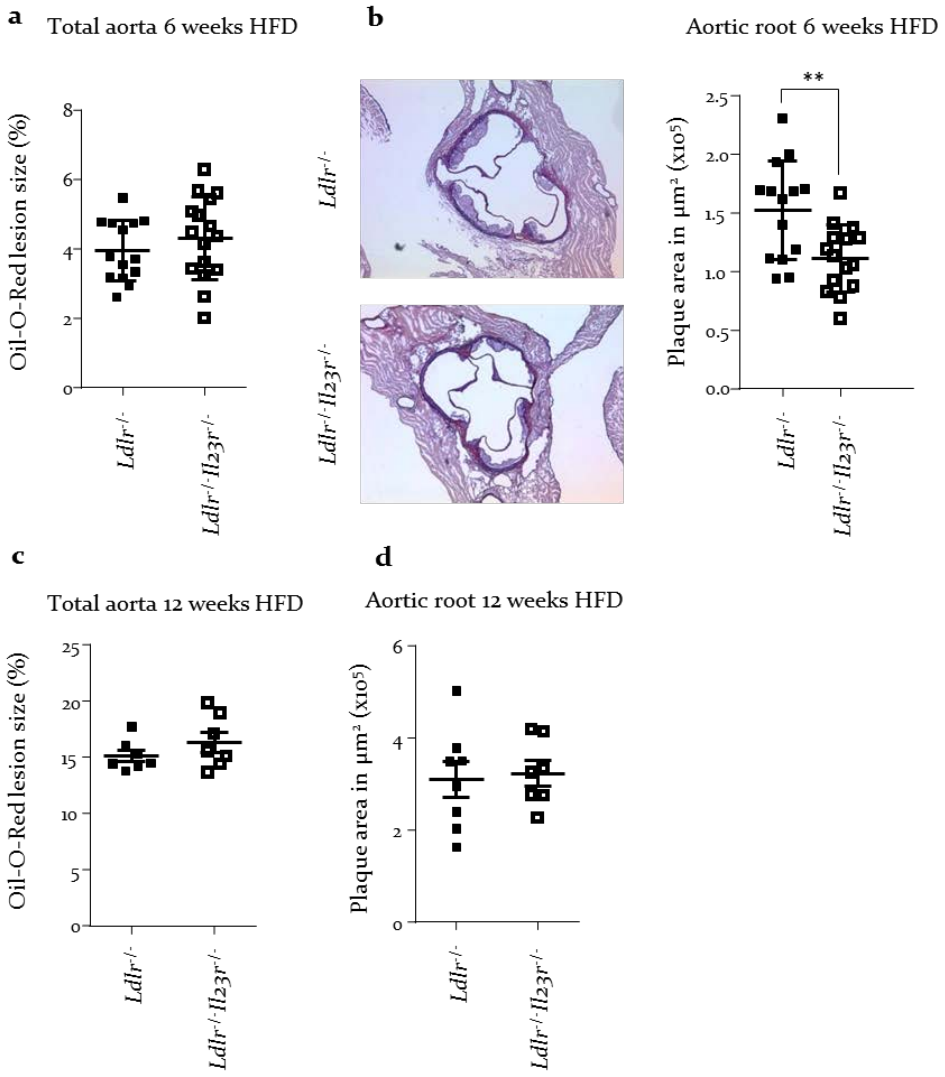


**Figure 38. *Il23r* deficiency protects against the development of atherosclerosis in the aortic root only at early time points of lesion formation.** Quantification of plaque area in Oil-Red-O stained aortas after (a) 6 and (c) 12 weeks of HFD, and quantification of plaque area in Aldehyde-Fuchsin-stained aortic root sections after (b) 6 and (d) 12 weeks of HFD in atherosclerotic *Ldlr*$^{-/-}$ (6 weeks, n=13; 12 weeks, n=8) and *Ldlr*$^{-/-}$*Il23r*$^{-/-}$ (6 weeks, n=16; 12 weeks, n=7). Representative images of the aortic root sections are shown. Data are presented as mean ± SEM; **p<0.01

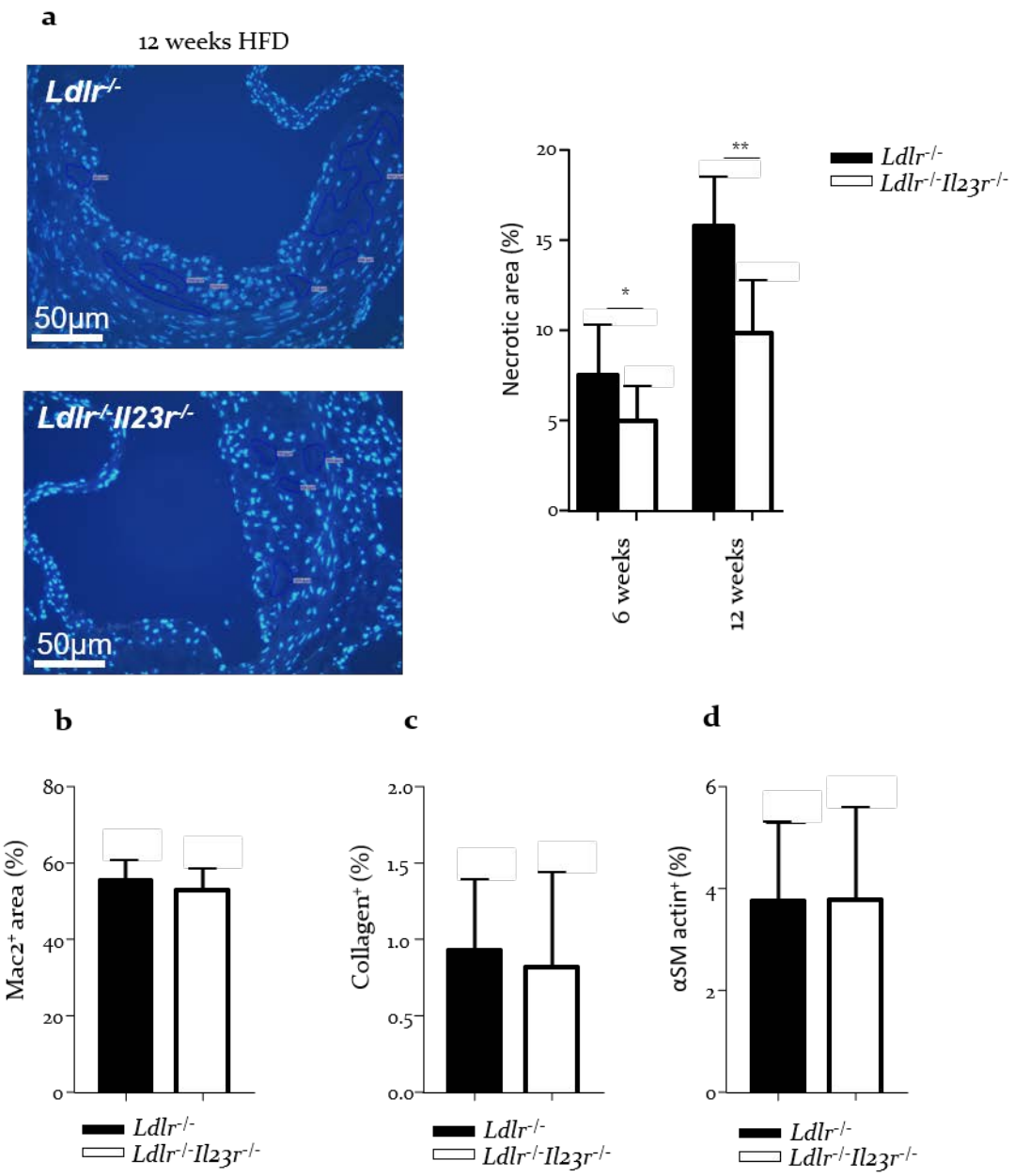


**Figure 39. Deficiency of IL-23R in *Ldlr*$^{-/-}$ mice fed 6 and 12 weeks a HFD reduced plaque necrosis.** Quantification of necrotic areas in the aortic root of *Ldlr*$^{-/-}$ (n=13) and *Ldlr*$^{-/-}$*Il23r*$^{-/-}$ mice (n=16) fed a HFD for 6 and 12 weeks. Representative images of DAPI stainings after 12 weeks of HFD are shown, scale bars: 50µm. To study macrophage, collagen and SMC content, slides were counterstained with (b) Mac-2, (c) Sirius red or (d) SMC actin. Data are presented as mean ± SEM; *p<0.05; **p<0.01

After 12 weeks of HFD, body weight and white blood cell counts were similar, as well as total serum cholesterol (Table 4). At this time point, lesion size was unaltered throughout the aorta but also in the aortic sinus (Figure 38c, d). However, plaque composition revealed that the necrotic core size was reduced in IL-23R-deficient *Ldlr*$^{-/-}$ mice (Figure 39a, right bars), while other parameters, such as macrophage (42.65% ± 7.22% *versus* 49.25% ± 5.75% of Mac2$^{+}$ area in plaques from *Ldlr*$^{-/-}$ compared to *Ldlr*$^{-/-}$ *Il23r*$^{-/-}$ mice; p=0.18), SMC (3.34% ± 1.09% *versus* 4.85% ± 3.68% of αSM actin$^{+}$ area in plaques from *Ldlr*$^{-/-}$ compared to *Ldlr*$^{-/-}$*Il23r*$^{-/-}$ mice; p=0.85) or collagen content (8.81% ± 2.66% *versus* 10.75% ± 2.79% of collagen$^{+}$ area in plaques from *Ldlr*$^{-/-}$ compared to *Ldlr*$^{-/-}$*Il23r*$^{-/-}$ mice; p=0.46) remained unaltered. These data suggest that *Il23r* deficiency protects against atherosclerosis development at early time points and reduced plaque necrosis both at early and late time points of lesion development.

**Table 4. Body weight, white blood cell (WBC) counts and serum cholesterol levels in *Ldlr*$^{-/-}$ (n=8) and *Ldlr*$^{-/-}$*Il23r*$^{-/-}$ mice (n=7) mice fed a HFD for 12 weeks.**

| | *Ldlr*$^{-/-}$ | *Ldlr*$^{-/-}$*Il23r*$^{-/-}$ | *p-value* |
|---|---|---|---|
| **Body weight (g)** | 28.78 ± 1.753 | 28.69 ± 2.274 | 0.99 |
| **WBC count (10³/ µl)** | 5.175 ± 3.483 | 4.550 ± 0.90 | 0.54 |
| **Cholesterol (µg/ml)** | 26513 ± 6728 | 28037 ± 2487 | 0.95 |

### 4.2.7. *Il23r* deficiency alters the Treg compartment

Several studies have pointed out that *Il23r* deficiency might impair the balance of $T_{reg}$/$Th_{17}$ in favor of $T_{reg}$ responses [222]. Analysis of IL-23R-deficient *Ldlr*$^{-/-}$ mice under homeostatic conditions reported no differences in $T_{reg}$ in any localization (described in 4.2.4). However, after 6 weeks of HFD increased levels and percentages of $T_{regs}$ were noted, especially in the blood (Figure 40a), but also in spleen (Figure 40b). Moreover, mRNA levels of *Foxp3* were upregulated in spleens of *Ldlr*$^{-/-}$*Il23r*$^{-/-}$ mice (Figure 40c), suggesting protective $T_{reg}$ responses in atherosclerotic mice fed a HFD. Increased percentages of $T_{regs}$ in the blood (4.73% ± 1.08% *versus* 5.93% ± 0.58% of CD25$^{+}$FoxP3$^{+}$ cells among CD4$^{+}$ T cells in *Ldlr*$^{-/-}$ compared to *Ldlr*$^{-/-}$*Il23r*$^{-/-}$ mice; *p<0.05) and spleen (13.41% ± 0.94% *versus* 15.34% ± 0.61% of CD25$^{+}$FoxP3$^{+}$ cells among CD4$^{+}$ T cells in *Ldlr*$^{-}$

$^{/-}$ compared to *Ldlr*$^{-/-}$*Il23r*$^{-/-}$ mice; ***p<0.001) were observed in *Ldlr*$^{-/-}$*Il23r*$^{-/-}$ mice after 12 weeks of HFD.

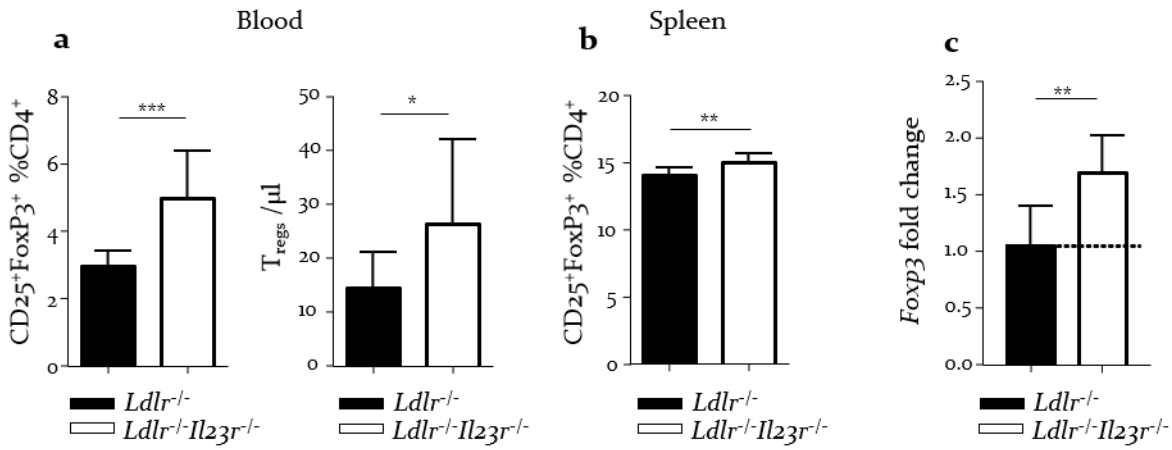


**Figure 40. $T_{reg}$ responses were increased in IL-23R-deficient *Ldlr*$^{-/-}$ mice after 6 weeks of HFD.** Total blood and splenocytes from *Ldlr*$^{-/-}$ (n=13) and *Ldlr*$^{-/-}$*Il23r*$^{-/-}$ mice (n=16) fed a HFD for 6 weeks were analyzed by flow cytometry. $T_{regs}$ were defined as $CD25^+FoxP3^+$ among $CD4^+$ T cells. (a) Percentages and cells per µl of blood of $T_{regs}$ in the blood and (b) spleen. (c) Quantitative PCR analysis of *Foxp3* mRNA expression in the spleen of *Ldlr*$^{-/-}$ (n=5) and *Ldlr*$^{-/-}$Il23r$^{-/-}$ mice (n=7) fed a HFD for 6 weeks. qPCR results were normalized to *Hprt* mRNA and are presented relative to *Ldlr*$^{-/-}$ controls. Data are presented as mean ± SEM; *p<0.05; **p<0.01.

It has previously been shown that naïve T cells do not express IL-23R and addition of IL-23 to cultures does not affect $T_{reg}$ generation [223]. Polarization of naïve T cells in the presence of TGF-β confirmed these findings, as $T_{reg}$ frequencies were similar in cultures using WT or IL-23R-deficient naïve T cells (66.77% ± 9.23% *versus* 71.67% ± 2.99% of $CD25^+FoxP3^+$ among $CD4^+$ T cells in WT compared to IL-23R-deficient naïve T cells, respectively; p=0.43). Petermann et al. reported that γδ T cells restrain $T_{reg}$ responses in an IL-23-dependent manner [224]. To assess whether *Il23r* deficiency impairs in vitro $T_{reg}$ polarization, spleens from WT or IL-23R-deficient *Ldlr*$^{-/-}$ animals were cultured in the presence or absence of TGF-β and IL-23. The percentage of $T_{regs}$ was higher in cultures from splenocytes from *Ldlr*$^{-/-}$*Il23r*$^{-/-}$ mice as compared to those from *Ldlr*$^{-/-}$ controls (Figure 41). However, the addition of IL-23 to cultures did not increase the percentage of $T_{regs}$. These results suggest either a cell-intrinsic mechanism promoting $T_{reg}$ differentiation in splenocytes from IL-23R-deficient *Ldlr*$^{-/-}$ mice when

exposure to TGF-β or that other effector cell type affected by the lack of IL-23R has the ability to modify regulatory T cell responses in an IL-23-independent manner.

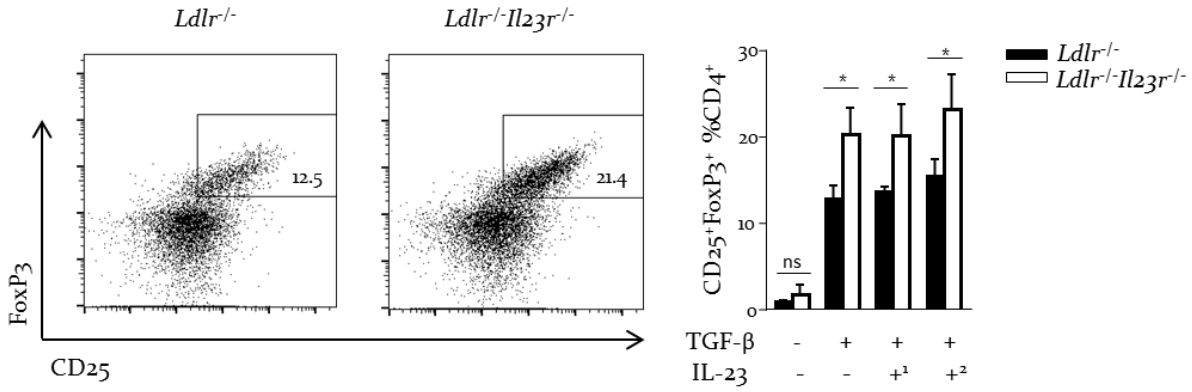


**Figure 41. Splenocytes from IL-23R-deficient *Ldlr*$^{-/-}$ mice showed an increased ability to polarize into $T_{reg}$.** Total splenocytes were activated with α-CD3 (5 μg/ml) and α-CD28 (1 μg/ml) and left untreated or cultured in the presence of TGF-β (4 ng/ml) and two different concentrations of IL-23 (1 = 20 ng/ml and 2 = 50 ng/ml). After 72 hours, the percentage of $CD4^+$ $CD25^+$ $FoxP3^+$ $T_{regs}$ were analyzed by flow cytometry. One of three independent experiments is shown. Data are presented as mean ± SEM; *p<0.05.

### 4.2.8. Altered cytokine profile in the aortic root of *Ldlr*$^{-/-}$*Il23r*$^{-/-}$ mice after 6 weeks of HFD

Given that HFD increased the release of pro-inflammatory cytokines among γδ T cells in the aortic root (Figure 37) and that *Ldlr*$^{-/-}$*Il23r*$^{-/-}$ mice showed a profound decreased in this subset, the cytokine profile in the aortic root after HFD might have been altered. The expression of several transcription factors and cytokines in aortic roots of *Ldlr*$^{-/-}$ and *Ldlr*$^{-/-}$*Il23r*$^{-/-}$ mice fed a HFD for 6 weeks was studied. mRNA levels of *Tbet* were higher among IL-23R-deficient *Ldlr*$^{-/-}$ mice, albeit differences were not significant (Figure 42). mRNA levels of *Rorc* were maintained (Figure 42). Of note, mRNA levels of *Ifng* and *Il10* were down- and upregulated in *Ldlr*$^{-/-}$*Il23r*$^{-/-}$ mice, respectively (Figure 42). This data suggest than *Il23r* deficiency is associated with an imbalance of pro- and anti-inflammatory in the aortic root cytokines under HFD-feeding.

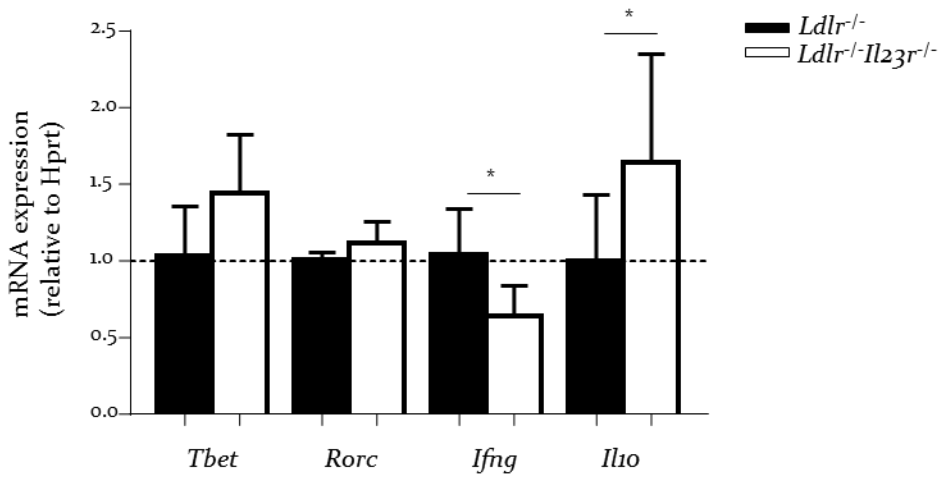


**Figure 42. Imbalance pro- and anti-inflammatory cytokine milieu in aortic sinus from *Ldlr*$^{-/-}$ *Il23r*$^{-/-}$ mice fed a HFD for 6 weeks.** Aortic root from *Ldlr*$^{-/-}$ (n=5) and *Ldlr*$^{-/-}$*Il23r*$^{-/-}$ mice (n=7) fed a HFD for 6 weeks were collected and immediately frozen in liquid nitrogen until use. Results were normalized to *Hprt* mRNA and are presented relative to *Ldlr*$^{-/-}$ controls. Data is presented as mean ± SEM; *p<0.05.

# 5. DISCUSSION I

## 5.1. The role of Batf3-dependent DCs in atherosclerosis

Accumulation of lipids and the consequent recruitment of circulating immune cells constitute the starting point of atherogenesis, characterized by the formation of plaques in the intima of the medium- and large-sized arteries. Despite our knowledge of how immune responses impact the formation of plaques, cholesterol-lowering statins remain the only approved drugs for the prevention and treatment of cardiovascular diseases.

Human and mouse plaques contain many different immune cells with the ability to modify the course of atherogenesis. Among them, DCs have gained attention within the last years given their ability to present antigens to T cells and produce cytokines, which may be used to reduce plaque formation and reduce cardiovascular outcomes such as myocardial infarction and strokes.

Early endeavors to define different DCs subsets have revealed different transcriptional requirements for individual DCs subpopulations. For example, the transcription factor ZBTB46 is selectively expressed by cDCs [97] and cDCs1 require the expression of BATF3, among others [94]. Recent studies have also proposed new surface markers to further discriminate among DCs subsets [95] and thus, define *bone fide* DC

$CD11c^+$ APCs are present in the arterial intima already at the steady state where they contribute to innate immunity by patrolling the tissue and avoiding damage [100]. Increased numbers of $CD11c^+MHCII^+$ cells in the aorta and the aortic root have been observed in experimental mouse models after feeding with a HFD [94]. In humans, the presence of $CD11c^+$ APCs has also been reported in plaques [226]. The mechanisms by which APCs can alter atherosclerosis development include polarization of T cell responses, secretion of cytokines and lipid metabolism [94], although the exact cell type responsible for the latter is not clear, as mouse models aiming to specifically deplete total cDCs have failed in the long-term [103]. In line with previous reports [98, 108, 109], this thesis shows that cDCs1 depletion does not alter total cholesterol levels

after 8 weeks of HFD, as *Ldlr*$^{-/-}$*Batf3*$^{-/-}$ mice showed similar circulating plasma cholesterol or triglycerides levels when compared to *Ldlr*$^{-/-}$ controls. These results highlight the importance of clearly define *bona fide* DCs, as the initial assumption that DCs control lipid metabolism might have been done by other CD11c-expressing population, such as macrophages.

Apart from cDCs, BATF3 has also been reported to be expressed in monocytes [104] and a previous report showed that the Ly6C$^{high}$ population was increased in the dermis of *Batf3*$^{-/-}$ animals [107]. Opposed to this data, *Ldlr*$^{-/-}$*Batf3*$^{-/-}$ animals in the steady state showed decreased frequencies of Ly6C$^{high}$ monocytes in spleen when compared to *Ldlr*$^{-/-}$ controls. There is currently no evidence showing any essential role of BATF3 in monocyte development or recruitment. However, a recent study has shown that depletion of CD8$^{+}$ T cells affects the percentages of Ly6C$^{high}$ monocytes in several compartments, including spleen [120]. Decreased percentages of CD8$^{+}$ T cells in spleens of *Ldlr*$^{-/-}$*Batf3*$^{-/-}$ mice after both feeding normal chow and HFD were observed. Batf3-dependent DCs are known to cross-present antigens to CD8$^{+}$ T cells and their depletion might have affected CD8$^{+}$ T cell homeostasis. It may be conceivable that a decrease in this immune cell population is, in part, responsible for reduced frequencies of Ly6C$^{high}$ monocytes, at least under steady state conditions. However, after feeding with a HFD, levels of CD8$^{+}$ T cells remained low without any difference in monocyte populations, suggesting other mechanisms to predominate in *Ldlr*$^{-/-}$*Batf3*$^{-/-}$ mice in atherosclerosis induced monopoiesis.

Batf3-deficient *Ldlr*$^{-/-}$ mice almost completely lack CD8α$^{+}$ and CD103$^{+}$ DCs in the spleen, as previously reported [104]. Furthermore, this work reports that *Batf3* deficiency led to the depletion of all CD103$^{+}$ DCs in the aorta. This deletion was not compensated by other members of the BATF family after chronic inflammation as the the absence of these DCs were also observed in the aorta of *Ldlr*$^{-/-}$*Batf3*$^{-/-}$ mice fed a HFD for 8 weeks

It has previously been shown that BATF3 is also highly expressed in pre-macrophages derived from yolk sac erythro-myeloid progenitor, which give rise to tissue-resident macrophages that again downregulate *Batf3* gene expression [211].

Given that embryo-derived resident macrophages are present in the aorta [86] one could speculate that *Batf3* deficiency also affects macrophage content. Multiple lines of evidence have pointed towards a non-essential role of BATF3 in macrophages development [104, 212, 213]. This thesis further supports these observations. Indeed, mRNA levels of *Batf3* are residual in BMDM when compared to isolated splenic $CD11c^+$ APCs. Deletion of *Batf3* did also not impair the ability of BMDM to take up lipids and become foam cells. Moreover, when $Ldlr^{-/-}Batf3^{-/-}$ mice were fed a HFD, the percentage of $CD11c^-F4/80^+$ macrophages in the root was unaffected. Altogether this data corroborate that BATF3 is specifically expressed by DCs and does not play a role in macrophage development or functionality.

Initially, Batf3-dependent DCs have been attributed to be protective in atherogenesis by inducing $T_{reg}$ responses in the aorta [98]. In the mentioned study, the authors used mice deficient for *Flt3*, which translated into reduced frequencies of $CD103^+$ DCs within the root. However, *Flt3* is also expressed in other immune cells that impact atherosclerosis development [101, 227, 228] and hence, whether or not cDCs1 were directly responsible for the observed phenotype is not clear.

Analysis of lesion burden in Batf3-deficient $Ldlr^{-/-}$ mice revealed no differences in the aorta or aortic root after feeding a HFD for 8 or 12 weeks of diet. Furthermore, the number of macrophages, SMCs, necrotic core or collagen in plaques was similar between groups, further suggesting that depletion of cDCs1 might not play an essential role in the development of atherosclerosis or in modifying plaque composition. Moreover, no differences in $T_{regs}$ responses were detected either at the steady state or after HFD feeding. These results are in line with a previous report using bone marrow chimeras aiming at elucidating the role of cross-presentation in atherosclerosis [108].

In contrast, a recent report using an $ApoE^{-/-}Batf3^{-/-}$ mouse model has reported aggravated atherosclerosis and increased percentages of macrophages in plaques of Batf3-deficient $ApoE^{-/-}$ mice after feeding a HFD for 12 weeks [109]. The authors argued that *Batf3* depletion disrupted the ability of $CD103^+$ DCs to secrete IL-12 leading to impaired $Th_1$ responses. One study has suggested that $CD103^+$ DCs are the major producer of IL-12 after infection with *L. monocytogenes* [107] and in line with this

evidence decreased $Th_1$ responses in spleens of *Ldlr*$^{-/-}$*Batf3*$^{-/-}$ mice fed a HFD were observed. However, this thesis clearly indicated no differences in plaque size or plaque composition. The reason for these discrepancies cannot be easily explained but might be related with the experimental model used. As highlighted by Getz et al. [229], although both *ApoE*$^{-/-}$ and *Ldlr*$^{-/-}$ mice are powerful models to study the effect of gene deletion on the development of atherosclerosis, they present advantages and disadvantages. For example, as reviewed in Chapter 1.3, *Apoe* deletion increases not only plasma cholesterol but also impairs immune responses, especially in macrophages [59]. Several studies have also reported contradictory results analyzing the same gene deletion using *ApoE*$^{-/-}$ and *Ldlr*$^{-/-}$ mice [230-233], which highlight the importance of studying both models to finally elucidate the role of a specific cell population in atherosclerosis.

Studying the function of DCs might lead to the development of new therapeutic targets for the treatment of atherosclerosis. These approaches might include the use of tolerogenic DCs, which are being explored for the treatment of other autoimmune diseases such as multiple sclerosis [234]; oxLDL-pulsed APCs, which has been successful in reducing plaque burden in mice [235] or even targeting of specific subsets with a proatherogenic potential, as it might be the case of pDCs [94]. This thesis provides evidence that Batf3-dependent DCs, including $CD8a^+$ and $CD103^+$ cells, do not impact lesion burden and thus may not serve as a target for the development of future treatments to modulate the course of the disease.

# 5. DISCUSSION II

## 5.2. The role of the IL-23 receptor in atherosclerosis

Since the initial discovery of IL-23, many attempts have tried to elucidate its contribution to immune responses. It is now well accepted that IL-23 is not only necessary to protect against extracellular pathogens [236] but is also responsible to confer pathogenicity to IL-23-responder cells characterized by the expression of the IL-23R [237]. Their role in autoimmunity is becoming evident [238] and many different clinical trials are currently testing the efficacy of antibodies against the specific subunit p19 for the treatment of disorders such as psoriasis, rheumatoid arthritis or Crohn´s disease [239]. Interestingly, these conditions share an accelerated course of atherosclerosis which confers an increased risk of cardiovascular outcomes in patients [240]. However, the exact contribution of IL-23 or the IL-23R in atherosclerosis remains elusive.

Previous epidemiological studies have suggested altered levels of IL-23 in the serum of patients affected by PAD [196] or CAD [197], and polymorphism conferring a loss-of-function of the IL-23R have been suggested to be related to improved cardiovascular outcomes [201]. However, these studies do not prove whether IL-23 is a cause or consequence of atherogenesis and thus it is not clear how its blockade might affect the course of the disease.

Although it is clear that TLR-activated APCs are able to secrete large amounts of IL-23 [180], there is no evidence that oxLDL can also modulate its expression. This thesis shows that oxLDL alone can induce upregulation of several surface markers associated with DC activation, such as a CD80 and CD40 in BM-APCs and in aortic $CD11c^{+}MHCII^{+}$ APCs in vivo. Previous reports analyzing the effect of oxLDL in APCs have provided conflicting data [157, 241-243]. However, this signal was not enough to induce the release of IL-23 by cultured cells in our experiments, suggesting that oxLDL requires an additional partner. Treating cells with TLR-2 or TLR-4 agonists and culturing them in the presence of oxLDL led to a marked increase in IL-23 release. Same results were obtained when BM-APCs were initially primed with LPS for 4 hours to induce

maturation and further incubated with oxLDL. These results suggest that oxLDL and TLR2/4 agonists synergize to promote the release of IL-23 and that oxLDL can also sustains IL-23 secretion in previously TLR-activated APCs. These in vitro results were also observed when culturing sectioned aortas from mice. However, this approach also led to the discovery that the addition of oxLDL without the presence of LPS also promoted the secretion of IL-23. Two different approaches may explain these differences when compared to in vitro observations. First, several papers have shown the presence of TLR ligands in aorta and plaques [43]. It is conceivable that resident or recruited APCs can be activated through different TLRs expressed by these cells and that further stimulation with oxLDL increases the secretion of IL-23. Second, BM-APCs differentiated with GM-CSF give rise to an inflammatory population that may not reflect the in vivo situation. Thus, ex vivo cultures of fresh aortas may contain different APC populations, either DCs or macrophages that are able to produce IL-23. In this line, a recent paper has shown that $CD11b^+$ cDCs1 are the major producer of IL-23 in a stroke model [199]. Moreover, a previous study has shown that IL-23 localizes with $CD11c^+$ APCs and $F4/80^+$ macrophages in plaques [179]. Further studies are needed to fully elucidate which cell type is responsible for IL-23 secretion in the aorta under homeostatic conditions and in mice fed a HFD.

Previous studies in humans have related increased levels of IL-23 in the serum to PAD [196]. Analysis of IL-23 serum levels in mice fed a HFD reported no differences after any time point analyzed. As human studies have analyzed patients with a long story of atherosclerosis it might be possible that elevated IL-23 is characteristic of very advanced stages of atherosclerosis, dissimilar to the experimental model used in this thesis. Another study has also shown that mRNA levels of *Il23a* and *Il23r* are elevated in human plaques [179]. In line with this, increased mRNA levels of *Il23a* specifically in the aortic root of mice fed a HFD for 6 weeks were observed. This could reflect an increased presence of oxLDL during atherogenesis, leading to sustained IL-23 secretion of TLR-activated APCs.

Responses to IL-23 require the presence of IL-23R. A previous study has characterized IL-23R expression in different organs, including lymph nodes, spleen and the lamina propria [189]. Awasthi and colleagues reported that IL-23R expression was

mainly found in γδ T cells, although its expression among different tissues varied significantly, with the highest proportion of IL-23R$^+$ found in the lamina propria. Apart from γδ T cells, also a minor population of CD4$^+$ T cells was found to express IL-23R, presumably belonging to $Th_{17}$ cells [189]. CD11c$^+$ and CD11b$^+$ cells, named as DCs and macrophages in this study, expressed detectable amounts of IL-23R exclusively in lymph nodes, but not spleen. In all cases, IL-23R expression was associated with secretion of IL-17.

In this thesis, IL-23R expression in the aorta and aortic root using *Ldlr*$^{-/-}$*Il23r*$^{gfp/+}$ mice was studied. Under homeostatic conditions, IL-23R was expressed mainly by γδ T cells and some TCR-β$^+$ conventional T cells, but not by other myeloid cells. Surprisingly, IL-23R expression showed a tissue-specific distribution. In the aortic root, almost all γδ T cells expressed the receptor, whereas markedly fewer γδ T cells were IL-23R$^+$ in the aorta. In line with previous reports associating IL-23R expression with IL-17, γδ T cells were the predominant producers of IL-17 in the aortic root and that this was associated with IL-23R expression. IL-23R$^+$ γδ T cells were able to co-express IL-17 and GM-CSF and this expression was enhanced after feeding mice a HFD for 6 and 12 weeks. Production of GM-CSF by γδ T cells has been previously reported. For example, GM-CSF secretion by $γδ_{17}$ T cells sustain neuroinflammation via myeloid cells that infiltrate the central nervous system (CNS) in an experimental autoimmune encephalomyelitis (EAE) mouse model [244]

In line with the expression of IL-23R in both the aorta and the aortic root, a profound decrease in the percentage of γδ T cells was observed in *Ldlr*$^{-/-}$*Il23r*$^{-/-}$ mice at the steady state and after feeding a HFD. In fact, IL-23 has been reported to be essential for the maintenance of $Th_{17}$ responses [236] and one can speculate that IL-23 secreted by APCs in the aorta is necessary to maintain the pool of γδ T cells and other IL-23-responding cells. The role of these IL-23R$^+$ cells in the aorta at the steady state is not clear and this thesis does not extricate their potential contribution to tissue homeostasis. Given that IL-23 has been shown to be important for the clearance of extracellular pathogens [236], it might be possible that under homeostatic conditions, basal secretion of IL-23 by APCs contributes to tissue defense.

After feeding a HFD, increased mRNA levels of *Il23a* in the aortic root but not in the aorta or spleen in *Ldlr*$^{-/-}$ mice compared to *Ldlr*$^{-/-}$ controls fed a chow diet were detected. Lesion size in *Ldlr*$^{-/-}$*Il23r*$^{-/-}$ mice was reduced in the aortic root after 6 weeks of diet, but not at 12 weeks. Importantly, at both time points the necrotic core area was reduced in the *Ldlr*$^{-/-}$*Il23r*$^{-/-}$ group compared to *Ldlr*$^{-/-}$ mice. These results point towards an important role of IL-23R in early plaque formation and plaque instability rather than promoting the further growth of atherosclerosis, at least during later stages of the disease.

Under steady state conditions, mice lacking the IL-23R presented decreased percentages of circulating CD115$^{+}$ monocytes. A previous report has also made the same observation using *Il23a*$^{-/-}$ mice [245]. Although after 6 weeks of diet the percentage of monocytes was similar between groups, one plausible explanation is that decreased frequencies of monocytes in IL-23R-deficient *Ldlr*$^{-/-}$ mice in steady state contributed to the reduced lesion size observed after 6 weeks of diet.

This thesis also reported that *Il23r* deficiency was accompanied by increased frequencies of $T_{regs}$ in the blood and in spleen in mice fed a HFD. These results suggest that $T_{regs}$ may have contributed to the observed phenotype, given their strong atheroprotective effect reported in the literature [152]. The reasons why IL-23R-deficient mice presented more $T_{regs}$ after feeding a HFD, but not at the steady state, have not been studied in detail in this thesis. The balance between $Th_{17}$ and $T_{reg}$ generation can be altered by disruption of the IL-23/IL-23R axis [222, 223]. However, how this axis impacted on the development of $T_{reg}$ is not fully understood. Neither naïve T cells nor $T_{regs}$ expresses the IL-23R and it is unlikely that IL-23 plays a direct role in $T_{reg}$ generation or maintenance once they have been polarized. Results presented here support this data, as polarization of total splenocytes in the presence of TGF-β revealed that addition of IL-23 did not affect frequencies of $T_{regs}$, although increased frequencies of IL-23R-deficient $T_{regs}$ were evident independently of the addition of IL-23. Interestingly, a recent paper has shown similar results in *Sgk1*$^{-/-}$ animals [246], a downstream molecule for the IL-23R. A previous study reported that γδ T cells restrain $T_{reg}$ responses in an IL-23-dependent manner [224]. It might be possible that disruption of the IL-23R signaling in splenic IL-23R$^{+}$ γδ T cells of *Ldlr*$^{-/-}$

*Il23r*$^{-/-}$ mice led to increased percentages of $T_{regs}$ when compared to controls. However, more studies are needed to conclude the relation between *Il23r* deficiency and $T_{reg}$ polarization.

Another intriguing finding was that IL-17 responses were unaltered in all compartments except in the aortic root of *Il23r*$^{-/-}$ animals. As introduced earlier, IL-17A is not an exclusive marker of pathogenic $Th_{17}$ responses and can also be produced by non-pathogenic $Th_{17}$ cells. This thesis reports that polarization of IL-23R-deficient naïve T cells showed a similar pattern of IL-17A secretion when cultured in the presence of the non-pathogenic cocktail TGF-β and IL-6. However, cultures in a TGF-β-independent manner clearly showed that $Th_{17}$ polarization was altered. Of note, IL-23R expression in spleen has already been shown to be low [189], which might reflect a protective role of IL-17 production in this location dependent on TGF-β only. These results are in line with a previous study using a *Sgk1*$^{-/-}$ mouse model [247]. These animals showed similar IL-17A responses when polarized using non-pathogenic conditions. However, re-stimulation with IL-23 led to a marked IL-17 response, similar to reported in vitro results. On the other hand, as in the aortic root, γδ T cells were the only producers of IL-17 and these cells were IL-23R$^{+}$, it was not surprising that, in this location, IL-17 was severely affected.

When analyzing the cytokine profile in the aortic root of *Ldlr*$^{-/-}$*Il23r*$^{-/-}$ mice fed a HFD for 6 weeks, decreased mRNA levels of *Ifng* and increased levels of *Il10* were noted. Non-pathogenic $Th_{17}$ cells are characterized not only by the expression of IL-17 but also by IL-10 [238], which confers them a non-pathogenic capacity. On the contrary, pathogenic $Th_{17}$ cells are characterized by IL-17, IFN-γ and GM-CSF expression [238]. Given that at the steady state GM-CSF expression was higher among IL-23R$^{+}$ cells, one can speculate that lack of IL-23R might skew atherosclerosis-induced pathogenic responses towards non-pathogenic responses characterized by the expression of IL-10 and reduced levels of INF-γ. Both cytokines have been shown to protect against atherosclerosis [248] or to promote it [249], respectively. Hence, both cytokines might have contributed to the phenotype described in this work. However, the possibility that the imbalance between pro- and anti-inflammatory cytokines in the aortic sinus of *Ldlr*$^{-/-}$*Il23r*$^{-/-}$ mice fed a HFD is driven by another cell type cannot be

excluded. For example, GM-CSF can manipulate the secretion of cytokines in macrophages, such as IL-10 [250].

Finally, apart from its described ability to induce pathogenicity, IL-23 has also been described to play a role during apoptosis. Several models have proposed that signaling through IL-23R contributes to Bcl2 activation, thereby promoting apoptosis [194]. Of note, a previous study using GM-CSF-deficient *Ldlr*$^{-/-}$ mice has observed smaller necrotic cores compared to *Ldlr*$^{-/-}$ controls when fed a HFD [179]. The authors argued that HFD promoted IL-23 production, which can act through IL-23R-responding macrophages. In the presence of oxLDL, IL-23 was shown to act synergistically to induce apoptosis and to contribute to necrotic core formation. During the work of this thesis, IL-23R was not expressed in any myeloid cells in the aorta or aortic root at the steady state or after HFD (the latter not shown). Moreover, no IL-23R expression in BM-APCs or BMDMs (data not shown) was detected when using the *Il23r*$^{gfp/+}$ reporter mice. The possibility that our model does not allow the detection of IL-23R expression in DCs or macrophages because the receptor is expressed at very low levels or may be secreted in *Il23r*$^{gfp/+}$ mice, as recently suggested in other immune cells [251] cannot be excluded. However, clear GFP expression in T cells was noted, and thus this Thesis showed that the reporter mouse provides valuable insight for the detection of IL-23R-bearing cells. The current data do not support the hypothesis that decreased necrotic core is related to diminished responsiveness to IL-23 by macrophages or DCs in IL-23R-deficient mice.

In summary, this thesis shows that atherosclerosis conditions sustain the secretion of IL-23 by TLR-activated APCs, which can act through IL-23R-responding cells. At the steady state, γδ T cells are the major subset in the aortic root expressing IL-23R and are characterized by the production of IL-17 and GM-CSF. *Il23r* deficiency led to a profound decrease of this subset in the aortic root and the aorta and an altered anti-inflammatory/pro-inflammatory cytokine balance after feeding mice a HFD. This dysregulation may be linked with decreased necrotic areas observed in transgenic mice, associated with plaque stability.

A model for these finding is summarized in Figure 43.

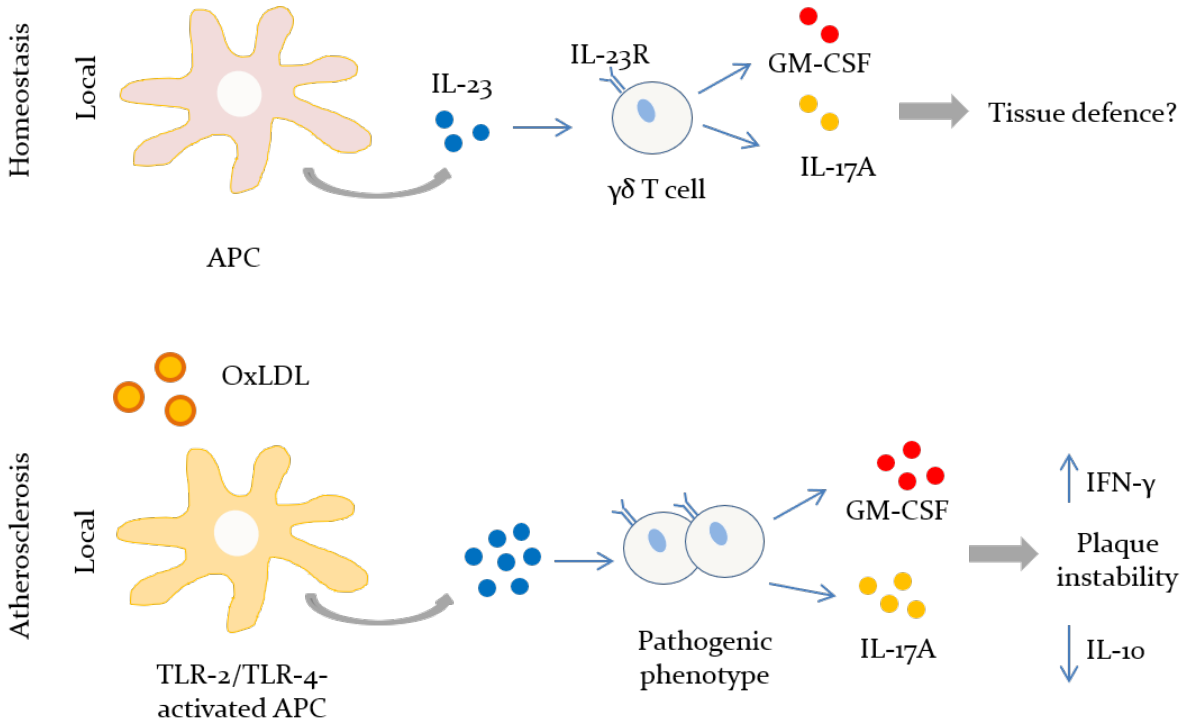


**Figure 43. Proposed mechanism by which IL-23R might influence atherosclerosis.** Under homeostatic conditions, local production of IL-23 by aortic APCs may contribute to tissue homeostasis by triggering responses in IL-23R$^+$ γδ T cells, characterized by the production of IL-17 and GM-CSF. Under atherogenic conditions, increased secretion of IL23 by TLR-activated APCs in the presence of oxLDL might induce a pathogenic phenotype in aortic IL-23R$^+$ cells. Increased production of IL-17 and GM-CSF might alter the fine balance between pro- and anti-inflammatory in the aortic sinus, leading to bigger necrotic areas and plaque instability.

## 6. REFERENCES


1. Hansson GK. Inflammation, atherosclerosis, and coronary artery disease. *N Engl J Med* 2005,**352**:1685-1695.
2. Virchow R. Der Ateromatose Prozess der Arterien. Wien Med Wochenschr. 1856:825–827.
3. Ross R, Glomset JA. The pathogenesis of atherosclerosis (first of two parts). *N Engl J Med* 1976,**295**:369-377.
4. Vanhoutte PM, Scott-Burden T. The endothelium in health and disease. *Tex Heart Inst J* 1994,**21**:62-67.
5. Rohlenova K, Veys K, Miranda-Santos I, De Bock K, Carmeliet P. Endothelial Cell Metabolism in Health and Disease. *Trends Cell Biol* 2017.
6. Chiu JJ, Chien S. Effects of disturbed flow on vascular endothelium: pathophysiological basis and clinical perspectives. *Physiol Rev* 2011,**91**:327-387.
7. Davignon J, Ganz P. Role of endothelial dysfunction in atherosclerosis. *Circulation* 2004,**109**:III27-32.
8. Michiels C. Endothelial cell functions. *J Cell Physiol* 2003,**196**:430-443.
9. Gimbrone MA, Jr., Garcia-Cardena G. Endothelial Cell Dysfunction and the Pathobiology of Atherosclerosis. *Circ Res* 2016,**118**:620-636.
10. Feingold KR, Grunfeld C. Introduction to Lipids and Lipoproteins. In: *Endotext*. Edited by De Groot LJ, Chrousos G, Dungan K*, et al.* South Dartmouth (MA); 2000.
11. Anitschkow NNC, S. Ueber experimentelle Cholesterinsteatose und ihre Bedeutung fur die Entstehung einiger pathologischer Prozesse. Zentralbl. Allg. Pathol. 1913;24:1-9
12. Kannel WB, Dawber TR, Kagan A, Revotskie N, Stokes J, 3rd. Factors of risk in the development of coronary heart disease--six year follow-up experience. The Framingham Study. Ann Intern Med. 1961;55:33-50
13. Castelli WP, Garrison RJ, Wilson PW, Abbott RD, Kalousdian S, Kannel WB. Incidence of coronary heart disease and lipoprotein cholesterol levels. The Framingham Study. *JAMA* 1986,**256**:2835-2838.

14. Gordon T, Castelli WP, Hjortland MC, Kannel WB, Dawber TR. High density lipoprotein as a protective factor against coronary heart disease. The Framingham Study. *Am J Med* 1977,**62**:707-714.
15. Williams KJ, Tabas I. The response-to-retention hypothesis of early atherogenesis. *Arterioscler Thromb Vasc Biol* 1995,**15**:551-561.
16. Steinberg D. The LDL modification hypothesis of atherogenesis: an update. *J Lipid Res* 2009,**50 Suppl**:S376-381.
17. Lusis AJ. Atherosclerosis. *Nature* 2000,**407**:233-241.
18. Wolf D, Stachon P, Bode C, Zirlik A. Inflammatory mechanisms in atherosclerosis. *Hamostaseologie* 2014,**34**:63-71.
19. Chistiakov DA, Melnichenko AA, Orekhov AN, Bobryshev YV. How do macrophages sense modified low-density lipoproteins? *Int J Cardiol* 2016.
20. Rader DJ, Pure E. Lipoproteins, macrophage function, and atherosclerosis: beyond the foam cell? *Cell Metab* 2005,**1**:223-230.
21. Jovinge S, Ares MP, Kallin B, Nilsson J. Human monocytes/macrophages release TNF-alpha in response to Ox-LDL. *Arterioscler Thromb Vasc Biol* 1996,**16**:1573-1579.
22. Frostegard J, Huang YH, Ronnelid J, Schafer-Elinder L. Platelet-activating factor and oxidized LDL induce immune activation by a common mechanism. *Arterioscler Thromb Vasc Biol* 1997,**17**:963-968.
23. Terkeltaub R, Banka CL, Solan J, Santoro D, Brand K, Curtiss LK. Oxidized LDL induces monocytic cell expression of interleukin-8, a chemokine with T-lymphocyte chemotactic activity. *Arterioscler Thromb* 1994,**14**:47-53.
24. Wang GP, Deng ZD, Ni J, Qu ZL. Oxidized low density lipoprotein and very low density lipoprotein enhance expression of monocyte chemoattractant protein-1 in rabbit peritoneal exudate macrophages. *Atherosclerosis* 1997,**133**:31-36.
25. Berliner JA, Schwartz DS, Territo MC, Andalibi A, Almada L, Lusis AJ, *et al.* Induction of chemotactic cytokines by minimally oxidized LDL. *Adv Exp Med Biol* 1993,**351**:13-18.
26. Parhami F, Fang ZT, Fogelman AM, Andalibi A, Territo MC, Berliner JA. Minimally modified low density lipoprotein-induced inflammatory responses in

endothelial cells are mediated by cyclic adenosine monophosphate. *J Clin Invest* 1993,**92**:471-478.

27. Huang YH, Ronnelid J, Frostegard J. Oxidized LDL induces enhanced antibody formation and MHC class II-dependent IFN-gamma production in lymphocytes from healthy individuals. *Arterioscler Thromb Vasc Biol* 1995,**15**:1577-1583.
28. Takei A, Huang Y, Lopes-Virella MF. Expression of adhesion molecules by human endothelial cells exposed to oxidized low density lipoprotein. Influences of degree of oxidation and location of oxidized LDL. *Atherosclerosis* 2001,**154**:79-86.
29. Vielma SA, Mironova M, Ku JR, Lopes-Virella MF. Oxidized LDL further enhances expression of adhesion molecules in Chlamydophila pneumoniae-infected endothelial cells. *J Lipid Res* 2004,**45**:873-880.
30. Khan BV, Parthasarathy SS, Alexander RW, Medford RM. Modified low density lipoprotein and its constituents augment cytokine-activated vascular cell adhesion molecule-1 gene expression in human vascular endothelial cells. *J Clin Invest* 1995,**95**:1262-1270.
31. Leitinger N, Tyner TR, Oslund L, Rizza C, Subbanagounder G, Lee H, *et al.* Structurally similar oxidized phospholipids differentially regulate endothelial binding of monocytes and neutrophils. *Proc Natl Acad Sci U S A* 1999,**96**:12010-12015.
32. Vora DK, Fang ZT, Liva SM, Tyner TR, Parhami F, Watson AD, *et al.* Induction of P-selectin by oxidized lipoproteins. Separate effects on synthesis and surface expression. *Circ Res* 1997,**80**:810-818.
33. Oinuma T, Yamada T, Sakurai I. Effects of copper-zinc type superoxide dismutase on the proliferation and migration of cultured vascular smooth muscle cells induced by oxidized low density lipoprotein. *J Atheroscler Thromb* 1997,**4**:79-84.
34. Liu J, Ren Y, Kang L, Zhang L. Oxidized low-density lipoprotein increases the proliferation and migration of human coronary artery smooth muscle cells through the upregulation of osteopontin. *Int J Mol Med* 2014,**33**:1341-1347.

35. Cherepanova OA, Pidkovka NA, Sarmento OF, Yoshida T, Gan Q, Adiguzel E*, et al.* Oxidized phospholipids induce type VIII collagen expression and vascular smooth muscle cell migration. *Circ Res* 2009,**104**:609-618.
36. Kiyan Y, Tkachuk S, Hilfiker-Kleiner D, Haller H, Fuhrman B, Dumler I. oxLDL induces inflammatory responses in vascular smooth muscle cells via urokinase receptor association with CD36 and TLR4. *J Mol Cell Cardiol* 2014,**66**:72-82.
37. Levitan I, Volkov S, Subbaiah PV. Oxidized LDL: diversity, patterns of recognition, and pathophysiology. *Antioxid Redox Signal* 2010,**13**:39-75.
38. Gough PJ, Gordon S. The role of scavenger receptors in the innate immune system. *Microbes Infect* 2000,**2**:305-311.
39. Endemann G, Stanton LW, Madden KS, Bryant CM, White RT, Protter AA. CD36 is a receptor for oxidized low density lipoprotein. *J Biol Chem* 1993,**268**:11811-11816.
40. Stewart CR, Stuart LM, Wilkinson K, van Gils JM, Deng J, Halle A*, et al.* CD36 ligands promote sterile inflammation through assembly of a Toll-like receptor 4 and 6 heterodimer. *Nat Immunol* 2010,**11**:155-161.
41. Dowling JK, Mansell A. Toll-like receptors: the swiss army knife of immunity and vaccine development. *Clin Transl Immunology* 2016,**5**:e85.
42. Trinchieri G, Sher A. Cooperation of Toll-like receptor signals in innate immune defence. *Nat Rev Immunol* 2007,**7**:179-190.
43. Falck-Hansen M, Kassiteridi C, Monaco C. Toll-like receptors in atherosclerosis. *Int J Mol Sci* 2013,**14**:14008-14023.
44. Nicolaou G, Erridge C. Toll-like receptor-dependent lipid body formation in macrophage foam cell formation. *Curr Opin Lipidol* 2010,**21**:427-433.
45. Pasini AF, Anselmi M, Garbin U, Franchi E, Stranieri C, Nava MC*, et al.* Enhanced levels of oxidized low-density lipoprotein prime monocytes to cytokine overproduction via upregulation of CD14 and toll-like receptor 4 in unstable angina. *Arterioscler Thromb Vasc Biol* 2007,**27**:1991-1997.
46. Mikita T, Porter G, Lawn RM, Shiffman D. Oxidized low density lipoprotein exposure alters the transcriptional response of macrophages to inflammatory stimulus. *J Biol Chem* 2001,**276**:45729-45739.

47. Groeneweg M, Kanters E, Vergouwe MN, Duerink H, Kraal G, Hofker MH, *et al.* Lipopolysaccharide-induced gene expression in murine macrophages is enhanced by prior exposure to oxLDL. *J Lipid Res* 2006,**47**:2259-2267.
48. Lafont A. Basic aspects of plaque vulnerability. *Heart* 2003,**89**:1262-1267.
49. Gistera A, Hansson GK. The immunology of atherosclerosis. *Nat Rev Nephrol* 2017,**13**:368-380.
50. Naghavi M, Libby P, Falk E, Casscells SW, Litovsky S, Rumberger J, *et al.* From vulnerable plaque to vulnerable patient: a call for new definitions and risk assessment strategies: Part I. *Circulation* 2003,**108**:1664-1672.
51. van der Wal AC, Becker AE, van der Loos CM, Das PK. Site of intimal rupture or erosion of thrombosed coronary atherosclerotic plaques is characterized by an inflammatory process irrespective of the dominant plaque morphology. *Circulation* 1994,**89**:36-44.
52. Frostegard J. Atherosclerosis in patients with autoimmune disorders. *Arterioscler Thromb Vasc Biol* 2005,**25**:1776-1785.
53. Bentzon JF, Otsuka F, Virmani R, Falk E. Mechanisms of plaque formation and rupture. *Circ Res* 2014,**114**:1852-1866.
54. Steinl DC, Kaufmann BA. Ultrasound imaging for risk assessment in atherosclerosis. *Int J Mol Sci* 2015,**16**:9749-9769.
55. Konstantinov IE, Jankovic GM. Alexander I. Ignatowski: a pioneer in the study of atherosclerosis. *Tex Heart Inst J* 2013,**40**:246-249.
56. Kapourchali FR, Surendiran G, Chen L, Uitz E, Bahadori B, Moghadasian MH. Animal models of atherosclerosis. *World J Clin Cases* 2014,**2**:126-132.
57. Emini Veseli B, Perrotta P, De Meyer GRA, Roth L, Van der Donckt C, Martinet W, *et al.* Animal models of atherosclerosis. *Eur J Pharmacol* 2017,**816**:3-13.
58. Ishibashi S, Brown MS, Goldstein JL, Gerard RD, Hammer RE, Herz J. Hypercholesterolemia in low density lipoprotein receptor knockout mice and its reversal by adenovirus-mediated gene delivery. *J Clin Invest* 1993,**92**:883-893.
59. Baitsch D, Bock HH, Engel T, Telgmann R, Muller-Tidow C, Varga G, *et al.* Apolipoprotein E induces antiinflammatory phenotype in macrophages. *Arterioscler Thromb Vasc Biol* 2011,**31**:1160-1168.

60. Larkin L, Khachigian LM, Jessup W. Regulation of apolipoprotein E production in macrophages (review). *Int J Mol Med* 2000,**6**:253-258.
61. Vitek MP, Brown CM, Colton CA. APOE genotype-specific differences in the innate immune response. *Neurobiol Aging* 2009,**30**:1350-1360.
62. Hansson GK, Libby P. The immune response in atherosclerosis: a double-edged sword. *Nat Rev Immunol* 2006,**6**:508-519.
63. Matsuura E, Kobayashi K, Lopez LR. Atherosclerosis in autoimmune diseases. *Curr Rheumatol Rep* 2009,**11**:61-69.
64. Matsuura E, Atzeni F, Sarzi-Puttini P, Turiel M, Lopez LR, Nurmohamed MT. Is atherosclerosis an autoimmune disease? *BMC Med* 2014,**12**:47.
65. Woollard KJ, Geissmann F. Monocytes in atherosclerosis: subsets and functions. *Nat Rev Cardiol* 2010,**7**:77-86.
66. Zernecke A, Shagdarsuren E, Weber C. Chemokines in atherosclerosis: an update. *Arterioscler Thromb Vasc Biol* 2008,**28**:1897-1908.
67. Hansson GK, Hermansson A. The immune system in atherosclerosis. *Nat Immunol* 2011,**12**:204-212.
68. Tacke F, Alvarez D, Kaplan TJ, Jakubzick C, Spanbroek R, Llodra J, *et al.* Monocyte subsets differentially employ CCR2, CCR5, and CX3CR1 to accumulate within atherosclerotic plaques. *J Clin Invest* 2007,**117**:185-194.
69. Audoy-Remus J, Richard JF, Soulet D, Zhou H, Kubes P, Vallieres L. Rod-Shaped monocytes patrol the brain vasculature and give rise to perivascular macrophages under the influence of proinflammatory cytokines and angiopoietin-2. *J Neurosci* 2008,**28**:10187-10199.
70. Auffray C, Fogg D, Garfa M, Elain G, Join-Lambert O, Kayal S, *et al.* Monitoring of blood vessels and tissues by a population of monocytes with patrolling behavior. *Science* 2007,**317**:666-670.
71. Rahman MS, Murphy AJ, Woollard KJ. Effects of dyslipidaemia on monocyte production and function in cardiovascular disease. *Nat Rev Cardiol* 2017,**14**:387-400.
72. Swirski FK, Libby P, Aikawa E, Alcaide P, Luscinskas FW, Weissleder R, *et al.* Ly-6Chi monocytes dominate hypercholesterolemia-associated monocytosis and give rise to macrophages in atheromata. *J Clin Invest* 2007,**117**:195-205.

73. Johnson JL, Newby AC. Macrophage heterogeneity in atherosclerotic plaques. *Curr Opin Lipidol* 2009,**20**:370-378.
74. Soehnlein O, Steffens S, Hidalgo A, Weber C. Neutrophils as protagonists and targets in chronic inflammation. *Nat Rev Immunol* 2017,**17**:248-261.
75. Hartwig H, Silvestre Roig C, Daemen M, Lutgens E, Soehnlein O. Neutrophils in atherosclerosis. A brief overview. *Hamostaseologie* 2015,**35**:121-127.
76. Drechsler M, Megens RT, van Zandvoort M, Weber C, Soehnlein O. Hyperlipidemia-triggered neutrophilia promotes early atherosclerosis. *Circulation* 2010,**122**:1837-1845.
77. Ionita MG, van den Borne P, Catanzariti LM, Moll FL, de Vries JP, Pasterkamp G, *et al.* High neutrophil numbers in human carotid atherosclerotic plaques are associated with characteristics of rupture-prone lesions. *Arterioscler Thromb Vasc Biol* 2010,**30**:1842-1848.
78. Moreno JA, Ortega-Gomez A, Delbosc S, Beaufort N, Sorbets E, Louedec L, *et al.* In vitro and in vivo evidence for the role of elastase shedding of CD163 in human atherothrombosis. *Eur Heart J* 2012,**33**:252-263.
79. Hansson GK. Immune and inflammatory mechanisms in the development of atherosclerosis. *Br Heart J* 1993,**69**:S38-41.
80. Soehnlein O, Weber C. Myeloid cells in atherosclerosis: initiators and decision shapers. *Semin Immunopathol* 2009,**31**:35-47.
81. Soehnlein O, Kai-Larsen Y, Frithiof R, Sorensen OE, Kenne E, Scharffetter-Kochanek K, *et al.* Neutrophil primary granule proteins HBP and HNP1-3 boost bacterial phagocytosis by human and murine macrophages. *J Clin Invest* 2008,**118**:3491-3502.
82. Gombart AF, Krug U, O'Kelly J, An E, Vegesna V, Koeffler HP. Aberrant expression of neutrophil and macrophage-related genes in a murine model for human neutrophil-specific granule deficiency. *J Leukoc Biol* 2005,**78**:1153-1165.
83. Shiohara M, Gombart AF, Sekiguchi Y, Hidaka E, Ito S, Yamazaki T, *et al.* Phenotypic and functional alterations of peripheral blood monocytes in neutrophil-specific granule deficiency. *J Leukoc Biol* 2004,**75**:190-197.
84. Murray PJ, Wynn TA. Protective and pathogenic functions of macrophage subsets. *Nat Rev Immunol* 2011,**11**:723-737.

85. Cochain C, Zernecke A. Macrophages in vascular inflammation and atherosclerosis. *Pflugers Arch* 2017,**469**:485-499.
86. Ensan S, Li A, Besla R, Degousee N, Cosme J, Roufaiel M, *et al.* Self-renewing resident arterial macrophages arise from embryonic CX3CR1(+) precursors and circulating monocytes immediately after birth. *Nat Immunol* 2016,**17**:159-168.
87. Chung EY, Kim SJ, Ma XJ. Regulation of cytokine production during phagocytosis of apoptotic cells. *Cell Res* 2006,**16**:154-161.
88. Rock KL, Kono H. The inflammatory response to cell death. *Annu Rev Pathol* 2008,**3**:99-126.
89. Durai V, Murphy KM. Functions of Murine Dendritic Cells. *Immunity* 2016,**45**:719-736.
90. Gil-Pulido J, Zernecke A. Antigen-presenting dendritic cells in atherosclerosis. *Eur J Pharmacol* 2017.
91. Steinman RM, Cohn ZA. Identification of a novel cell type in peripheral lymphoid organs of mice. I. Morphology, quantitation, tissue distribution. *J Exp Med* 1973,**137**:1142-1162.
92. Steinman RM, Witmer MD. Lymphoid dendritic cells are potent stimulators of the primary mixed leukocyte reaction in mice. *Proc Natl Acad Sci U S A* 1978,**75**:5132-5136.
93. Nussenzweig MC, Steinman RM, Gutchinov B, Cohn ZA. Dendritic cells are accessory cells for the development of anti-trinitrophenyl cytotoxic T lymphocytes. *J Exp Med* 1980,**152**:1070-1084.
94. Gil-Pulido J, Zernecke A. Antigen-presenting dendritic cells in atherosclerosis. *Eur J Pharmacol* 2017,**816**:25-31.
95. Guilliams M, Dutertre CA, Scott CL, McGovern N, Sichien D, Chakarov S, *et al.* Unsupervised High-Dimensional Analysis Aligns Dendritic Cells across Tissues and Species. *Immunity* 2016,**45**:669-684.
96. Miller JC, Brown BD, Shay T, Gautier EL, Jojic V, Cohain A, *et al.* Deciphering the transcriptional network of the dendritic cell lineage. *Nat Immunol* 2012,**13**:888-899.

97. Satpathy AT, Kc W, Albring JC, Edelson BT, Kretzer NM, Bhattacharya D*, et al.* Zbtb46 expression distinguishes classical dendritic cells and their committed progenitors from other immune lineages. *J Exp Med* 2012,**209**:1135-1152.

98. Choi JH, Cheong C, Dandamudi DB, Park CG, Rodriguez A, Mehandru S*, et al.* Flt3 signaling-dependent dendritic cells protect against atherosclerosis. *Immunity* 2011,**35**:819-831.

99. Hume DA. Macrophages as APC and the dendritic cell myth. *J Immunol* 2008,**181**:5829-5835.

100. Roufaiel M, Gracey E, Siu A, Zhu SN, Lau A, Ibrahim H*, et al.* CCL19-CCR7-dependent reverse transendothelial migration of myeloid cells clears Chlamydia muridarum from the arterial intima. *Nat Immunol* 2016,**17**:1263-1272.

101. Busch M, Westhofen TC, Koch M, Lutz MB, Zernecke A. Dendritic cell subset distributions in the aorta in healthy and atherosclerotic mice. *PLoS One* 2014,**9**:e88452.

102. Gautier EL, Huby T, Saint-Charles F, Ouzilleau B, Pirault J, Deswaerte V*, et al.* Conventional dendritic cells at the crossroads between immunity and cholesterol homeostasis in atherosclerosis. *Circulation* 2009,**119**:2367-2375.

103. Rombouts M, Cools N, Grootaert MO, de Bakker F, Van Brussel I, Wouters A*, et al.* Long-Term Depletion of Conventional Dendritic Cells Cannot Be Maintained in an Atherosclerotic Zbtb46-DTR Mouse Model. *PLoS One* 2017,**12**:e0169608.

104. Hildner K, Edelson BT, Purtha WE, Diamond M, Matsushita H, Kohyama M*, et al.* Batf3 deficiency reveals a critical role for CD8alpha+ dendritic cells in cytotoxic T cell immunity. *Science* 2008,**322**:1097-1100.

105. Carbone FR, Heath WR. Cross-priming: its beginnings. *J Immunol* 2010,**185**:1353-1354.

106. Suffia I, Reckling SK, Salay G, Belkaid Y. A role for CD103 in the retention of CD4+CD25+ Treg and control of Leishmania major infection. *J Immunol* 2005,**174**:5444-5455.

107. Martinez-Lopez M, Iborra S, Conde-Garrosa R, Sancho D. Batf3-dependent CD103+ dendritic cells are major producers of IL-12 that drive local Th1 immunity against Leishmania major infection in mice. *Eur J Immunol* 2015,**45**:119-129.

108. Legein B, Janssen EM, Theelen TL, Gijbels MJ, Walraven J, Klarquist JS*, et al.* Ablation of CD8alpha(+) dendritic cell mediated cross-presentation does not impact atherosclerosis in hyperlipidemic mice. *Sci Rep* 2015,**5**:15414.

109. Li Y, Liu X, Duan W, Tian H, Zhu G, He H*, et al.* Batf3-dependent CD8alpha+ Dendritic Cells Aggravates Atherosclerosis via Th1 Cell Induction and Enhanced CCL5 Expression in Plaque Macrophages. *EBioMedicine* 2017,**18**:188-198.

110. Klein L, Kyewski B, Allen PM, Hogquist KA. Positive and negative selection of the T cell repertoire: what thymocytes see (and don't see). *Nat Rev Immunol* 2014,**14**:377-391.

111. Tse K, Tse H, Sidney J, Sette A, Ley K. T cells in atherosclerosis. *Int Immunol* 2013,**25**:615-622.

112. Jonasson L, Holm J, Skalli O, Bondjers G, Hansson GK. Regional accumulations of T cells, macrophages, and smooth muscle cells in the human atherosclerotic plaque. *Arteriosclerosis* 1986,**6**:131-138.

113. Zhou X, Stemme S, Hansson GK. Evidence for a local immune response in atherosclerosis. CD4+ T cells infiltrate lesions of apolipoprotein-E-deficient mice. *Am J Pathol* 1996,**149**:359-366.

114. Cochain C, Zernecke A. Protective and pathogenic roles of CD8(+) T cells in atherosclerosis. *Basic Res Cardiol* 2016,**111**:71.

115. Ilhan F, Kalkanli ST. Atherosclerosis and the role of immune cells. *World J Clin Cases* 2015,**3**:345-352.

116. Grivel JC, Ivanova O, Pinegina N, Blank PS, Shpektor A, Margolis LB*, et al.* Activation of T lymphocytes in atherosclerotic plaques. *Arterioscler Thromb Vasc Biol* 2011,**31**:2929-2937.

117. Kolbus D, Ramos OH, Berg KE, Persson J, Wigren M, Bjorkbacka H*, et al.* CD8+ T cell activation predominate early immune responses to hypercholesterolemia in Apoe(-)(/)(-) mice. *BMC Immunol* 2010,**11**:58.

118. Elhage R, Gourdy P, Brouchet L, Jawien J, Fouque MJ, Fievet C*, et al.* Deleting TCR alpha beta+ or CD4+ T lymphocytes leads to opposite effects on site-specific atherosclerosis in female apolipoprotein E-deficient mice. *Am J Pathol* 2004,**165**:2013-2018.

119. Kyaw T, Winship A, Tay C, Kanellakis P, Hosseini H, Cao A, *et al.* Cytotoxic and proinflammatory CD8+ T lymphocytes promote development of vulnerable atherosclerotic plaques in apoE-deficient mice. *Circulation* 2013,**127**:1028-1039.

120. Cochain C, Koch M, Chaudhari SM, Busch M, Pelisek J, Boon L, *et al.* CD8+ T Cells Regulate Monopoiesis and Circulating Ly6C-high Monocyte Levels in Atherosclerosis in Mice. *Circ Res* 2015,**117**:244-253.

121. Bevan MJ. Helping the CD8(+) T-cell response. *Nat Rev Immunol* 2004,**4**:595-602.

122. Leavy O. Regulatory T cells: CD8+ TReg cells join the fold. *Nat Rev Immunol* 2010,**10**:680.

123. Zhou J, Dimayuga PC, Zhao X, Yano J, Lio WM, Trinidad P, *et al.* CD8(+)CD25(+) T cells reduce atherosclerosis in apoE(-/-) mice. *Biochem Biophys Res Commun* 2014,**443**:864-870.

124. Luckheeram RV, Zhou R, Verma AD, Xia B. CD4(+)T cells: differentiation and functions. *Clin Dev Immunol* 2012,**2012**:925135.

125. Lazarevic V, Glimcher LH, Lord GM. T-bet: a bridge between innate and adaptive immunity. *Nat Rev Immunol* 2013,**13**:777-789.

126. Mallat Z, Taleb S, Ait-Oufella H, Tedgui A. The role of adaptive T cell immunity in atherosclerosis. *J Lipid Res* 2009,**50 Suppl**:S364-369.

127. Baidya SG, Zeng QT. Helper T cells and atherosclerosis: the cytokine web. *Postgrad Med J* 2005,**81**:746-752.

128. Gupta S, Pablo AM, Jiang X, Wang N, Tall AR, Schindler C. IFN-gamma potentiates atherosclerosis in ApoE knock-out mice. *J Clin Invest* 1997,**99**:2752-2761.

129. Whitman SC, Ravisankar P, Elam H, Daugherty A. Exogenous interferon-gamma enhances atherosclerosis in apolipoprotein E-/- mice. *Am J Pathol* 2000,**157**:1819-1824.

130. Tedgui A, Mallat Z. Cytokines in atherosclerosis: pathogenic and regulatory pathways. *Physiol Rev* 2006,**86**:515-581.

131. Panousis CG, Zuckerman SH. Interferon-gamma induces downregulation of Tangier disease gene (ATP-binding-cassette transporter 1) in macrophage-derived foam cells. *Arterioscler Thromb Vasc Biol* 2000,**20**:1565-1571.

132. Wurtz O, Bajenoff M, Guerder S. IL-4-mediated inhibition of IFN-gamma production by CD4+ T cells proceeds by several developmentally regulated mechanisms. *Int Immunol* 2004,**16**:501-508.

133. Engelbertsen D, Andersson L, Ljungcrantz I, Wigren M, Hedblad B, Nilsson J, *et al.* T-helper 2 immunity is associated with reduced risk of myocardial infarction and stroke. *Arterioscler Thromb Vasc Biol* 2013,**33**:637-644.

134. King VL, Cassis LA, Daugherty A. Interleukin-4 does not influence development of hypercholesterolemia or angiotensin II-induced atherosclerotic lesions in mice. *Am J Pathol* 2007,**171**:2040-2047.

135. King VL, Szilvassy SJ, Daugherty A. Interleukin-4 deficiency decreases atherosclerotic lesion formation in a site-specific manner in female LDL receptor-/- mice. *Arterioscler Thromb Vasc Biol* 2002,**22**:456-461.

136. Khew-Goodall Y, Wadham C, Stein BN, Gamble JR, Vadas MA. Stat6 activation is essential for interleukin-4 induction of P-selectin transcription in human umbilical vein endothelial cells. *Arterioscler Thromb Vasc Biol* 1999,**19**:1421-1429.

137. Barks JL, McQuillan JJ, Iademarco MF. TNF-alpha and IL-4 synergistically increase vascular cell adhesion molecule-1 expression in cultured vascular smooth muscle cells. *J Immunol* 1997,**159**:4532-4538.

138. Vadiveloo PK, Stanton HR, Cochran FW, Hamilton JA. Interleukin-4 inhibits human smooth muscle cell proliferation. *Artery* 1994,**21**:161-181.

139. Elliott MJ, Gamble JR, Park LS, Vadas MA, Lopez AF. Inhibition of human monocyte adhesion by interleukin-4. *Blood* 1991,**77**:2739-2745.

140. Daugherty A, Rateri DL, King VL. IL-5 links adaptive and natural immunity in reducing atherosclerotic disease. *J Clin Invest* 2004,**114**:317-319.

141. Miller AM, Xu D, Asquith DL, Denby L, Li Y, Sattar N, *et al.* IL-33 reduces the development of atherosclerosis. *J Exp Med* 2008,**205**:339-346.

142. Binder CJ, Shaw PX, Chang MK, Boullier A, Hartvigsen K, Horkko S, *et al.* The role of natural antibodies in atherogenesis. *J Lipid Res* 2005,**46**:1353-1363.

143. Vignali DA, Collison LW, Workman CJ. How regulatory T cells work. *Nat Rev Immunol* 2008,**8**:523-532.

144. Lahoute C, Herbin O, Mallat Z, Tedgui A. Adaptive immunity in atherosclerosis: mechanisms and future therapeutic targets. *Nat Rev Cardiol* 2011,**8**:348-358.

145. Rosenblum MD, Remedios KA, Abbas AK. Mechanisms of human autoimmunity. *J Clin Invest* 2015,**125**:2228-2233.

146. Wigren M, Bjorkbacka H, Andersson L, Ljungcrantz I, Fredrikson GN, Persson M, *et al.* Low levels of circulating CD4+FoxP3+ T cells are associated with an increased risk for development of myocardial infarction but not for stroke. *Arterioscler Thromb Vasc Biol* 2012,**32**:2000-2004.

147. Ait-Oufella H, Salomon BL, Potteaux S, Robertson AK, Gourdy P, Zoll J, *et al.* Natural regulatory T cells control the development of atherosclerosis in mice. *Nat Med* 2006,**12**:178-180.

148. Mor A, Planer D, Luboshits G, Afek A, Metzger S, Chajek-Shaul T, *et al.* Role of naturally occurring CD4+ CD25+ regulatory T cells in experimental atherosclerosis. *Arterioscler Thromb Vasc Biol* 2007,**27**:893-900.

149. Andersson J, Libby P, Hansson GK. Adaptive immunity and atherosclerosis. *Clin Immunol* 2010,**134**:33-46.

150. Grainger DJ, Mosedale DE, Metcalfe JC, Bottinger EP. Dietary fat and reduced levels of TGFbeta1 act synergistically to promote activation of the vascular endothelium and formation of lipid lesions. *J Cell Sci* 2000,**113 ( Pt 13)**:2355-2361.

151. Maganto-Garcia E, Tarrio ML, Grabie N, Bu DX, Lichtman AH. Dynamic changes in regulatory T cells are linked to levels of diet-induced hypercholesterolemia. *Circulation* 2011,**124**:185-195.

152. Foks AC, Lichtman AH, Kuiper J. Treating atherosclerosis with regulatory T cells. *Arterioscler Thromb Vasc Biol* 2015,**35**:280-287.

153. Spitz C, Winkels H, Burger C, Weber C, Lutgens E, Hansson GK, *et al.* Regulatory T cells in atherosclerosis: critical immune regulatory function and therapeutic potential. *Cell Mol Life Sci* 2016,**73**:901-922.

154. Ghoreschi K, Laurence A, Yang XP, Tato CM, McGeachy MJ, Konkel JE, *et al.* Generation of pathogenic T(H)17 cells in the absence of TGF-beta signalling. *Nature* 2010,**467**:967-971.

155. Stockinger B, Omenetti S. The dichotomous nature of T helper 17 cells. *Nat Rev Immunol* 2017,**17**:535-544.

156. Nordlohne J, von Vietinghoff S. Interleukin 17A in atherosclerosis - Regulation and pathophysiologic effector function. *Cytokine* 2017.

157. Frostegard J, Zhang Y, Sun J, Yan K, Liu A. Oxidized Low-Density Lipoprotein (OxLDL)-Treated Dendritic Cells Promote Activation of T Cells in Human Atherosclerotic Plaque and Blood, Which Is Repressed by Statins: microRNA let-7c Is Integral to the Effect. *J Am Heart Assoc* 2016,**5**.

158. Lim H, Kim YU, Sun H, Lee JH, Reynolds JM, Hanabuchi S*, et al.* Proatherogenic conditions promote autoimmune T helper 17 cell responses in vivo. *Immunity* 2014,**40**:153-165.

159. Akhavanpoor M, Akhavanpoor H, Gleissner CA, Wangler S, Doesch AO, Katus HA*, et al.* The Two Faces of Interleukin-17A in Atherosclerosis. *Curr Drug Targets* 2017,**18**:863-873.

160. Taleb S, Tedgui A. IL-17 in atherosclerosis: the good and the bad. *Cardiovasc Res* 2018,**114**:7-9.

161. Ding R, Gao W, He Z, Liao M, Wu F, Zou S*, et al.* Effect of serum interleukin 21 on the development of coronary artery disease. *APMIS* 2014,**122**:842-847.

162. Rattik S, Hultman K, Rauch U, Soderberg I, Sundius L, Ljungcrantz I*, et al.* IL-22 affects smooth muscle cell phenotype and plaque formation in apolipoprotein E knockout mice. *Atherosclerosis* 2015,**242**:506-514.

163. Shaposhnik Z, Wang X, Weinstein M, Bennett BJ, Lusis AJ. Granulocyte macrophage colony-stimulating factor regulates dendritic cell content of atherosclerotic lesions. *Arterioscler Thromb Vasc Biol* 2007,**27**:621-627.

164. Zbinden S, Zbinden R, Meier P, Windecker S, Seiler C. Safety and efficacy of subcutaneous-only granulocyte-macrophage colony-stimulating factor for collateral growth promotion in patients with coronary artery disease. *J Am Coll Cardiol* 2005,**46**:1636-1642.

165. Vantourout P, Hayday A. Six-of-the-best: unique contributions of gammadelta T cells to immunology. *Nat Rev Immunol* 2013,**13**:88-100.

166. Carding SR, Egan PJ. Gammadelta T cells: functional plasticity and heterogeneity. *Nat Rev Immunol* 2002,**2**:336-345.

167. Prinz I, Silva-Santos B, Pennington DJ. Functional development of gammadelta T cells. *Eur J Immunol* 2013,**43**:1988-1994.

168. Chien YH, Zeng X, Prinz I. The natural and the inducible: interleukin (IL)-17-producing gammadelta T cells. *Trends Immunol* 2013,**34**:151-154.

169. Vanderlaan PA, Reardon CA. Thematic review series: the immune system and atherogenesis. The unusual suspects:an overview of the minor leukocyte populations in atherosclerosis. *J Lipid Res* 2005,**46**:829-838.

170. Cheng HY, Wu R, Hedrick CC. Gammadelta (gammadelta) T lymphocytes do not impact the development of early atherosclerosis. *Atherosclerosis* 2014,**234**:265-269.

171. Smith E, Prasad KM, Butcher M, Dobrian A, Kolls JK, Ley K, *et al.* Blockade of interleukin-17A results in reduced atherosclerosis in apolipoprotein E-deficient mice. *Circulation* 2010,**121**:1746-1755.

172. Kleindienst R, Xu Q, Willeit J, Waldenberger FR, Weimann S, Wick G. Immunology of atherosclerosis. Demonstration of heat shock protein 60 expression and T lymphocytes bearing alpha/beta or gamma/delta receptor in human atherosclerotic lesions. *Am J Pathol* 1993,**142**:1927-1937.

173. Vu DM, Tai A, Tatro JB, Karas RH, Huber BT, Beasley D. gammadeltaT cells are prevalent in the proximal aorta and drive nascent atherosclerotic lesion progression and neutrophilia in hypercholesterolemic mice. *PLoS One* 2014,**9**:e109416.

174. Vignali DA, Kuchroo VK. IL-12 family cytokines: immunological playmakers. *Nat Immunol* 2012,**13**:722-728.

175. Wang X, Wei Y, Xiao H, Liu X, Zhang Y, Han G, *et al.* A novel IL-23p19/Ebi3 (IL-39) cytokine mediates inflammation in Lupus-like mice. *Eur J Immunol* 2016,**46**:1343-1350.

176. Collison LW, Chaturvedi V, Henderson AL, Giacomin PR, Guy C, Bankoti J, *et al.* IL-35-mediated induction of a potent regulatory T cell population. *Nat Immunol* 2010,**11**:1093-1101.

177. Oppmann B, Lesley R, Blom B, Timans JC, Xu Y, Hunte B, *et al.* Novel p19 protein engages IL-12p40 to form a cytokine, IL-23, with biological activities similar as well as distinct from IL-12. *Immunity* 2000,**13**:715-725.

178. Espigol-Frigole G, Planas-Rigol E, Ohnuki H, Salvucci O, Kwak H, Ravichandran S, *et al.* Identification of IL-23p19 as an endothelial proinflammatory peptide that promotes gp130-STAT3 signaling. *Sci Signal* 2016,**9**:ra28.

179. Subramanian M, Thorp E, Tabas I. Identification of a non-growth factor role for GM-CSF in advanced atherosclerosis: promotion of macrophage apoptosis and plaque necrosis through IL-23 signaling. *Circ Res* 2015,**116**:e13-24.

180. Schuetze N, Schoeneberger S, Mueller U, Freudenberg MA, Alber G, Straubinger RK. IL-12 family members: differential kinetics of their TLR4-mediated induction by Salmonella enteritidis and the impact of IL-10 in bone marrow-derived macrophages. *Int Immunol* 2005,**17**:649-659.

181. Roses RE, Xu S, Xu M, Koldovsky U, Koski G, Czerniecki BJ. Differential production of IL-23 and IL-12 by myeloid-derived dendritic cells in response to TLR agonists. *J Immunol* 2008,**181**:5120-5127.

182. Parham C, Chirica M, Timans J, Vaisberg E, Travis M, Cheung J, *et al.* A receptor for the heterodimeric cytokine IL-23 is composed of IL-12Rbeta1 and a novel cytokine receptor subunit, IL-23R. *J Immunol* 2002,**168**:5699-5708.

183. Teng MW, Bowman EP, McElwee JJ, Smyth MJ, Casanova JL, Cooper AM, *et al.* IL-12 and IL-23 cytokines: from discovery to targeted therapies for immune-mediated inflammatory diseases. *Nat Med* 2015,**21**:719-729.

184. Gaffen SL, Jain R, Garg AV, Cua DJ. The IL-23-IL-17 immune axis: from mechanisms to therapeutic testing. *Nat Rev Immunol* 2014,**14**:585-600.

185. Zuniga LA, Jain R, Haines C, Cua DJ. Th17 cell development: from the cradle to the grave. *Immunol Rev* 2013,**252**:78-88.

186. Annunziato F, Cosmi L, Liotta F, Maggi E, Romagnani S. Type 17 T helper cells-origins, features and possible roles in rheumatic disease. *Nat Rev Rheumatol* 2009,**5**:325-331.

187. Marks BR, Nowyhed HN, Choi JY, Poholek AC, Odegard JM, Flavell RA, *et al.* Thymic self-reactivity selects natural interleukin 17-producing T cells that can regulate peripheral inflammation. *Nat Immunol* 2009,**10**:1125-1132.

188. Cua DJ, Tato CM. Innate IL-17-producing cells: the sentinels of the immune system. *Nat Rev Immunol* 2010,**10**:479-489.

189. Awasthi A, Riol-Blanco L, Jager A, Korn T, Pot C, Galileos G, *et al.* Cutting edge: IL-23 receptor gfp reporter mice reveal distinct populations of IL-17-producing cells. *J Immunol* 2009,**182**:5904-5908.

190. Kebir H, Ifergan I, Alvarez JI, Bernard M, Poirier J, Arbour N, *et al.* Preferential recruitment of interferon-gamma-expressing TH17 cells in multiple sclerosis. *Ann Neurol* 2009,**66**:390-402.

191. Eid RE, Rao DA, Zhou J, Lo SF, Ranjbaran H, Gallo A, *et al.* Interleukin-17 and interferon-gamma are produced concomitantly by human coronary artery-infiltrating T cells and act synergistically on vascular smooth muscle cells. *Circulation* 2009,**119**:1424-1432.

192. Shi WY, Che CY, Liu L. Human interleukin 23 receptor induces cell apoptosis in mammalian cells by intrinsic mitochondrial pathway associated with the down-regulation of RAS/mitogen-activated protein kinase and signal transducers and activators of transcription factor 3 signaling pathways. *Int J Mol Sci* 2013,**14**:24656-24669.

193. Cocco C, Canale S, Frasson C, Di Carlo E, Ognio E, Ribatti D, *et al.* Interleukin-23 acts as antitumor agent on childhood B-acute lymphoblastic leukemia cells. *Blood* 2010,**116**:3887-3898.

194. Li H, Hsu HC, Wu Q, Yang P, Li J, Luo B, *et al.* IL-23 promotes TCR-mediated negative selection of thymocytes through the upregulation of IL-23 receptor and RORgammat. *Nat Commun* 2014,**5**:4259.

195. Liao Y, Hu X, Guo X, Zhang B, Xu W, Jiang H. Promoting effects of IL23 on myocardial ischemia and reperfusion are associated with increased expression of IL17A and upregulation of the JAK2STAT3 signaling pathway. *Mol Med Rep* 2017.

196. David A, Saitta S, De Caridi G, Benedetto F, Massara M, Risitano DC, *et al.* Interleukin-23 serum levels in patients affected by peripheral arterial disease. *Clin Biochem* 2012,**45**:275-278.

197. Abbas A, Gregersen I, Holm S, Daissormont I, Bjerkeli V, Krohg-Sorensen K, *et al.* Interleukin 23 levels are increased in carotid atherosclerosis: possible role for the interleukin 23/interleukin 17 axis. *Stroke* 2015,**46**:793-799.

198. Khojasteh-Fard M, Abolhalaj M, Amiri P, Zaki M, Taheri Z, Qorbani M, *et al.* IL-23 gene expression in PBMCs of patients with coronary artery disease. *Dis Markers* 2012,**33**:289-293.

199. Gelderblom M, Gallizioli M, Ludewig P, Thom V, Arunachalam P, Rissiek B, *et al.* IL-23 (Interleukin-23)-Producing Conventional Dendritic Cells Control the Detrimental IL-17 (Interleukin-17) Response in Stroke. *Stroke* 2018,**49**:155-164.
200. Abdollahi E, Tavasolian F, Momtazi-Borojeni AA, Samadi M, Rafatpanah H. Protective role of R381Q (rs11209026) polymorphism in IL-23R gene in immune-mediated diseases: A comprehensive review. *J Immunotoxicol* 2016,**13**:286-300.
201. Mangino M, Braund P, Singh R, Steeds R, Stevens S, Channer KS, *et al.* Association analysis of IL-12B and IL-23R polymorphisms in myocardial infarction. *J Mol Med (Berl)* 2008,**86**:99-103.
202. Zhang M, Cai ZR, Zhang B, Cai X, Li W, Guo Z, *et al.* Functional polymorphisms in interleukin-23 receptor and susceptibility to coronary artery disease. *DNA Cell Biol* 2014,**33**:891-897.
203. Duerr RH, Taylor KD, Brant SR, Rioux JD, Silverberg MS, Daly MJ, *et al.* A genome-wide association study identifies IL23R as an inflammatory bowel disease gene. *Science* 2006,**314**:1461-1463.
204. Di Meglio P, Di Cesare A, Laggner U, Chu CC, Napolitano L, Villanova F, *et al.* The IL23R R381Q gene variant protects against immune-mediated diseases by impairing IL-23-induced Th17 effector response in humans. *PLoS One* 2011,**6**:e17160.
205. Genetic Analysis of Psoriasis C, the Wellcome Trust Case Control C, Strange A, Capon F, Spencer CC, Knight J, *et al.* A genome-wide association study identifies new psoriasis susceptibility loci and an interaction between HLA-C and ERAP1. *Nat Genet* 2010,**42**:985-990.
206. Kave M, Shadman M, Alizadeh A, Samadi M. Analysis of the association between IL-23R rs11209026 polymorphism and incidence of atherosclerosis. *Int J Immunogenet* 2015,**42**:341-345.
207. Heinen AP, Wanke F, Moos S, Attig S, Luche H, Pal PP, *et al.* Improved method to retain cytosolic reporter protein fluorescence while staining for nuclear proteins. *Cytometry A* 2014,**85**:621-627.
208. Sukovich DA, Kauser K, Shirley FD, DelVecchio V, Halks-Miller M, Rubanyi GM. Expression of interleukin-6 in atherosclerotic lesions of male ApoE-

knockout mice: inhibition by 17beta-estradiol. *Arterioscler Thromb Vasc Biol* 1998,**18**:1498-1505.

209. Edelson BT, Kc W, Juang R, Kohyama M, Benoit LA, Klekotka PA, *et al.* Peripheral CD103+ dendritic cells form a unified subset developmentally related to CD8alpha+ conventional dendritic cells. *J Exp Med* 2010,**207**:823-836.

210. Seillet C, Jackson JT, Markey KA, Brady HJ, Hill GR, Macdonald KP, *et al.* CD8alpha+ DCs can be induced in the absence of transcription factors Id2, Nfil3, and Batf3. *Blood* 2013,**121**:1574-1583.

211. Mass E, Ballesteros I, Farlik M, Halbritter F, Gunther P, Crozet L, *et al.* Specification of tissue-resident macrophages during organogenesis. *Science* 2016,**353**.

212. Goldmann T, Wieghofer P, Jordao MJ, Prutek F, Hagemeyer N, Frenzel K, *et al.* Origin, fate and dynamics of macrophages at central nervous system interfaces. *Nat Immunol* 2016,**17**:797-805.

213. Ferris ST, Carrero JA, Mohan JF, Calderon B, Murphy KM, Unanue ER. A minor subset of Batf3-dependent antigen-presenting cells in islets of Langerhans is essential for the development of autoimmune diabetes. *Immunity* 2014,**41**:657-669.

214. Tussiwand R, Lee WL, Murphy TL, Mashayekhi M, Kc W, Albring JC, *et al.* Compensatory dendritic cell development mediated by BATF-IRF interactions. *Nature* 2012,**490**:502-507.

215. Murphy TL, Tussiwand R, Murphy KM. Specificity through cooperation: BATF-IRF interactions control immune-regulatory networks. *Nat Rev Immunol* 2013,**13**:499-509.

216. Sato K, Fujita S. Dendritic cells: nature and classification. *Allergol Int* 2007,**56**:183-191.

217. Siegemund S, Schutze N, Freudenberg MA, Lutz MB, Straubinger RK, Alber G. Production of IL-12, IL-23 and IL-27p28 by bone marrow-derived conventional dendritic cells rather than macrophages after LPS/TLR4-dependent induction by Salmonella Enteritidis. *Immunobiology* 2007,**212**:739-750.

218. Jongstra-Bilen J, Zhang CX, Wisnicki T, Li MK, White-Alfred S, Ilaalagan R, *et al.* Oxidized Low-Density Lipoprotein Loading of Macrophages Downregulates

TLR-Induced Proinflammatory Responses in a Gene-Specific and Temporal Manner through Transcriptional Control. *J Immunol* 2017,**199**:2149-2157.

219. van Bergenhenegouwen J, Kraneveld AD, Rutten L, Garssen J, Vos AP, Hartog A. Lipoproteins attenuate TLR2 and TLR4 activation by bacteria and bacterial ligands with differences in affinity and kinetics. *BMC Immunol* 2016,**17**:42.
220. Erbel C, Dengler TJ, Wangler S, Lasitschka F, Bea F, Wambsganss N, *et al.* Expression of IL-17A in human atherosclerotic lesions is associated with increased inflammation and plaque vulnerability. *Basic Res Cardiol* 2011,**106**:125-134.
221. Nakashima Y, Raines EW, Plump AS, Breslow JL, Ross R. Upregulation of VCAM-1 and ICAM-1 at atherosclerosis-prone sites on the endothelium in the ApoE-deficient mouse. *Arterioscler Thromb Vasc Biol* 1998,**18**:842-851.
222. Astry B, Venkatesha SH, Moudgil KD. Involvement of the IL-23/IL-17 axis and the Th17/Treg balance in the pathogenesis and control of autoimmune arthritis. *Cytokine* 2015,**74**:54-61.
223. Izcue A, Hue S, Buonocore S, Arancibia-Carcamo CV, Ahern PP, Iwakura Y, *et al.* Interleukin-23 restrains regulatory T cell activity to drive T cell-dependent colitis. *Immunity* 2008,**28**:559-570.
224. Petermann F, Rothhammer V, Claussen MC, Haas JD, Blanco LR, Heink S, *et al.* gammadelta T cells enhance autoimmunity by restraining regulatory T cell responses via an interleukin-23-dependent mechanism. *Immunity* 2010,**33**:351-363.
225. Libby P. Inflammation in atherosclerosis. *Arterioscler Thromb Vasc Biol* 2012,**32**:2045-2051.
226. Van Vre EA, Bosmans JM, Van Brussel I, Maris M, De Meyer GR, Van Schil PE, *et al.* Immunohistochemical characterisation of dendritic cells in human atherosclerotic lesions: possible pitfalls. *Pathology* 2011,**43**:239-247.
227. Mackarehtschian K, Hardin JD, Moore KA, Boast S, Goff SP, Lemischka IR. Targeted disruption of the flk2/flt3 gene leads to deficiencies in primitive hematopoietic progenitors. *Immunity* 1995,**3**:147-161.
228. Maraskovsky E, Brasel K, Teepe M, Roux ER, Lyman SD, Shortman K, *et al.* Dramatic increase in the numbers of functionally mature dendritic cells in Flt3

ligand-treated mice: multiple dendritic cell subpopulations identified. *J Exp Med* 1996,**184**:1953-1962.

229. Getz GS, Reardon CA. Do the Apoe-/- and Ldlr-/- Mice Yield the Same Insight on Atherogenesis? *Arterioscler Thromb Vasc Biol* 2016,**36**:1734-1741.

230. Song L, Schindler C. IL-6 and the acute phase response in murine atherosclerosis. *Atherosclerosis* 2004,**177**:43-51.

231. Schieffer B, Selle T, Hilfiker A, Hilfiker-Kleiner D, Grote K, Tietge UJ, *et al.* Impact of interleukin-6 on plaque development and morphology in experimental atherosclerosis. *Circulation* 2004,**110**:3493-3500.

232. Zirlik A, Maier C, Gerdes N, MacFarlane L, Soosairajah J, Bavendiek U, *et al.* CD40 ligand mediates inflammation independently of CD40 by interaction with Mac-1. *Circulation* 2007,**115**:1571-1580.

233. Lutgens E, Lievens D, Beckers L, Wijnands E, Soehnlein O, Zernecke A, *et al.* Deficient CD40-TRAF6 signaling in leukocytes prevents atherosclerosis by skewing the immune response toward an antiinflammatory profile. *J Exp Med* 2010,**207**:391-404.

234. Thomson AW, Robbins PD. Tolerogenic dendritic cells for autoimmune disease and transplantation. *Ann Rheum Dis* 2008,**67 Suppl 3**:iii90-96.

235. Habets KL, van Puijvelde GH, van Duivenvoorde LM, van Wanrooij EJ, de Vos P, Tervaert JW, *et al.* Vaccination using oxidized low-density lipoprotein-pulsed dendritic cells reduces atherosclerosis in LDL receptor-deficient mice. *Cardiovasc Res* 2010,**85**:622-630.

236. Riol-Blanco L, Lazarevic V, Awasthi A, Mitsdoerffer M, Wilson BS, Croxford A, *et al.* IL-23 receptor regulates unconventional IL-17-producing T cells that control bacterial infections. *J Immunol* 2010,**184**:1710-1720.

237. Lee Y, Awasthi A, Yosef N, Quintana FJ, Xiao S, Peters A, *et al.* Induction and molecular signature of pathogenic TH17 cells. *Nat Immunol* 2012,**13**:991-999.

238. Croxford AL, Mair F, Becher B. IL-23: one cytokine in control of autoimmunity. *Eur J Immunol* 2012,**42**:2263-2273.

239. Tang C, Chen S, Qian H, Huang W. Interleukin-23: as a drug target for autoimmune inflammatory diseases. *Immunology* 2012,**135**:112-124.

240. Sherer Y, Shoenfeld Y. Mechanisms of disease: atherosclerosis in autoimmune diseases. *Nat Clin Pract Rheumatol* 2006,**2**:99-106.

241. Nickel T, Schmauss D, Hanssen H, Sicic Z, Krebs B, Jankl S, *et al.* oxLDL uptake by dendritic cells induces upregulation of scavenger-receptors, maturation and differentiation. *Atherosclerosis* 2009,**205**:442-450.

242. Perrin-Cocon L, Coutant F, Agaugue S, Deforges S, Andre P, Lotteau V. Oxidized low-density lipoprotein promotes mature dendritic cell transition from differentiating monocyte. *J Immunol* 2001,**167**:3785-3791.

243. Zaguri R, Verbovetski I, Atallah M, Trahtemberg U, Krispin A, Nahari E, *et al.* 'Danger' effect of low-density lipoprotein (LDL) and oxidized LDL on human immature dendritic cells. *Clin Exp Immunol* 2007,**149**:543-552.

244. Papotto PH, Reinhardt A, Prinz I, Silva-Santos B. Innately versatile: gammadelta17 T cells in inflammatory and autoimmune diseases. *J Autoimmun* 2018,**87**:26-37.

245. Indramohan M, Sieve AN, Break TJ, Berg RE. Inflammatory monocyte recruitment is regulated by interleukin-23 during systemic bacterial infection. *Infect Immun* 2012,**80**:4099-4105.

246. Wu C, Chen Z, Xiao S, Thalhamer T, Madi A, Han T, *et al.* SGK1 Governs the Reciprocal Development of Th17 and Regulatory T Cells. *Cell Rep* 2018,**22**:653-665.

247. Wu C, Yosef N, Thalhamer T, Zhu C, Xiao S, Kishi Y, *et al.* Induction of pathogenic TH17 cells by inducible salt-sensing kinase SGK1. *Nature* 2013,**496**:513-517.

248. Pinderski LJ, Fischbein MP, Subbanagounder G, Fishbein MC, Kubo N, Cheroutre H, *et al.* Overexpression of interleukin-10 by activated T lymphocytes inhibits atherosclerosis in LDL receptor-deficient Mice by altering lymphocyte and macrophage phenotypes. *Circ Res* 2002,**90**:1064-1071.

249. Voloshyna I, Littlefield MJ, Reiss AB. Atherosclerosis and interferon-gamma: new insights and therapeutic targets. *Trends Cardiovasc Med* 2014,**24**:45-51.

250. Bergamini A, Bolacchi F, Bongiovanni B, Cepparulo M, Ventura L, Capozzi M, *et al.* Granulocyte-macrophage colony-stimulating factor regulates cytokine

production in cultured macrophages through CD14-dependent and -independent mechanisms. *Immunology* 2000,**101**:254-261.

251. Edo A, Espinosa-Parrilla JF. Soluble interleukin 23 receptor gene therapy with adeno-associated vectors for the treatment of multiple sclerosis. *Neural Regen Res* 2017,**12**:1605-1606.

**ACKNOWLEDGMENTS**

"There is strength in numbers". I completely agree. Writing a thesis is a really long journey and cannot be completed without the support and help of many different and important protagonists, who have contributed at different levels during this trip and who need to be recognized as a big part of this work.

First of all, I need to give a big and special thanks to Alma, who not only allowed me to enter to the fascinating world of atherosclerosis but also gave me priceless ideas and suggestions, that inevitably ended in the thesis that today is presented here. I need also to thank the trust she put on my hands regarding mouse maintenance or student supervision, among others, which enhanced important skills needed for a successful career. Thanks a lot.

I also need to express my gratitude to Manfred Lutz and Ana Eulalio, members of my thesis Committee, who gave me valuable inputs and helped me to canalize some aspects of the work. In a similar way, I say thanks to Thomas Korn in München, who provided the IL-23R mouse model.

I cannot forget my colleagues, Melanie Schott, Yvonne Kerstan, Petra Werner, Petra Hönig-Liedl, Sandra Vorlova, Clement Cochain and Maja Bundalo, which apart from helping me with my work also made every day in the lab smoother. Also Doris and Lilo, responsible for genotyping the lines I were in charge with, and Elfriede, who was always prepared for my "we are ride of this product!" and "this machine is not working!" moments. Thanks, Silvia Schülein and Petra Hufnagel especially at the end of 2017, for listening to all the FACS-related problems and helping me with "The Neverending Story", and Elke Butt. A special thanks to Nuria, who not only was my colleague but also my best friend in the lab. Thanks a lot for always being there to listen to all my crazy thoughts, ranging from those days in where I want to leave the thesis to those difficult personal moments not related to the work. Moltes mercès!

Thanks also to the animal keepers in the ZEMM, as they had an enormous responsibility in maintaining most of the lines that have been used for this thesis.

As this journey required not only academic but also emotional support I do not want to forget those last ones. I want to start with Ana and Reichel, who always understood all the different emotions coming throughout the whole process. I need to continue with “Los Ramoncines”, Barbara, Hector and Unai, whose sometimes meaningless conversations were exactly what I need to completely disconnect after a difficult day in the lab. Thanks again for your friendship and your presence, even in the distance. A special thanks to those who enter my life at the starting point of the thesis, Jose, Cris, Juan and Susy, who contributed to making life easier especially when you leave back your country and need to start everything from zero.

I want to finish these acknowledgments with the most important part of my life, without them nothing would have been possible. Many thanks to you, Alex, my life-partner, for not only dealing with the rollercoaster emotions during the Ph.D. work but also for supporting and encouraging me to achieve my final goal and not leaving me to give up.

Finally, I need to give a big, big thanks to my parents Jesus and Mercedes, and my sister, Bea because they made the person who I am today. I cannot express with words how invaluable was, is and will be your help for me and I am sure this Ph.D. could have never seen the light without you. Muchas gracias por ser como sois. Nunca cambiéis.

# LIST OF PUBLICATIONS

This Thesis led to the publication of the following original articles and review:

**Gil-Pulido J**, Cochain C, Manthey H, Rösch M, Amezaga N, Iwakura Y, Prinz I, Waisman A, Korn T, Zernecke A. Interleukin-23 signaling activates γδ T cells that locally control early atherosclerotic lesion formation and plaque necrosis in mice. *Submitted*

**Gil-Pulido J**, Zernecke A. Antigen-presenting dendritic cells in atherosclerosis. *Eur J Pharmacol* 2017,**816**:25-31.

**Gil-Pulido J**, Cochain C, Lippert MA, Schneider N, Butt E, Amezaga N, *et al.* Deletion of *Batf3*-dependent antigen-presenting cells does not affect atherosclerotic lesion formation in mice. *PLoS One* 2017,**12**:e0181947.

Other original articles published derived from external collaborations:

Gotru SK*, **Gil-Pulido J***, Beyersdorf N, Diefenbach A, Becker IC, Vogtle T, et al. Cutting Edge: Imbalanced Cation Homeostasis in MAGT1-Deficient B Cells Dysregulates B Cell Development and Signaling in Mice. J Immunol 2018,200:2529-2534.

*Equally contribution

# CURRICULUM VITAE

## AFFIDAVIT

I hereby confirm that my thesis entitled “The role of Batf3-dependent dendritic cells and the IL-23 receptor in atherosclerosis” is the results of my own work. I did not receive any help or support from commercial consultants. All sources and/or materials applied are listed and specified in the thesis.

Furthermore, I confirm that this thesis has not yet been submitted as part of another examination process neither in identical nor in similar form.

Place, Data Signature

## EIDESSTATTLICHE ERKLÄRUNG

Hiermit erkläre ich an Eides statt, die Dissertation „Die Rolle von Batf3-abhängigen dendritischen Zellen und des IL-23-Rezeptors in der Atherosklerose“ eigenständig, d.h. insbesondere selbständig und ohne Hilfe eines kommerziellen Promotionsberaters, angefertigt und keine anderen als die von mir angegebenen Quellen und Hilfsmittel verwendet zu haben.

Ich erkläre außerdem, dass die Dissertation weder in gleicher noch in ähnlicher Form bereits in einem anderen Prüfungsverfahren vorgelegen hat.

Ort, Datum Unterschrift